1996

Multicomponent Interdiffusion In Micellar Solutions And Microemulsions

Ling Hao

MULTICOMPONENT INTERDIFFUSION IN MICELLAR SOLUTIONS AND MICROEMULSIONS

by

Ling Hao

Department of Chemistry

Submitted in partial fulfillment
of the requirements for the degree of
Doctor of Philosophy

Faculty of Graduate Studies
The University of Western Ontario
London, Ontario
July 1996

ISBN 0-612-15054-2

ABSTRACT

This thesis focuses on multicomponent interdiffusion in micellar solutions and microemulsions. The Taylor dispersion technique is used to measure ternary diffusion coefficients for aqueous micellar solutions of: sodium dodecylsulfate (SDS)/NaCl; SDS/alcohol solubilizates; and sodium cholate (SC)/alcohol solubilizates. Ternary diffusion coefficients are also reported for water/sodium bis(2-ethylhexyl) sulfosuccinate (AOT)/*n*-heptane and water/*2*-propanol/*n*-hexane water-in-oil microemulsions. The results include cross-diffusion coefficients, which provide new insights into the interactions between diffusing surfactants and solubilizates.

The diffusion coefficient of SDS in aqueous salt solutions determined by Taylor dispersion is found to be smaller than the diffusion coefficient of the micelles indicated by the popular quasi-elastic light scattering (QELS) method. To clarify the disagreement between the two methods, an expression is developed for the spectrum of light scattered by concentration fluctuations in a multicomponent solution. The spectrum shows that QELS gives the lower eigenvalue of the diffusion coefficient matrix for SDS/NaCl solutions rather than the diffusion coefficient of the SDS micelles.

In aqueous SDS/alcohol solubilizate solutions, the diffusion of the solubilized portion of each alcohol was expected to cotransport large amounts of SDS. In fact, diffusing octanol produces large countercurrent coupled flows of SDS. Nernst-Planck equations are used to develop a model for the diffusion of solubilizates and ionic micelles.

The binary diffusion coefficient of aqueous SC, an important biosurfactant, solutions is determined by the Taylor dispersion technique. The results are used to estimate the critical micelle concentration and the average aggregation number of SC micelles. Ternary diffusion coefficients reported for aqueous SC/*n*-decanol and SC/*n*-octanol solutions suggest that diffusion in SC/solubilizate systems is similar to that of SDS/octanol solutions.

In water/AOT/*n*-heptane water-in-oil microemulsions, the water and AOT components were expected to diffuse together through the heptane-continuous medium as

surfactant-coated water droplets. Surprisingly, the Taylor results show that the diffusion coefficient of AOT is up to 3 times larger than the diffusion coefficient of water. Moreover, concentration gradients in AOT produce cocurrent coupled flows of water, but gradients in water produce counterflows of AOT. This unexpected behaviour is attributed to changes in the average droplet size along the diffusion path. A size distribution model is proposed to describe the interdiffusion in microemulsions. The diffusion coefficients predicted for water/AOT/*n*-heptane are in good agreement with the measured diffusion coefficients.

Ternary diffusion coefficients are also measured for water/*2*-propanol/*n*-hexane water-in-oil microemulsions. The results show that diffusing water produces significant counterflows of *2*-propanol. A chemical equilibrium model is developed to describe coupled diffusion in water/*2*-propanol/*n*-hexane microemulsions.

ACKNOWLEDGEMENTS

First of all, I wish to express my sincerest appreciation to Dr. D.G. Leaist, my supervisor, for his invaluable guidance, assistance and encouragement throughout this thesis work. His exceptional intelligence, scientific attitude and working enthusiasm with endless ideas and energy deeply impress me.

I would like to extend my thanks to Dr. A.R. Allnatt, Dr. R.R. Martin, Dr. A.C. Weedon, and Dr. C.J. Willis for their advice and support throughout the course of this research.

Special thanks to Hui Lü, Zhiping Deng, Lizhong Sun, Zhanfeng Yin, Dien Li, Yongfeng Hu, Qiwei Zhu and Hai Du for their unforgettable help over the past few years, especially during my initial hard time here. I am also grateful to Ruanhui Lu and Rob Donkers for their friendship and help.

I am indebted to Dr. H.J. Baldwin and Mrs. Cheryl O'Meara for their warm assistance throughout the duration of this program.

I have a deep feeling of indebtedness to my dear parents, Minen Hao and Fang Qi, and sister Ping Hao, for their moral support and lasting encouragement.

Finally, I want to present my unreserved, heartful gratitude to my lovely, beautiful wife Boxiu for her love, full support, understanding, and patience.

This thesis is dedicated to my wife and parents.

TABLE OF CONTENTS

LIST OF FIGURES

LIST OF TABLES

Chapter 1

INTRODUCTION

1.1. General Considerations

Diffusion, the transport of matter by random thermal motions, is one of the most fundamental processes in nature. Because diffusion is slow, it often limits the rates of important chemical, biological, geological and environmental processes. For example, the rates of many chemical reactions are limited by how rapidly the reactants can diffuse together. In addition to practical applications, studies of diffusion provide fundamental information regarding the motion, sizes and shapes of molecules and ions, the interactions between them, and also the structure of liquid solutions.

Over the past decade, diffusion measurements have become increasingly popular for the characterization of solutions of micelles and microemulsions which are formed by the self-association of surfactants. Surfactants find increasing applications in catalysis, enhanced oil recovery, and the production of paints, dyestuffs, cosmetics, pesticides, fibers and plastics.

Intradiffusion Diffusion in micellar solutions and microemulsions is usually studied by NMR[1-8] or radioactive tracer methods[9,10]. These techniques give "intradiffusion" coefficients[11,12], D^*, for the transport of labelled species in solutions of uniform chemical composition:

$$J^* = -D^* \nabla C^* \qquad (1.1)$$

J^* denotes the flux of labelled species, and ∇C^* the gradient in concentration of labelled species. For example, octanol tagged with radioactive ^{14}C can be used to study the intradiffusion of partially solubilized octanol in aqueous solutions of sodium dodecylsulfate micelles. Because the intradiffusion coefficient is the concentration-weighted average of the diffusion coefficients of the solution species containing the radioactive labels, intradiffusion experiments provide invaluable information about the extent of solubilization and counterion binding.

Binary Interdiffusion Mass transport caused by chemical concentration gradients is called "interdiffusion" or "mutual diffusion". Unlike intradiffusion, which involves the interchange of labelled and unlabelled species in solutions of uniform chemical composition, interdiffusion generates net flows of chemical substances. In solubilization processes, for example, micelles diffuse to oil droplets to form water-soluble aggregates of oil and surfactant. Interdiffusion in a two-component solution consisting of a solute dissolved in a solvent is described by Fick's equation

$$J = -D\nabla C \tag{1.2}$$

J is the flux of solute, D the binary interdiffusion coefficient, and ∇C the gradient in concentration of the solute. Although equations (1.1) and (1.2) are mathematically identical, interdiffusion differs fundamentally from intradiffusion. In general, there is no exact relationship between interdiffusion and intradiffusion coefficients.

Binary Interdiffusion in Micellar Solutions Interdiffusion in micellar solutions has been studied by a variety of techniques, including quasi-elastic light scattering[13-20], electrochemical measurements[21-33], and Taylor dispersion[34-37]. Aqueous sodium dodecylsulfate (SDS) solutions, in particular, have been thoroughly studied over a wide range of concentration[14-16,35-37]. The interdiffusion coefficient of aqueous SDS drops sharply at the critical micelle concentration (cmc), marking the onset of the aggregation of surfactant monomers to form micelles. As the concentration is raised above the cmc, the diffusion coefficient increases steadily, despite the increasing of solution viscosity.

The unexpected increase in the rate of diffusion of SDS above the cmc has been attributed to micelle-micelle interactions[14,34], monomer-micelle exchange kinetics[34], micelle rearrangement and electrostatic interactions[35]. Weinheimer *et al.*[36] expressed the diffusion coefficient of a dissolved surfactant as a weighted average of the diffusion coefficients of the monomer and micellar aggregates, implying the existence of local equilibrium of the micellar aggregation and dissociation reactions. Leaist[37] showed that the sudden drop in the surfactant diffusion coefficient at the cmc is a thermodynamic effect, analogous to the limiting behaviour $D \rightarrow 0$ at a critical mixing point caused by the vanishing of free energy gradients - the driving forces for diffusion. The increase in the

diffusion coefficient of aqueous SDS above the cmc is due to a 10-fold decrease in the frictional force acting on the micellized electrolyte. The frictional force opposing the diffusion of a dissolved species is proportional to the effective radius of the species which in turn is proportional to the cube root of the volume of the species. Because the volume of a micellar aggregate of n monomers is proportional to n, the frictional force acting on the micelle increases only as $n^{1/3}$, and hence the frictional force *per monomer* actually *decreases* with the aggregation number as $n^{1/3}/n = n^{-2/3}$.

1.2. Motivation

Multicomponent Interdiffusion In practical applications, solutions of micelles or microemulsions usually contain more than two components (e.g., solvent, surfactant, cosurfactant, salt, solubilizates). Interdiffusion in a solution containing three or more components is called multicomponent interdiffusion. It has long been recognized that multicomponent interdiffusion differs substantially from binary diffusion[38]. For example, diffusion in multicomponent solutions is "coupled", which means that a gradient in the concentration of a component causes diffusional flows of other components in the mixture. Interdiffusion in a 3-component system (ternary interdiffusion) consisting of solvent and solutes 1 and 2 is described by the equations

$$J_1 = -D_{11}\nabla C_1 - D_{12}\nabla C_2 \tag{1.3}$$

$$J_2 = -D_{21}\nabla C_1 - D_{22}\nabla C_2 \tag{1.4}$$

where J_1, J_2 and ∇C_1, ∇C_2 are the fluxes and gradients in concentration of the solute components. D_{11} and D_{22} are the "main" diffusion coefficients which give the fluxes of components 1 and 2 down their own gradients. D_{12} and D_{21} are cross-diffusion coefficients which measure the coupled flux of component 1 caused by the gradient in component 2, and *vice versa*. Cross-diffusion coefficients can be especially large for associating solutes or for mixed electrolytes which interact electrostatically[39,40]. In some cases a diffusing solute can produce fluxes of other solutes which exceed its own flux[41,42]. It is not uncommon for components to diffuse against their concentration gradients, from regions of lower to higher

concentration. The electric field generated by the diffusion of macroions together with mobile counterions can drive especially large coupled flows of supporting electrolytes. In aqueous solution of proteins containing added salt, for instance, each mole of diffusing protein can cotransport hundreds of moles of salt[43].

Interdiffusion in Micellar Solutions and Microemulsions In solutions of micellar electrolytes, such as aqueous sodium dodecylsulfate (SDS), the mobilities of the micelles and counterions differ widely. As a result, diffusion of micellar electrolytes will generate a relatively large electric field which can drive substantial coupled flows of added salt. In previous studies, however, diffusion of micellar electrolytes in salt solutions was often treated as a binary process[14-16,34-37,44,45]. The neglect of coupled diffusion led to a scatter in the diffusivities reported for SDS in aqueous NaCl solutions[15]. It was not until 1986[46] that the importance of coupled diffusion in aqueous SDS/NaCl solutions was recognized, and models were developed for the diffusion of ionic micelles in salt solutions.

So far there have been few studies of multicomponent interdiffusion in microemulsion systems, in spite of the practical importance and potentially interesting features of transport in these systems. Except for a pioneering study by Vitagliano *et al.*[47], interdiffusion in microemulsions has always been treated as a pseudo-binary process, despite the presence of at least three different components: oil, water, and surfactant. Vitagliano *et al.*[48] used Gouy interferometry to measure ternary diffusion in a water-in-oil microemulsion prepared from water, AOT(sodium bis(2-ethylhexyl) sulfosuccinate), and heptane. The AOT surfactant was found to cotransport large amounts of water. In the Gouy experiments, diffusion coefficients were calculated from the pattern of interference fringes produced when a beam of monochromatic light passes through the gradient in refractive index produced by concentration gradients in a column of solution. Unfortunately, unwanted convection was frequently produced by density inversions resulting from the upward coupled diffusion of a denser component or the downward coupled diffusion of a less-dense component[49-56]. As a result of the gravitational instability problems, diffusion coefficients were measured for only one composition of the water/AOT/heptane microemulsion system.

Although the main features of multicomponent diffusion in solutions of micelles + salt are understood, no models are yet available to describe interdiffusion in microemulsions or micelles + solubilizate solutions. Understanding mass transport in micellar solutions and microemulsions is still a considerable challenge.

Objectives of this Thesis The Taylor dispersion technique[57-60] has been successfully employed in previous studies to determine diffusion coefficents for a wide range of systems, including binary and multicomponent solutions[61-74]. In a Taylor diffusion experiment, samples of solution are injected into a laminar carrier solution of different composition flowing in a long capillary tube. Diffusion coefficients are calculated from the refractive-index profiles across the dispersed sample peaks at the tube outlet. This technique is rapid, convenient, and capable of good accuracy (1-2% error in D). Because diffusion occurs in fine-bore tubing, Taylor dispersion measurements are free of errors from gravitational instabilities. The purpose of the work reported in this thesis is to extend the Taylor dispersion technique to studies of multicomponent diffusion in the ternary micellar solutions: aqueous SDS/NaCl, aqueous SDS/solubilized alcohol, and aqueous sodium cholate (SC)/solubilized alcohol. Ternary diffusion coefficients for the water-in-oil microemulsions water/AOT/heptane and water/2-propanol/hexane are also reported. The results, including cross-diffusion coefficients, provide new insights into the interactions between diffusing surfactants and solubilizates. In addition, new models are developed to describe interdiffusion in aqueous solutions of ionic surfactant/solubilizate and water-in-oil microemulsions.

1.3. Outline of this Thesis

A brief description of diffusion equations and surfactant solutions is given in Chapters 2 and 3, respectively. The Taylor dispersion technique employed in this thesis work is described in Chapter 4 after a brief review of the major methods for measuring interdiffusion coefficients. Ternary diffusion coefficients for aqueous sodium dodecylsulfate (SDS)/sodium chloride solutions are presented in Chapter 5. The Taylor results are compared with apparent micelle diffusion coefficients determined by light scattering, and the interesting descrepancies between the two sets of data are discussed.

Chapter 6 deals with the interdiffusion of *n*-alcohol solubilizates in aqueous SDS solutions. Based on the experimental results, a model is developed for the interdiffusion of solubilizates in solutions of ionic micelles. The new model takes into consideration changes in the extent of counterion binding and solubilization, as well as the electric field induced by diffusion of the charged species. To examine the wider applicability of the model, the interdiffusion of solubilizates in solutions of sodium cholate, an important ionic biosurfactant, are reported in Chapter 7. In Chapter 8, ternary interdiffusion coefficients are reported for water/AOT/heptane water-in-oil microemulsions over a wide range of concentration, and a size distribution model is developed to help interpret microemulsion diffusion behaviour. Ternary diffusion coefficients for water/2-propanol/hexane water-in-oil microemulsions are reported in Chapter 9. Finally, a summary of this thesis work is given in Chapter 10.

1.4. References

1. B. Lindman and B. Brun, *J. Colloid Interface Sci.*, **43**, 388 (1973)
2. P. Stilbs, *J. Colloid Interface Sci.*, **87**, 385 (1982); **89**, 547 (1982)
3. D. Langevin, *Annu. Rev. Chem.*, **43**, 341 (1992)
4. B. Lindman, P. Stilbs and M.E. Moseley, *J. Colloid Interface Sci.*, **83**, 569 (1981)
5. P. Nilsson and B. Lindman, *J. Phys. Chem.*, **86**, 271 (1982)
6. P. Guéring and B. Lindman, *Langmuir*, **1**, 464 (1985)
7. M.T. Clarkson, D. Beaglehole and P.T. Callaghan, *Phys. Rev. Lett.*, **54**, 1722 (1985)
8. B. Lindman, N. Kamenka, M.-C. Puyal, B. Brun and B. Jonsson, *J. Phys. Chem.*, **88**, 53 (1984)
9. D. Stigter, R.J. Williams and K.J. Mysels, *J. Phys. Chem.*, **59**, 330 (1955)
10. H. Fabre, N. Kamenka and B. Lindman, *J. Phys. Chem.*, **85**, 3493 (1981)
11. W.A. Wakeham, A. Nagashima and J.V. Sengers ed., *Measurement of the Transport Properties of Fluids*, Chapter 9, Blackwell Scientific Publications, London, 1991
12. H.J.V. Tyrrell and K.R. Harris, *Diffusion in Liquids: A Theoretical and Experimental Study*, Chapter 5 and 7, Butterworths, London, 1984
13. N.A. Mazer, G.B. Benedek and M.C. Carey, *J. Phys. Chem.*, **80**, 1076 (1976)

14. M. Corti and V. Degiorgio, *J. Phys. Chem.*, **85**, 711 (1981)

15. J.P. Kratohvil and T.M. Aminabhavi, *J. Phys. Chem.*, **86**, 1254 (1982)

16. A. Rohde and E. Sackmann, *J. Phys. Chem.*, **80**, 1598 (1980)

17. R. Finsey, A. Devrise and H.J. Lekkerker, *J. Chem. Soc. Faraday Trans. 2*, **76**, 767 (1980)

18. C. Hermansky and R.A. Mackay, *J. Colloid Interface Sci.*, **73**, 324 (1980)

19. H.M. Cheung, S. Qutubuddin, R.V. Edwards and J.A. Mann, *Langmuir*, **3**, 744 (1987)

20. E. Gulari, B. Bedwell and S. Alkhafaji, *J. Colloid Interface Sci.*, **77**, 202 (1980)

21. R. Zana and R.A. Mackay, *Langmuir*, **5**, 1242 (1989)

22. A. Berthod and J. Georges, *J. Colloid Interface Sci.*, **106**, 194 (1985)

23. P. Yeh and T. Kuwana, *J. Electrochem. Soc.*, **123**, 1334 (1976)

24. Y. Ohsawa, Y. Shimazaki and S. Aoyagui, *J. Electroanal. Chem.*, **114**, 235 (1980)

25. G.L. McIntire, D.M. Chiappardi, R.L. Casselberry and H.N. Blount, *J. Phys. Chem.*, **86**, 2632 (1982)

26. J. Georges and A. Berthod, *Electrochim. Acta*, **28**, 735 (1983)

27. J. Georges and S. Desmetre, *Electrochim. Acta*, **29**,521 (1984)

28. J. Georges and S. Desmetre, *J. Colloid Interface Sci.*, **118**, 192 (1987)

29. J. Texter, F.R. Horch, S. Qutubuddin and E. Dayalan, *J. Colloid Interface Sci.*, **135**, 263 (1990)

30. E. Dayalan, S. Qutubuddin and J. Texter, *J. Colloid Interface Sci.*, **143**, 423 (1991)

31. E. Dayalan, S. Qutubuddin and A. Hussam, *Langmuir*, **6**, 715 (1990)

32. R.A. Mackay, S.A. Myers, L. Bodalbhai and A. Brajter-Toth, *Anal. Chem.*, **62**, 1084 (1990)

33. A. C. Lam and Robert S. Schechter, *J. Colloid Interface Sci.*, **120**, 42 (1987)

34. V. Degiorgio and M. Corti, *J. Colloid Interface Sci.*, **101**, 289 (1984)

35. D.F. Evans, S. Mukherjee, D.J. Mitchell and B.W. Ninham, *J. Colloid Interface Sci.*, **93**, 184 (1983)

36. R.M. Weinheimer, D.F. Evans and E.L. Cussler, *J. Colloid Interface Sci.*, **80**, 357 (1981)

37. D.G. Leaist, *J. Colloid Interface Sci.*, **111**, 230 (1986)

38. E.L. Cussler, *Multicomponent Diffusion*, Elsevier Scientific Publishing Company, Amsterdam, 1976

39. L. Ambrosone, L. Paduano, R. Sartorio and V. Vitagliano, *J. Solution Chem.*, **22**, 1119 (1993)

40. V. Vitagliano, *Pure Appl. Chem.*, **63**, 1441 (1991)

41. E.L. Cussler and M.M. Breuer, *Nature*, **235**, 74 (1972)

42. E.L. Cussler, *AIChE J.*, **18**, 812 (1972)

43. D.G. Leaist, *J. Phys. Chem.*, **90**, 6600 (1986); **93**, 474 (1989)

44. A. Rohde and E. Sackmann, *J. Colloid Interface Sci.*, **70**, 494 (1979)

45. L.O. Sundelof, *J. Chem. Soc. Faraday Trans. 2*, **77**, 1779 (1981)

46. D.G. Leaist, *J. Colloid Interface Sci.*, **111**, 240 (1986)

47. L. Costantino, C. Della Volpe, O. Ortona and V. Vitagliano, *J. Colloid Interface Sci.*, **148**, 72 (1992)

48. L. Costantino, C. Della Volpe, O. Ortona and V. Vitagliano, *J. Chem. Soc. Faraday Trans.*, **88**, 61 (1992)

49. P.L. Vitagliano, C. Della Volpe and V. Vitagliao, *J. Solution Chem.*, **13**, 549 (1984)

50. D.G. Miller and V. Vitagliano, *J. Phys. Chem.*, **90**, 1706 (1986)

51. V. Vitagliano, G. Borriello, C. D. Vople and O. Ortona, *J. Solution Chem.*, **15**, 811 (1986)

52. L. Paduano, V. Vitagliano, C. D. Vople and L. Costantino, *J. Solution Chem.*, **21**, 623 (1992)

53. H.E. Huppert and M.A. Hallworth, *J. Phys. Chem.*, **88**, 2902 (1984)

54. C.F. Chen and D.H. Johnson, *J. Fluid Mech.*, **138**, 405 (1984)

55. J.S. Turner, *Annu. Rev. Fluid Mech.*, **17**, 11 (1985)

56. P.L. Vitagliano, L. Ambrosone and V. Vitagliano, *J. Phys. Chem.*, **96**, 1431 (1992)

57. G.I. Taylor, *Proc. Roy. Soc.*, **A219**, 186 (1953)

58. G.I. Taylor, *Proc. Phys. Soc.*, **B67**, 857 (1954)

59. R. Aris, *Proc. Roy. Soc.*, **A235**, 67 (1956)

60. W.E. Price, *J. Chem. Soc. Faraday Trans. 1*, **84**, 2431 (1988)

61. D.G. Leaist, *J. Chem. Soc. Faraday Trans.*, **87**, 597 (1991); **88**, 2897 (1992)

62. D.G. Leaist, *J. Phys. Chem.*, **94**, 5180 (1990)

63. Z. Deng and D.G. Leaist, *Can. J. Chem.*, **69**, 1548 (1991)

64. Z. Deng and D.G. Leaist, *J. Solution Chem.*, **21**, 15 (1992)

65. H. Lu and D.G. Leaist, *J. Chem. Soc. Faraday Trans.*, **87**, 3667 (1991)

66. D.G. Leaist and L. Hao, *J. Phys. Chem.*, **97**, 7763, 1464 (1993); **99**, 12896 (1995)

67. D.G. Leaist, *Can. J. Chem.*, **68**, 33 (1990)

68. D.G. Leaist, *Electrochimica Acta*, **36**, 309 (1991)

69. D.G. Leaist, L. Hao and R. Ibrahimov, *J. Chem. Soc. Faraday Trans.*, **89**, 515 (1993)

70. D.G. Leaist and L. Hao, *J. Chem. Soc. Faraday Trans.*, **89**,2775 (1993); **90**, 133 (1994); **91**, 2837 (1995)

71. D.G. Leaist, *J. Solution Chem.*, **20**, 175 (1991); **21**, 1035 (1992)

72. D.G. Leaist, *Ber. Bunsenges. Phys. Chem.*, **95**, 119 (1991)

73. D.G. Leaist and L. Hao, *J. Solution Chem.*, **23**, 263 (1993)

74. L. Hao and D.G. Leaist, *J. Solution Chem.*, **24**, 523 (1995)

Chapter 2

EQUATIONS FOR DIFFUSION IN LIQUIDS

2.1. Fick's Laws of Diffusion

Studies of diffusion appear to date back to Graham's pioneering work[1] on the diffusion of gases in the 1820s and 1830s. Studies of diffusion in liquids soon followed. The early experiments showed that diffusion in liquids was at least several orders of magnitude slower than diffusion in gases. In 1850 Fick made a crucial advance[1] by showing that the rate of diffusion of a substance is proportional to its concentration gradient.

$$J = -D\nabla C \tag{2.1}$$

J is the flux of substance in moles per unit area per unit time and C the concentration of diffusing substance in moles per unit volume. D, the diffusion coefficient, is a function of temperature and pressure as well as the concentration and the nature of the diffusing substance. Equation (2.1) is known as Fick's first law of diffusion.

By means of analogies with Fourier's work on the conduction of heat, Fick also developed the basic equation for "unsteady" diffusion (also called "transient" diffusion) in which the concentration of the diffusing substance changes with time along the diffusion path,

$$\frac{\partial C}{\partial t} = \nabla(D\nabla C) \tag{2.2}$$

If the changes in concentration are sufficiently small, the diffusion coefficient can be treated as a constant. Under these conditions equation (2.2) simplifies to

$$\frac{\partial C}{\partial t} = D\nabla^2 C \tag{2.3}$$

where D is the "differential" diffusion coefficient at concentration C. Equation (2.3) is often called Fick's second law. Fick's laws provide the foundation for the empirical description of diffusion processes.

2.2. Interdiffusion in Two-Component Mixtures — Binary Diffusion

Counterintuitively, the interdiffusion of two different chemical substances is described by a *single* diffusion coefficient. Consider binary diffusion in a system containing components 1 and 2, such as octanol(1) + water(2). According to Fick's first law, the fluxes of the two components in the volume-fixed frame of reference (laboratory coordinates) are given by

$$J_1 = -D_1 \nabla C_1 \tag{2.4}$$

$$J_2 = -D_2 \nabla C_2 \tag{2.5}$$

In this frame of reference the net flow of volume is zero:

$$J_1 V_1 + J_2 V_2 = 0 \tag{2.6}$$

V_1 and V_2 are the partial molar volumes of components 1 and 2, respectively. In view of the restriction imposed by equation (2.6), there is only one independent diffusion flux.

According to the definition of partial molar volumes (V_i), it follows that

$$C_1 V_1 + C_2 V_2 = 1 \tag{2.7}$$

At constant temperature and pressure, the Gibbs-Duhem equation gives

$$C_1 \nabla V_1 + C_2 \nabla V_2 = 0 \tag{2.8}$$

From equations (2.7) and (2.8) we get

$$V_1 \nabla C_1 + V_2 \nabla C_2 = 0 \tag{2.9}$$

and hence

$$V_1 = -\frac{\nabla C_2}{\nabla C_1} V_2 \tag{2.10}$$

Substituting equations (2.4), (2.5) and (2.10) into (2.6) gives

$$(D_1\nabla C_1)\left(\frac{\nabla C_2}{\nabla C_1}V_2\right) - (D_2\nabla C_2)V_2 = 0 \qquad (2.11)$$

which shows that

$$D_1 = D_2 = D \qquad (2.12)$$

Therefore, interdiffusion in a two-component mixture is described by a single diffusion coefficient, D.

2.3. Interpretation of the Binary Interdiffusion Coefficient

In 1876, Gibbs[2] made an important advance in the theory of diffusion by showing that the fundamental driving forces for diffusion are gradients in chemical potential, not concentration gradients. In 1931, Onsager[3] used the nonequilibrium thermodynamic relation

$$J = -L\nabla\mu \qquad (2.13)$$

to describe the flux of diffusing substance. $\nabla\mu$ is the gradient in chemical potential of the substance and L is the Onsager phenomenological coefficient.

To understand the physical meaning of the D and L coefficients, it is helpful to express the diffusion flux as

$$J = Cv \qquad (2.14)$$

where v is the diffusion speed of the solute. By using a mechanical analogy, the molar mobility, U_m, of a diffusing substance is defined as the ratio of its diffusion speed to the driving force[2],

$$U_m = -v/\nabla\mu = L/C \qquad (2.15)$$

From equations (2.1), (2.13) and (2.15) it is evident that

$$D = U_m \frac{\partial\mu}{\partial \ln C} \qquad (2.16)$$

Equation (2.16) shows that interdiffusion coefficients are products of both mobility (U_m) and thermodynamic ($\partial\mu/\partial\ln C'$) factors. The thermodynamic contribution to D is often overlooked.

2.4. Binary Interdiffusion in Nonelectrolyte Solutions

The chemical potential μ of a nonelectrolyte solute can be expressed as

$$\mu = \mu^0 + RT\ln\gamma C' \tag{2.17}$$

μ^0 is the standard chemical potential, R the gas constant, T the temperature, and γ the activity coefficient. Substituting equation (2.17) into (2.16) gives

$$D = RTU_m\left(1 + \frac{d\ln\gamma}{d\ln C'}\right) \tag{2.18}$$

As $C' \rightarrow 0$, $d\ln\gamma/d\ln C' \rightarrow 0$, and we get

$$D^0 = RTU_m^0 \tag{2.19}$$

where U_m^0 is the molar mobility of the solute in an infinitely dilute solution.

Stokes[4] derived an expression for the mobility U^0 of a spherical molecule in a continuum fluid:

$$U^0 = 1/6\pi\eta r \tag{2.20}$$

Stokes law can be used to relate the diffusion coefficients of a solute molecule to its effective molecular radius, r, and the solvent viscosity, η,

$$D^0 = RT/6\pi N\eta r = kT/6\pi\eta r \tag{2.21}$$

where N is the Avogadro constant and k is the Boltzmann constant. Equation (2.21), which is often called the Stokes-Einstein equation, is frequently used to estimate the size of a diffusing species. It holds reasonably well for molecules that are approximately spherical and much larger than the solvent molecules. In Chapters 8 and 9 of this thesis, the Stokes-Einstein equation is used to estimate the diffusion coefficients and sizes of microemulsion droplets.

2.5. Interdiffusion in Electrolyte Solutions

When dissolved in water, strong electrolytes dissociate into individual cations and anions. The diffusion of ionic species is coupled by the electric field which is generated by the diffusion of the ions with different mobilities. The diffusion-induced electric field slows down the more mobile ions and speeds up the slower ones so that all parts of the solution remain electrically neutral. The driving force for the diffusion of each ion is the gradient in its electrochemical potential rather than its chemical potential. The electrochemical potential of ion i, $\tilde{\mu}_i$, is defined as the sum of the ion's chemical potential μ_i and its electric potential energy $z_iF\phi$:

$$\tilde{\mu}_i = \mu_i + z_iF\phi = \mu_i^0 + RT\ln\gamma_i c_i + z_iF\phi \tag{2.22}$$

where c_i is the concentration of ion i in moles per unit volume, z_i its valence, F the Faraday constant, and ϕ the electric potential. The driving force for the diffusion of ion i is therefore

$$-\nabla\tilde{\mu}_i = -RT\nabla\ln\gamma_i c_i - z_iF\nabla\phi \tag{2.23}$$

According to the definition of electric field,

$$E = -\nabla\phi \tag{2.24}$$

equation (2.23) can be rewritten as

$$-\nabla\tilde{\mu}_i = -RT\nabla\ln\gamma_i c_i + z_iFE \tag{2.25}$$

In dilute solutions, the term $\nabla\ln\gamma_i$ is negligible, and equation (2.25) simplifies to

$$-\nabla\tilde{\mu}_i = -RT\nabla\ln c_i + z_iFE \tag{2.26}$$

The diffusion velocity of ion i, v_i, is proportional to the sum of the forces acting on the ion,

$$v_i = -u_i\nabla\tilde{\mu}_i = -u_iRT\nabla\ln c_i + u_iz_iFE \tag{2.27}$$

where u_i is the molar mobility of ion i. The flux of ion i is

$$j_i = c_i v_i = -RTu_i \nabla c_i + u_i c_i z_i FE \tag{2.28}$$

Recognizing that RTu_i is the diffusion coefficient of ion i gives

$$j_i = -D_i \nabla c_i + (F/RT) D_i c_i z_i E \tag{2.29}$$

This relation is the well known Nernst-Planck equation[5]. It will be used later in this thesis to develop a model for interdiffusion in aqueous solutions of ionic surfactants and solubilizates. The first term on the right side of equation (2.29) is the flux of ion i caused by "pure diffusion" of the ion down its concentration gradient. The second term is the flux of the ion driven by the diffusion-induced electric field.

2.6. Interdiffusion in Binary Electrolyte Solutions

Consider interdiffusion in a solution consisting of a solvent and a dissolved salt that dissociates into p cations and q anions:

$$M_pX_q = pM^{z+} + qX^{z-} \tag{2.30}$$

Although there are two kinds of ions, the cations and anions must diffuse at the same rate to keep the solution electrically neutral, $v_+ = v_- = v$:

$$v = -u_+(\nabla \mu_+ - z_+ FE) = - \quad '\mu_- - z_- FE) \tag{2.31}$$

Combination of equations (2.14), (2.15), and (2.31) with the expressions for the electroneutrality condition and the chemical potential of the electrolyte

$$pz_+ + qz_- = 0 \tag{2.32}$$

$$\mu = p\tilde{\mu}_+ + q\tilde{\mu}_- \tag{2.33}$$

gives

$$J = Cv = -\frac{u_+ u_-}{pu_- + qu_+} \frac{\partial \mu}{\partial \ln C} \nabla C = -D \nabla C \tag{2.34}$$

and hence

$$D = \frac{u_+ u_-}{pu_- + qu_+} \frac{\partial \mu}{\partial \ln C} \tag{2.35}$$

The chemical potential of the electrolyte is given by the expression

$$\mu = \mu^0 + RT\ln(\gamma_\pm^{p+q} c_+^p c_-^q) = \mu^0 + RT\ln[\gamma_\pm^{p+q} (pC)^p (qC)^q] \tag{2.36}$$

where $\gamma_\pm$ is the mean ionic molar activity coefficient of the electrolyte. For an infinitely dilute solution, $\partial \ln\gamma_\pm / \partial \ln C = 0$, and we obtain

$$\frac{\partial \mu}{\partial \ln C} = (p+q)RT\left(1 + \frac{\partial \ln \gamma_\pm}{\partial \ln C}\right) = (p+q)RT \tag{2.37}$$

Substituting the expression

$$\lambda_i^0 = |z_i| F^2 u_i^0 \tag{2.38}$$

for the limiting equivalent conductivity into equation (2.35) gives

$$D^0 = \frac{(p+q)\lambda_+^0 \lambda_-^0}{pz_+(\lambda_+^0 + \lambda_-^0)} \frac{RT}{F^2} \tag{2.39}$$

The limiting diffusion coefficients of ions are proportional to their mobilities

$$D_i^0 = RTu_i^0 \tag{2.40}$$

and hence

$$D_i^0 = \frac{\lambda_i^0 RT}{|z_i| F^2} \tag{2.41}$$

This equation is often used to estimate the diffusion coefficients of ions in solution from the limiting equivalent conductivities. It follows from equations (2.39) and (2.41) that

$$D^0 = \frac{(p+q) D_+^0 D_-^0}{q D_+^0 + p D_-^0} \tag{2.42}$$

This equation is often used to estimate the diffusion coefficient of an electrolyte in solution from known ion diffusion coefficients.

2.7. Ternary Interdiffusion in Liquids

As mentioned in Chapter 1, interdiffusion in a multicomponent solution differs from that in a binary system. For example, adding a third component to a binary mixture changes the rates of diffusion of other components in the mixture. In 1892, Arrhenius[6] observed that when hydrochloric acid diffused in an aqueous sodium chloride solution, the flux of the hydrogen ion was 80% faster than that of the diffusion of hydrochloric acid in pure water. He correctly related this result to electrostatic coupling between the diffusing ions. In fact, any kind of interaction between components diffusing in a multicomponent system generates coupled fluxes. In 1945 Onsager developed generalized Fick's laws to describe multicomponent interdiffusion[1]:

$$J_i = -\sum_k D_{ik} \nabla C_k \tag{2.43}$$

$$\frac{\partial C_i}{\partial t} = \sum_k D_{ik} \nabla^2 C_k \tag{2.44}$$

J_i and C_k denote the flux of component i and the concentration of component k, respectively. In a three-component (ternary) system, there are 3 fluxes (J_0, J_1, J_2), but only two fluxes are independent because of the volume-fixed constraint

$$J_0 V_0 + J_1 V_1 + J_2 V_2 = 0 \tag{2.45}$$

The subscript 0 denotes the most abundant component, usually the solvent. From these considerations it follows that the interdiffusion of solutes 1 and 2 in a solvent (0) is described by the coupled equations

$$J_1 = -D_{11} \nabla C_1 - D_{12} \nabla C_2 \tag{2.46}$$

$$J_2 = -D_{21} \nabla C_1 - D_{22} \nabla C_2 \tag{2.47}$$

$$\frac{\partial C_1}{\partial t} = D_{11} \nabla^2 C_1 + D_{12} \nabla^2 C_2 \tag{2.48}$$

$$\frac{\partial C_2}{\partial t} = D_{21} \nabla^2 C_1 + D_{22} \nabla^2 C_2 \tag{2.49}$$

Equations (2.48) and (2.49) hold if the changes in concentration along with diffusion path are sufficiently small. In this thesis equations (2.45) through (2.49) are used to describe ternary interdiffusion in the micellar solutions and microemulsions.

The diagonal terms D_{11} and D_{22} are called *main* diffusion coefficients. They measure the flux of each component produced by its own concentration gradient. The off-diagonal terms D_{12} and D_{21}, which are called *cross*-diffusion coefficients, give the flux of each component caused by the gradient in the concentration of the other component. Non-zero values for cross-coefficient D_{12} or D_{21} indicate that diffusing components interact. In general, the matrix $\boldsymbol{D}$ of multicomponent diffusion coefficients is not symmetric i.e., $D_{12} \neq D_{21}$. Studies of multicomponent interdiffusion in micellar solutions and microemulsions could provide new insights into the interaction of the components in these solutions.

2.8. Multicomponent Interdiffusion in Electrolyte Solutions

For interdiffusion in electrolyte solutions, as discussed in Section 2.5., the diffusion-induced electric field slows down the more mobile ions and speeds up the slower ones so that all parts of the solution remain electrically neutral. As a result, diffusion of mixed electrolytes is strongly coupled by the diffusion-induced electric field.

Surprisingly, the electric field can also produce coupled flows of uncharged molecules. Consider the diffusion of octanol solubilized in sodium dodecylsulfate (SDS) micellar solutions. In this case there are many different solute species: free octanol molecules as well as ionic species such as Na^+, DS^-, $(Na^+)_m(DS^-)_n^{m-n}$, and $(Na^+)_m(DS^-)_n(ROH)_p^{m-n}$. Here, m, n, and p are stoichiometric variables to represent a series of micellar species. Because the solubilized portion of the octanol is transported in charged micellar species, a coupled flux of octanol is driven by the diffusion-induced electric field. Nernst-Planck equations are extremely useful in such cases because they provide a detailed model of diffusion for any number of different solute species and association equilibria.

Although a multicomponent solution may contain many different solute species, the diffusion of only a few components may be independent. In such cases Fick's laws provide a more convenient and concise description of diffusion in terms of the fluxes of independent solute components, such as total octanol and total SDS. If Nernst-Planck equations are

combined with multicomponent Fick equations, the D_{ik} coefficients for the total components can be estimated in terms of the concentrations and diffusion coefficients of the constituent species that actually diffuse in the solution[7].

The fluxes of the total solute components, J_i, used in the Fick equations can always be expressed as simple linear combination of the fluxes of the constituent species, j_s.

$$J_i = \sum_s \nu_{is} j_s \tag{2.50}$$

ν_{is} gives the number of moles of diffusing solute component i contributed per mole of species s. According to the Nernst-Planck equation (2.29), the flux of solute species s is the sum of the purely diffusional flux $j_{s(D)}$ caused by the gradient ∇c_s in the concentration of that species plus the flux $j_{s(E)}$ driven by the diffusion-induced electric field:

$$j_s = j_{s(D)} + j_{s(E)} \tag{2.51}$$

$$j_{s(D)} = -D_s \nabla c_s \tag{2.52}$$

$$j_{s(E)} = (F/RT) z_s c_s D_s E \tag{2.53}$$

The multicomponent Fick diffusion coefficient D_{ik} gives the flux of component i caused by the gradient in the concentration of component k:

$$D_{ik} = -J_i / (\nabla C_k)_{C_{m \neq k}} \tag{2.54}$$

If there is no external electric field applied to the solution, the zero-current must be satisfied

$$\sum_s z_s j_s = 0 \tag{2.55}$$

and hence

$$\sum_s z_s j_{s(E)} = -\sum_s z_s j_{s(D)} = \sum_s z_s D_s \nabla c_s \tag{2.56}$$

To simplify the equations, it is convenient to define the transference number t_s of species as the fraction of the total electric current carried by species s

$$t_i = z_i j_{i(E)} \Big/ \sum_i z_i j_{i(E)} \tag{2.57}$$

Substitution of equations (2.53) and (2.56) into equation (2.57) gives

$$j_{i(E)} = (t_i/z_i)\sum_h z_h D_h \nabla c_h \tag{2.58}$$

which allows the Nernst-Planck equations to be rewritten as

$$j_i = -D_i \nabla c_i + (t_i/z_i)\sum_h z_h D_h \nabla c_h \tag{2.59}$$

Notice that the electric field has been expressed in terms of the concentration gradients and diffusion coefficients of the species.

Substitution of equations (2.50) and (2.59) into equation (2.54) gives

$$D_{ik} = \frac{\sum_i \nu_{is}\left[D_i (\nabla c_i)_{C_{mst}} - (t_s/z_s)\sum_h z_h D_h (\nabla c_h)_{C_{mst}} \right]}{(\nabla C_k)_{C_{mst}}} \tag{2.60}$$

which simplifies to

$$D_{ik} = \sum_i \nu_{is}\left[D_i (\partial c_i/\partial C_k)_{C_{mst}} - (t_s/z_s)\sum_h z_h D_h (\partial c_h/\partial C_k)_{C_{mst}} \right] \tag{2.61}$$

This result shows that multicomponent diffusion coefficients can be estimated in terms of the diffusion coefficients, concentrations and charges of the solute species. Also, the interdiffusion coefficients can be decomposed

$$D_{ik} = D_{ik(D)} + D_{ik(E)} \tag{2.62}$$

into the contribution $D_{ik(D)}$ from pure diffusion down concentration gradients:

$$D_{ik(D)} = \sum_i \nu_{is} D_s \frac{\partial c_s}{\partial C_k} \tag{2.63}$$

and the contribution $D_{ik(E)}$

$$D_{ik(E)} = -\sum_h \sum_s \frac{\nu_{sh} t_h}{z_h} z_i D_s \frac{\partial c_s}{\partial C_k} \tag{2 64}$$

from the migration of charged species in the diffusion-induced electric field. Equations (2.50) through (2.64) are used to discuss interdiffusion in sodium dodecylsulfate/solubilized alcohol and sodium cholate/solubilized alcohol solutions, as presented in Chapters 6 and 7.

2.9. References

1. E.L. Cussler, *Diffusion: Mass Transfer in Fluids Systems*, Chapter 2 and 6-8, Cambridge University Press, London, 1984

2. D.G. Leaist, *Encyclopedia of Applied Physics*, Vol. 5, G.L. Trigg ed., VCH Publishers, Inc., 1992, p. 61-74

3. L. Onsager, *Phys. Rev.*, **37**, 405 (1931); **38**, 2265 (1931)

4. G.G. Stokes, *Mathematical and Physical Papers*,Vol. 3, Cambridge University Press, London, 1903

5. A.J. Bard and L.R. Faulkner, *Electrochemical Methods: Fundamentals and Applications*, Wiley, New York, 1980

6. E.L. Cussler, *Multicomponent Diffusion*, Elsevier Scientific Publishing Company, Amsterdam, 1976

7. D.G. Leaist and L. Hao, *J. Chem Soc. Faraday Trans.*, **89**, 2775 (1993)

Chapter 3

MICELLES AND MICROEMULSIONS

As shown by the equations summarized in Chapter 2, diffusion coefficients are products of both mobility and thermodynamic factors. A basic knowledge of these factors is helpful in order to interpret the interdiffusion coefficients in microemulsions and micellar solutions.

3.1. Chemical Equilibrium in Micellar Solutions

Surfactants tend to adsorb at interfaces and lower interfacial surface tensions[1]. A surfactant molecule or ion contains a nonpolar hydrophobic group and a polar hydrophilic group. A good example is sodium dodecylsulfate (SDS), an anionic surfactant. The dodecylsulfate ion consists of a nonpolar hydrophobic alkyl chain ($C_{12}H_{25}$-) and a polar hydrophilic sulfate group (-OSO_3^-). Often the hydrophilic part of a surfactant molecule or ion is called the *head* and the hydrophobic part - usually an alkyl chain - is called the *tail*. Surfactants are usually classified on the basis of the charge carried by the polar head group as *anionic*, *cationic*, *nonionic*, or *zwitterionic*. *Lecithin*, *cephalin*, and *bile acids* are important examples of *biosurfactants*.

In addition to their ability to adsorb at various interfaces (liquid/gas, liquid/liquid, liquid/solid), many dissolved surfactants spontaneously aggregate by self-association above a narrow concentration range. Aggregates of surfactant monomers are called micelles, and the concentration above which micelles form is called the *critical micelle concentration* (cmc). The formation of micelles is energetically favoured because of the reduction of the hydrocarbon-water surface area. This is often explained in terms of the "hydrophobic effect".

Many books[2-4], conference proceedings[5-10], review articles[11,12], and scientific papers[13-23] on micelle formation have been published. There are two widely-accepted models for the thermodynamic description of surfactant aggregation: the pseudo-phase separation model and the chemical equilibrium model. The phase separation model

assumes that micelles are microdroplets of a separate phase dispersed in a continuous bulk solution phase, while the chemical equilibrium model regards micelles as chemical species formed by the association of multiple surfactant monomers. Both models show advantages in describing certain properties of micellar solutions, but they cannot cover all aspects of surfactant solutions. Although many reports on micelle formation and solubilization into micelles favour the phase separation model[13-17], both models are useful in discussions of diffusion in micellar solutions and microemulsions and both models will be used in this thesis to interpret the diffusion behaviour of multicomponent surfactant solutions.

3.2. Micelles

3.2.1. The Chemical Equilibrium Model

Nonionic Micelles Consider a simple association equilibrium between surfactant monomers (S_1) and micelles (S_n) of aggregation number n. For monodisperse micelles of a nonionic surfactant, the micellization process can be described as follows.

$$nS_1 \rightleftharpoons S_n \tag{3.1}$$

The equilibrium constant, K_n, for the formation of monodisperse micelles of aggregation number n is given by

$$K_n = a_n / a_1^n \tag{3.2}$$

where a_n and a_1 are the activities of micelles and surfactant monomers, respectively. For dilute solutions, the activities can be replaced by the corresponding concentrations, c_n and c_1, and equation (3.2) becomes

$$K_n = c_n / c_1^n \tag{3.3}$$

Ionic Micelles For the formation of micelles in ionic surfactant solutions, counterion binding must be taken into consideration. For a 1-1 ionic surfactant, such as sodium dodecylsulfate (SDS), the following equilibrium is used to describe the micellization process:

$$m\mathrm{Na}^+ + n\mathrm{DS}^- \rightleftharpoons \mathrm{Na}_m(\mathrm{DS})_n^{(m-n)} \tag{3.4}$$

where m and n are the number of sodium counterions and dodecylsulfate surfactant ions per micelle. Accordingly, the micellization constant K_{mn} is written as

$$K_{mn} = \frac{c_{Na_m(DS)_n^{(m-n)}}}{c_{Na}^{m} c_{DS}^{n}} \tag{3.5}$$

for the formation of monodisperse micelles in ionic surfactant solutions.

The chemical equilibrium model stresses the interactions of associating species in surfactant solutions. This model will be used to develop the new models for interdiffusion in micellar solutions and microemulsions.

3.2.2. The Phase Separation Model

It is well known that the concentration dependence of the refractive index, conductivity, surface tension, and other solution properties change suddenly in the vicinity of cmc. Analogous behaviour is observed at phase transitions. A stronger case can be made for the treatment of micellar solutions as two-phase systems by noting that surfactant micelles resemble microdroplets of a "w" phase dispersed in the bulk solution "main" phase. The equilibrium distribution of molecules or ions i between the micelle and bulk solution pseudo-phases can be expressed in the form

$$K_i = \frac{c_i^{(m)}}{c_i^{(b)}} \tag{3.6}$$

where K_i is the distribution equilibrium constant of component i, $c_i^{(m)}$ the concentration of component i in moles per unit volume of micellar phase, and $c_i^{(b)}$ the concentration of component i in moles per unit volume of the continueous phase. The distribution of each component in different phases directly influences its own interdiffusion coefficient as well as the interdiffusion coefficients of the other components.

3.3. Structures of Micelles

Depending on the total surfactant concentration, six different surfactant phases have been observed, each with a different structure of the surfactant aggregates[24]. The isotropic micellar phase exists at low surfactant concentrations. At higher surfactant concentrations, cylindrical, cubic, hexagonal liquid crystalline, and lamellar (normal or reverse) phases

Figure 3-1 Schematic diagram of the different structures of surfactant aggregates

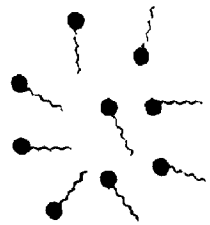

Surfactant Monomers

Spherical Micelles

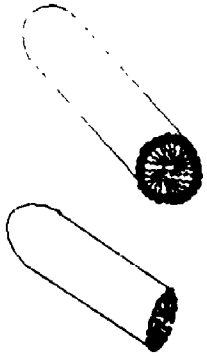

Cylindrical Micelles

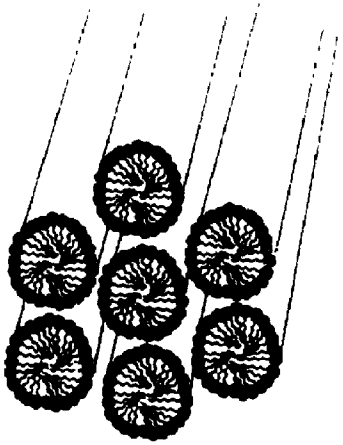

Hexagonal Phase

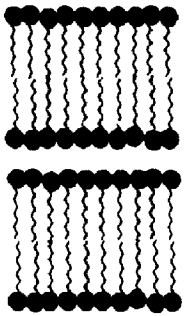

Lamellar Phase

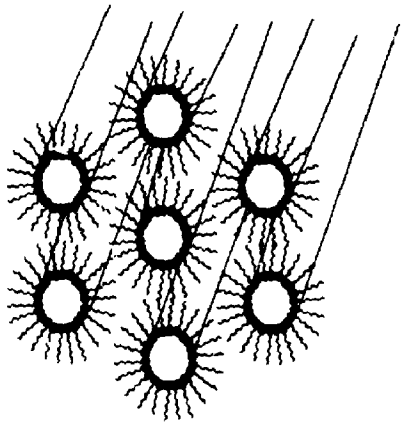

Reverse Hexagonal Phase

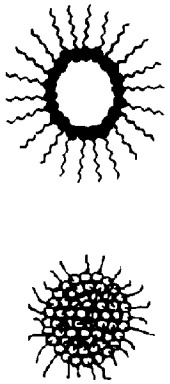

Reverse Spherical Micelles

exist (see Figure 3-1). Small-angle neutron scattering experiments on dilute solutions of sodium dodecylsulfate and other ionic micelles[25,26] support the spherical micelle model developed by Reich[27]. The spherical micelle model is adopted in this thesis because the solutions studied here are sufficiently dilute.

Solubilization is one of the most striking features of micellar solutions. Many practical applications stem from solubilization, and it has important consequences for mass transport. There are three possible solubilization sites in a surfactant aggregate[28]. Taking a spherical micelle in an aqueous solution as an example, hydrocarbons and other nonpolar compounds are thought to be incorporated primarily into the micelle interior, forming swollen micelles or microemulsion droplets (Figure 3-2a). Some solubilizate molecules may insert between two surfactant head groups in the "palisade" layer (Figure 3-2b). Polar solubilizate molecules may adsorb on the micellar surface (Figure 3-2c).

3.4. Microemulsions

Micelles are able to solubilize sparingly soluble compounds, leading to the formation of microemulsions. For example, benzene is almost insoluble in water but it can dissolve in the hydrocarbon cores of dodecylsulfate micelles. Similarly, water is almost insoluble in heptane, but it can dissolve in AOT-heptane mixtures. First, the water dissolves in the polar cores of AOT micelles, forming swollen micelles. The micelles increase in size as more water is added. Eventually the swollen micelles grow into microemulsion droplets. Micelles are therefore the precursors of microemulsions.

At present, there is no precise or commonly agreed upon definition of microemulsions. In fact, there has been much debate about term "microemulsion". Other terms, such as "swollen micelles" or "solubilized micelles", are prefered by some authors[28]. The debate focuses on distinguishing microemulsions from micellar solutions[29,30]. Historically, microemulsions were defined from a phenomenological viewpoint by the observation of a homogeneous, transparent, and low-viscosity system containing a considerable amount of dispersed phase and a stabilizing surfactant and possibly cosurfactant. At low volume fractions of the dispersed phase, however, the system closely resembles a true micellar solution. The transition between micelles and

Figure 3-2 Three possible sites for the incorporation of solubilizates into micelles

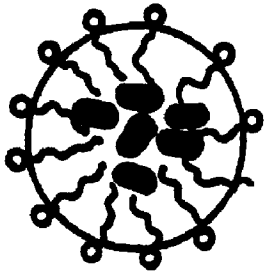

(a) Micelle Interior

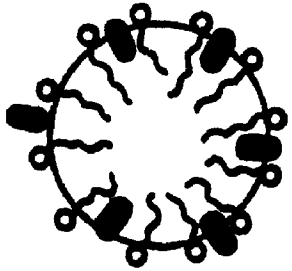

(b) Palisade Layer

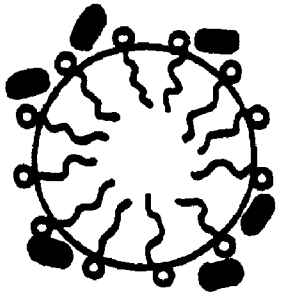

(c) Micellar Surface

Figure 3-3 Schematic diagram of oil-in-water and water-in-oil microemulsions stabilized by an interfacial film of surfactant and cosurfactant

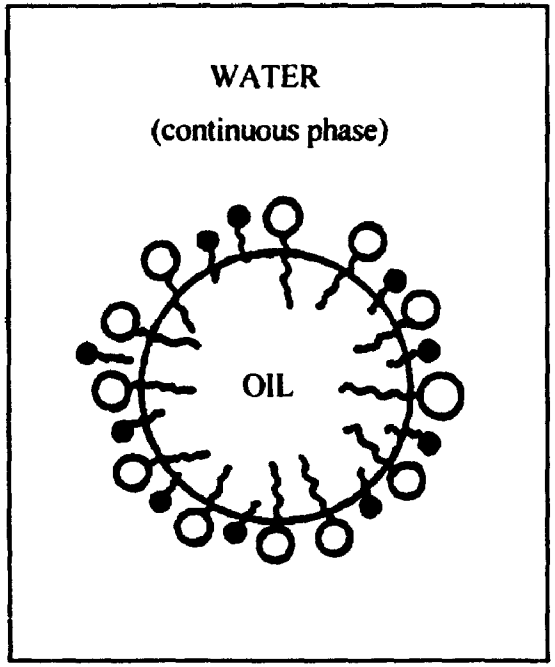

OIL-IN-WATER

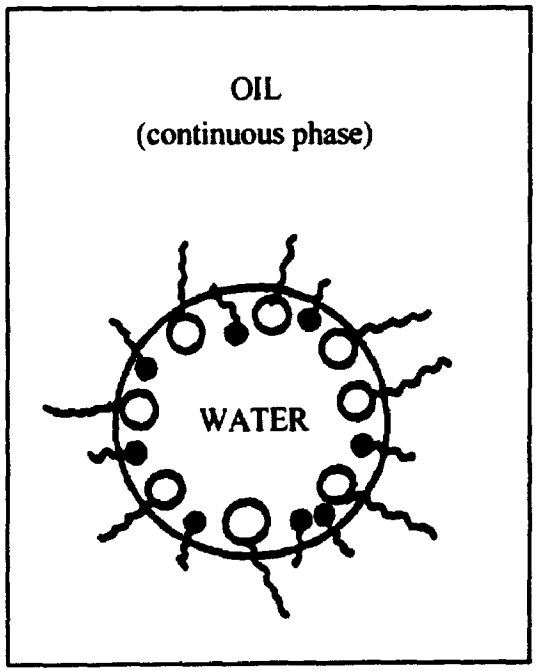

WATER-IN-OIL

microemulsions generally shows no apparent break in the concentration dependence of the system properties[31]. In some cases, however, it has been shown that the kinetics of solubilization of oil is much slower for oil-in-water microemulsions than for normal micelles[32].

In spite of the controversy mentioned above, microemulsions are usually defined as a thermodynamically stable, isotropically clear dispersion of two immiscible liquids, consisting of microdomains of one or both liquids stabilized by an interfacial film of surfactant[33]. Two kinds of microemulsions are commonly encountered: oil-in-water (o/w) and water-in-oil (w/o) globular droplets, as shown in Figure 3-3[28]. Theories dealing with the formation of microemulsions are available elsewhere[28,34] and will not be described here.

The stability of microemulsions is very important to our studies of interdiffusion. It should be noted, however, that microemulsion droplets are dynamic, not static aggregates. It has been shown[35-37] that the droplet dynamics are characterized by two relaxation times: t_1, which is related to the residence time of an individual surfactant molecule in a particular droplet; and t_2, which measures the lifetime of an entire droplet (the average time from the formation of a micelle to its decomposition). Although these relaxation times depend on a number of variables, such as the surfactant concentration and the molecular structure of the surfactant, t_1 is generally in the 10 ns to 1 ms range, and t_2 is usually in the 1 ms to 1 second range[35-37]. Even though macroscopic concentration gradients exist in microemulsion diffusion experiments, microemulsions are still locally in equilibrium because diffusion relaxation times are typically orders of magnitude larger than either t_1 or t_2.

3.5. References

1. M. Bender, *Interfacial Phenomena in Biological Systems*, Dekker, New York, 1991
2. C. Tanford, *The Hydrophobic Effect: Formation of Micelles and Biological Membranes*, Wiley, New York, 1973
3. M.J. Schick, *Nonionic Surfactants*, Dekker, New York, 1967
4. E. Jungermann, *Cationic Surfactants*, Dekker, New York, 1970

5. V. Degiorgio and M. Corti, *Physics of Amphiphiles: Micelles, Vesicles and Microemulsions*, Proceedings of the International School of Physics "Enrico Fermi", North-Holland, Amsterdam, 1985

6. K.L. Mittal and P. Bothorel, *Surfactants in Solution*, Plenum Press, New York, 1986

7. K.L. Mittal and B. Lindman, *Surfactants in Solution*, Plenum Press, New York, 1984

8. K.L. Mittal and E.J. Fendler, *Solution Behavoir of Surfactants: Theoretical and Applied Aspects*, Plenum Press, New York, 1982

9. K.L. Mittal, *Solution Chemistry of Surfactants*, Plenum Press, New York, 1979

10. K.L. Mittal, *Micellization, Solubilization, and Microemulsions*, Plenum Press, New York, 1977

11. H. Wennerstrom and B. Lindman, *Phys. Rep.*, **52**, 1 (1979)

12. L.R. Pratt, B. Owenson and Z. Sun, *Adv. Colloid Interface Sci.*, **26**, 69 (1986)

13. I.B.C. Matheson and A.D. King, Jr., *J. Colloid Interface Sci.*, **66**, 464 (1978)

14. W. Prapaitrakul and A.D. King, Jr., *J. Colloid Interface Sci.*, **106**, 186 (1985)

15. E. Ruckenstein and R. Krishnan, *J. Colloid Interface Sci.*, **71**, 321 (1979)

16. E.Lissi, E. Abuin and Z.N. Rocha, *J. Phys. Chem.*, **84**, 2406 (1980)

17. J.C. Ericksson, S. Ljunggren and U. Henriksson, *J. Chem. Soc. Faraday Trans. 2*, **81**, 833 (1985)

18. J.N. Phillips, *Trans. Faraday Soc.*, **51**, 561 (1955)

19. Y. Moroi, *Micelles: Theoretical and Applied Aspects*, Plenum Press, New York, 1992, p.58

20. Y. Moroi and Y. Sakamoto, *J. Phys. Chem.*, **92**, 5189 (1988)

21. H.N. Singh, S. Swarup and S.M. Saleem, *J. Colloid Interface Sci.*, **68**, 128 (1979)

22. E.J.R. Sudholter and J.B.F.N. Engberts, *J. Phys. Chem.*, **83**, 1854 (1979)

23. M.F. Emerson and A. Holtzer, *J. Phys. Chem.*, **71**, 1898 (1967)

24. M.J. Lawrence, Chem. Soc. Rev., **23**(6), 417 (1994)

25. J.B. Hayter and J. Penfold, *J. Chem. Soc. Faraday Trans. 1*, **77**, 1851 (1981)

26. D.W.R. Gruen, *J. Phys. Chem.*, **89**, 146 (1985); **89**, 153 (1985)

27. I. Reich, *J. Phys. Chem.*, **60**, 257 (1956)

28. Darsh T. Wasan, Martin E. Ginn and Dinesh O. Shah, *Surfactants in Chemical/Process Engineering*, Marcel Dekker, Inc., New York, 1988, p. 318-350

29. L.M. Prince, *J. Colloid Interface Sci.*, **52**, 182 (1975)

30. M.P. Pileni and S. Chevalier, *J. Colloid Interface Sci.*, **92**, 326 (1983)

31. H.F. Eicke, *Microemulsions*, I.D. Rodd ed., Plenum Press, New York, 1982, p. 17

32. D.B. Siano, *J. Colloid Interface Sci.*, **93**, 1 (1983)

33. Andrew C. Lam and Robert S. Schechter, *J. Colloid Interface Sci.*, **120**, 56 (1987)

34. P. Becher, *Surfactants in Solution*, Vol. 3, K.L. Mittal and B. Lindman eds., Plenum Press, New York, 1984, p.1925

35. P.A. Winsor, *Chem. Rev.*, **68**, 1 (1968)

36. E.A.G. Aniansson, S.N. Wall, M. Almgren, H. Hoffman, I. Killmann. W. Ulbricht, R. Zana, J. Lang and C. Tondre, *J. Phys. Chem.*, **80**, 905 (1976)

37. A.C. Lam and R.S. Schechter, *J. Colloid Interface Science*, **120**, 56 (1987)

Chapter 4

THE TAYLOR DISPERSION TECHNIQUE

4.1. Introduction

Many techniques are used to study diffusion in micellar solutions[1-14] and microemulsions[15-23]. NMR and capillary-tube techniques, the most popular methods, can be only used to measure intradiffusion coefficients. Other popular techniques, such as light-scattering and electrochemical methods[19-21], give apparent diffusion coefficients for micelles or microemulsion droplets rather than the true diffusion coefficients of the components defined by Fick's laws. Techniques that can be employed to determine interdiffusion coefficients are listed in Table 4-1[24].

Diaphragm-Cell Method In a diaphragm-cell experiment, dissolved substances diffuse from one solution compartment to another through a porous diaphragm, such as a filter paper or a sintered glass disc. This method can be used to measure intra- as well as inter-diffusion coefficients of micellar solutions[5] with high accuracy, but the experiments are time-consuming. Moreover, it is quite difficult to quantitatively determine the concentrations of the diffusing components in a multicomponent system. Because the sintered glass disc used in many diaphragm cells has large surface area, it can adsorb and immobilize surfactants. This would decrease the measured diffusion coefficients.

Conductimetric Method[25,26] In this technique, an initial concentration gradient is produced by injecting solution into the lower end of a short (3-6 cm) diffusion column. The rate of decay of the concentration gradient is followed by measuring the electrical conductivity across pairs of small platinum electrodes located near the top and bottom of the solution column. Interdiffusion coefficients are calculated from the rate of decay of the difference in conductivity measured at the upper and lower electrodes. This technique has been used to measure the interdiffusion coefficients of micellar solutions[13,19,27,28]. Despite the high accuracy of the conductimetric method (0.2%), this technique is limited to studies of interdiffusion in electrolyte solutions, and like diaphragm-cell experiments, the run times are inconveniently long (~ days).

Table 4-1 Experimental methods for the determination of the diffusion coefficients of liquids.

	Diffusion type			
Method	Intra-	Inter-	Accuracy	Experiment time
Diaphragm cell	Yes	Yes	Good (0.5-1%)	Days
Conductance	–	Yes	High (0.2%)	Days
Gouy	–	Yes	High (≤ 0.1%)	Hours
Rayleigh	–	Yes	High (≤ 0.1%)	Hours
QELS	–	Yes	Moderate (~5%)	Hours
Taylor dispersion	Yes	Yes	Moderate (1-2%)	Hours

Quasi-Elastic Light Scattering (QELS) QELS is based on the principle that fluctuations in the intensity of light scattered from a solution are related to microscopic fluctuations in the local composition which in turn are governed by interdiffusion coefficients. This technique is often used to study the interdiffusion of macromolecules and surfactant aggregates, which scatter light relatively efficiently[7-9,14,17,18,22]. This technique is convenient and immune to errors from convection. Moreover, it can be used to measure the polydispersity of macromolecules and aggregates. However, QELS does have some limitations. Because the intensity of light scattered by large molecules or ions usually overwhelms the intensity from smaller species, it is generally believed that QELS gives the diffusivity of the largest species in a solution, such as micelles or microemulsion droplets[29]. The work on aqueous SDS/NaCl solutions described in the following chapter shows that QELS measures the lowest eigenvalue of the interdiffusion coefficient matrix $\boldsymbol{D}$ instead of true multicomponent interdiffusion coefficients.

Gouy and Rayleigh Interferometry In Gouy and Rayleigh experiments, diffusion coefficients are calculated from the pattern of interference fringes produced when a beam of monochromatic light passes through a concentration gradient - and hence a refractive-index gradient - in a column of solution. High accuracy (0.1%) is the main advantage of interferometric techniques. In addition, they can be used to measure multicomponent interdiffusion coefficients. When applied to microemulsions[15,16], however, interferometric techniques are prone to gravitational instabilities and convection[30-33]. This undesirable behaviour is caused by density inversions produced when coupled diffusion drives a relative dense component upward into less dense solution, or *vice versa*.

Taylor Dispersion This technique has become increasingly popular for measuring diffusion in liquids, because of its convenience and short run times. In a dispersion experiment, a small amount of solution is injected into a laminar carrier stream of slightly different composition flowing in a long capillary tube. The injected sample spreads out into a nearly Gaussian profile as it flows along the tube. Diffusion coefficients are calculated from the shape of the eluted peak which can be measured with a flow-through differential refractometer or another suitable detector. Gravitational instabilities and unwanted convection are negligible because the carrier stream is confined to narrow-bore capillary

tubing. Recently, this technique has been extended to measure the interdiffusion coefficients[12,13,34-36] of multicomponent solutions.

4.2. The Principle of Taylor Dispersion Technique

The theoretical description of dispersion in a laminar carrier stream in a capillary tube was provided by Taylor in 1950s[37]. His mathematical treatment related the dispersion of a pulse of soluble substance in a solvent to a dispersion coefficient. Aris[38] worked out a more general solution to the dispersion problem. Alizadeh *et al.*[39] have discussed in detail the application of Taylor dispersion to diffusion measurements.

4.2.1. Binary Diffusion

When a solute is injected into a laminar carrier stream of solvent, the solute near the center of the tube flows more rapidly than the solute near the tube wall. Consequently, the injected solute spreads out as it flows along the tube, as shown in Figure 4-1. The dispersion process is governed by the equation[37]

$$\frac{\partial C}{\partial t} = K\nabla^2 C \tag{4.1}$$

where K is a dispersion coefficient and C is the radially-averaged solute concentration in the frame of reference moving at the average speed u of the carrier stream. Equation (4.1) bears a striking resemblance to Fick's equation for transient diffusion.

Aris[38] showed that the dispersion coefficient is given by

$$K = D + \frac{r^2u^2}{48D} \tag{4.2}$$

where r is the inner radius of the capillary tube. For liquid-phase diffusion, the term $r^2u^2/48D$ is usually several orders of magnitude larger than D, and hence

$$K = \frac{r^2u^2}{48D} \qquad \text{(liquids)} \tag{4.3}$$

Equation (4.1) can be solved to give the radially-averaged concentration of the dispersed substance at the tube outlet, a distance L downstream from the point of injection:

Figure 4-1 Schematic description of Taylor dispersion of solution injected into a carrier stream in a capillary tube

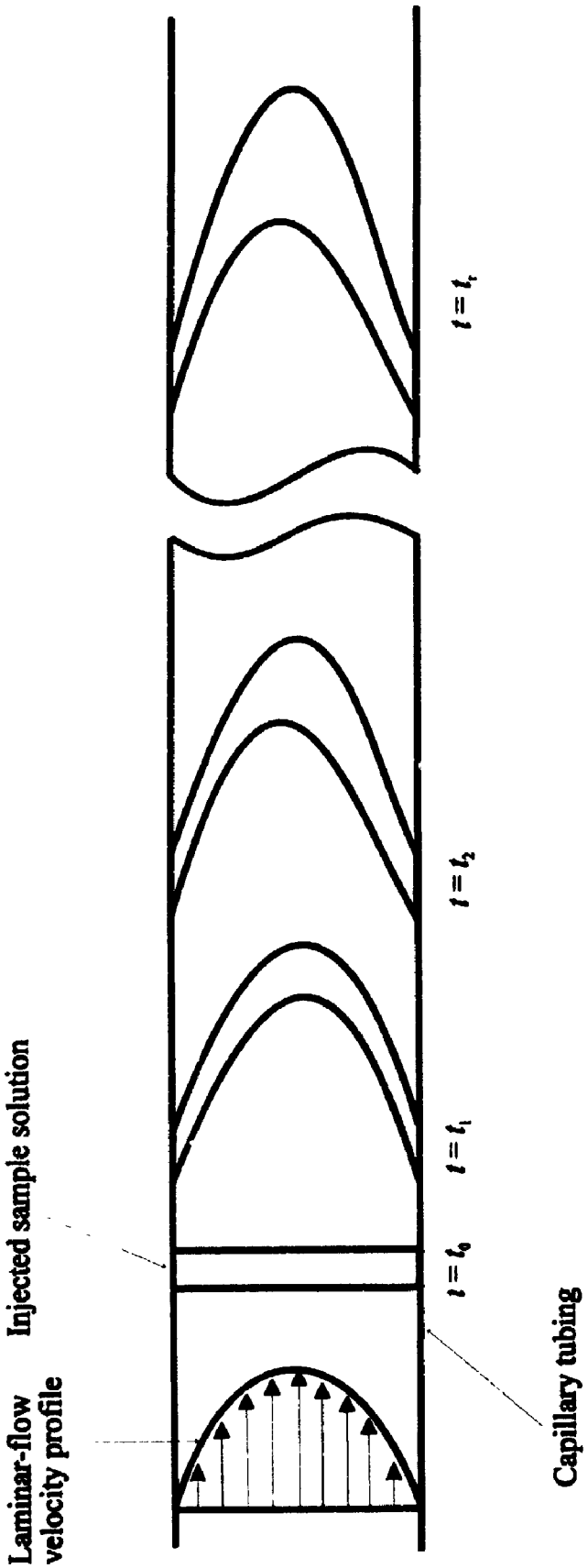
Laminar-flow velocity profile
Injected sample solution
Capillary tubing
t = t0
t = t1
t = t2
t = tf

$$C(t) = \bar{C} + \frac{\Delta C' \Delta V}{\pi r^2 u}\sqrt{\frac{12D}{\pi t}}\exp\left[-\frac{12D(t-t_r)^2}{r^2 t}\right] \quad (4.4)$$

where t_r is the retention time defined by

$$t_r = L/u \quad (4.5)$$

ΔV is the volume of the injected sample of solution, $\Delta C'$ the difference in concentration between the injected solution and the carrier stream, $\bar{C}$ the background concentration of the carrier stream. Equation (4.4) shows that the excess injected solute spreads out into a Gaussian distribution of variance $r^2t_r/24D$ as it flows along the capillary tube since $12D(t-t_r)^2/r^2t \approx 12D(t-t_r)^2/r^2t_r$ across the solute peak. Equation (4.4) is valid provided $D << r^2u^2/48D$ and longitudinal diffusion is negligible[40]:

$$L/u >> 0.8r^2/D \quad (4.6)$$

It is difficult in practice to measure the concentration of the eluted solute directly. Instead, the broadened distribution of solute is usually followed by using a liquid-chromatography flow-through detector at the tube outlet. The output voltages of these detectors vary in proportion to changes in the refractive index, conductivity, or UV absorbance of the eluted solution.

In this study, sensitive differential refractometers are used as detectors. The refractometer output voltage $V(t)$ and the refractive index of the eluted solution $n(t)$ are related as follows

$$V(t) = a_0 + a_1 t + s[n(t) - \bar{n}] \quad (4.7)$$

where s is the detector sensitivity, and $\bar{n}$ is the refractive index of the carrier solution at concentration $\bar{C}$. The linear baseline voltage $a_0 + a_1t$ is included in practice to allow for small drifts in the refractometer signal. The refractive index difference $n(t) - \bar{n}$ along the diffusion path is a function of the concentration of the solute:

$$n(t) - \bar{n} = R[C(t) - \bar{C}] \quad (4.8)$$

where $R = \partial n/\partial C$. Combining equations (4.4), (4.7) and (4.8) yields

$$V(t) = a_0 + a_1 t + V_{max}(t_r/t)^{1/2} \exp\left[-\frac{12D(t-t_r)^2}{r^2 t}\right] \quad (4.9)$$

where V_{max} is the peak height given by

$$V_{max} = sR\frac{\Delta C \Delta V}{\pi r^3 u}\sqrt{\frac{12D}{\pi t_r}} \quad (4.10)$$

a_0, a_1, V_{max}, t_r and D are determined by using least squares to fit equation (4.9) to the measured detector voltages[41].

4.2.2. Ternary Diffusion

It was not until 1988 that Price[42] developed the theory of Taylor dispersion for three-component systems. Consider a ternary carrier solution containing solutes 1 and 2 at concentrations $\bar{C}_1$ and $\bar{C}_2$. At time $t = 0$ a small volume ΔV of solution of composition $\bar{C}_1 + \Delta C_1$ and $\bar{C}_2 + \Delta C_2$ is injected into the carrier stream. Price showed that the radially-averaged concentrations $C_i(t)$ of the dispersed solutes at the tube outlet can be expressed as follows.

$$C_i(t) = \bar{C}_i + \left(\frac{2}{\pi r^3 u}\right)\left(\frac{3}{\pi t}\right)^{1/2}\sum_{k=1}^{2} B_{ik} D_k^{1/2} \exp\left[-\frac{12D_k(t-t_r)^2}{r^2 t}\right] \quad (i = 1, 2) \quad (4.11)$$

where D_1 and D_2 are the eigenvalues of the 2×2 matrix $\boldsymbol{D}$ of the ternary diffusion coefficients

$$D_1 = [D_{11} + D_{22} + (D_{11} - D_{22})[1 + (\frac{4D_{12}D_{21}}{(D_{11}-D_{22})^2})]^{1/2}]/2 \quad (4.12)$$

$$D_2 = [D_{11} + D_{22} - (D_{11} - D_{22})[1 + (\frac{4D_{12}D_{21}}{(D_{11}-D_{22})^2})]^{1/2}]/2 \quad (4.13)$$

The B_{ik} coefficients are abbreviations for

$$B_{11} = \Delta V[(D_{22} - D_1)\Delta C_1 - D_{12}\Delta C_2]/(D_2 - D_1) \quad (4.14)$$

$$B_{12} = \Delta V[(D_{22} - D_2)\Delta C_1 - D_{12}\Delta C_2]/(D_1 - D_2) \quad (4.15)$$

$$B_{21} = \Delta V[(D_{11} - D_1)\Delta C_2 - D_{21}\Delta C_1]/(D_2 - D_1) \quad (4.16)$$

$$B_{22} = \Delta V[(D_{11} - D_2)\Delta C_2 - D_{21}\Delta C_1]/(D_1 - D_2) \quad (4.17)$$

Equation (4.11) is valid provided eigenvalues D_1 and D_2 satisfy the following condition[41]

$$\frac{0.8r^2}{D_i} < t_r < \frac{Lr}{50D_i} \quad (4.18)$$

The broadened distribution of the solutes can be followed by measuring the refractive index profile $n(t)$ across the eluted sample peak:

$$n(t) = \bar{n} + R_1[C_1(t) - \bar{C}_1] + R_2[C_2(t) - \bar{C}_2] \quad (4.19)$$

where $R_1 = \partial n/\partial C_1$ and $R_2 = \partial n/\partial C_2$ are the molar refractivities of the solutes at the carrier-stream composition $\bar{C}_1$, $\bar{C}_2$. Equations (4.11), (4.14) - (4.17), and (4.19) lead to the expression

$$V(t) = a_0 + a_1 t + V_{max}(t_r/t)^{1/2}[W_1\exp(-\frac{12D_1(t-t_r)^2}{r^2 t}) + (1 - W_1)\exp(-\frac{12D_2(t-t_r)^2}{r^2 t})] \quad (4.20)$$

for the detector voltage, where W_1 and $1 - W_1$ are the normalized weights of the exponential terms

$$W_1 = \frac{(a+b\alpha_1)D_1^{1/2}}{[(a+b\alpha_1)D_1^{1/2} + (1-a-b\alpha_1)D_2^{1/2}]} \quad (4.21)$$

and

$$\alpha_1 = R_1\Delta C_1/(R_1\Delta C_1 + R_2\Delta C_2) \quad (4.22)$$

is the fraction of the initial refractive index difference due to solute 1. Parameters a and b are constants for a given system and carrier stream composition. According to equation (4.20), the detector signals for ternary c fusion resemble two overlapping Gaussians, centred on t_r, with variances $r^2t_r/24D_1$ and $r^2t_r/24D_2$.

Fitting equation (4.20) to the measured detector voltages gives the values of a, b, D_1 and D_2, from which the D_{ik} coefficients can be calculated:

$$D_{11} = D_1 + [a(1 - a - b)/b](D_1 - D_2) \quad (4.23)$$

$$D_{12} = (R_2/R_1)(a/b)(1 - a)(D_1 - D_2) \quad (4.24)$$

$$D_{21} = (R_1/R_2)[(a + b)(1 - a - b)/b](D_2 - D_1) \quad (4.25)$$

$$D_{22} = D_2 + [a(1 - a - b)/b](D_2 - D_1) \quad (4.26)$$

Details of the procedure have been reported elsewhere[41,43].

4.3. Experimental Equipment

Teflon dispersion tubes (~ 3000 cm long) were used in this work. The inner radius of each tube (*ca.* 0.045 cm) was determined by weighing the tube when empty and when filled with water of known density. Each tube was coiled in a 75-cm-diameter helix and held at a constant temperature in a thermostat.

A schematic diagram of the Taylor dispersion equipment is shown in Figure 4-2. A metering pump (Gilson model MP2) maintained a steady flow of carrier solution through each tube. Flow rates (typically 0.5 cm s^{-1}) were adjusted to give retention times (typically 2 hours) satisfying the condition expressed by inequality (4.18). At the start of each run a narrow pulse of sample solution was injected into a carrier stream of the solution through a Teflon injection valve (Rheodyne model 50) with a 20 μL sample loop. The broadened distribution of dispersed samples was monitored at the tube outlet with a sensitive flow-through differential refractometer (Waters model 410, Hewlett-Packard model 1047A, or Gilson model 131, each with 10 μL flow cell) capable of resolving changes in refractive index as small as 1×10^{-8}. The refractive indices of the flowing and injected solutions differed by 0.001-0.002. When the injected solute reaches the detector, however, the difference in refractive index across the eluted sample decayed to much smaller values, typically 2×10^{-5}, because the injected solute is diluted and dispersed in the carrier stream.

Figure 4-2 Schematic diagram of Taylor dispersion experimental equipment:

1 - Sample loop

2 - Refractometer

S - Sample refractometer cell (flowing solution)

R - Reference refractometer cell (trapped carrier solution)

E - Shut-off valve (open during each run, closed to flush refractometer cells)

P - Purge valve (closed during each run, open to flush refractometer cells)

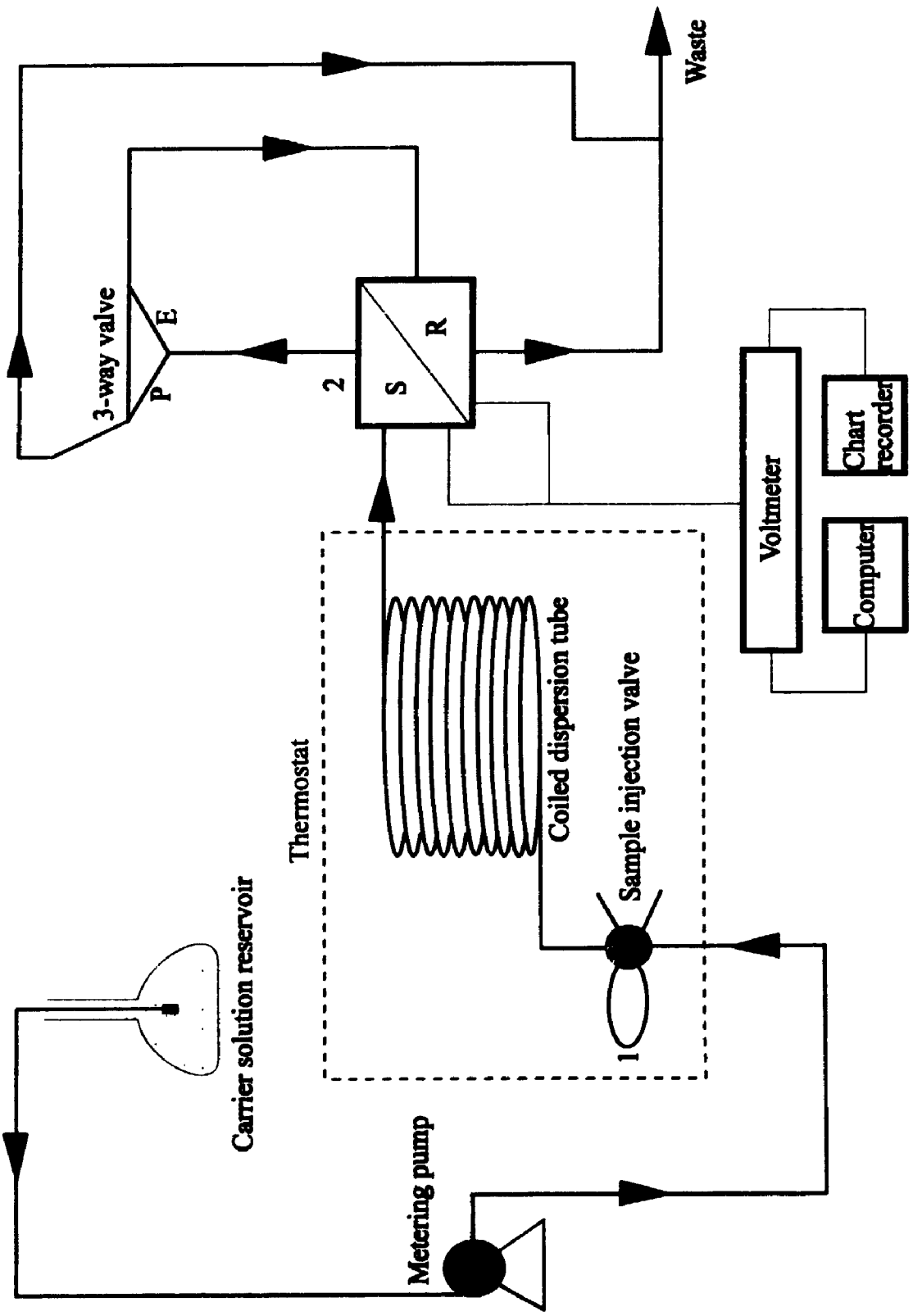
Waste
3-way valve
E
P
2
S
R
Voltmeter
Chart recorder
Computer
Thermostat
Coiled dispersion tube
Sample injection valve
1
Carrier solution reservoir
Metering pump

Table 4-2 Binary interdiffusion coefficients of aqueous sucrose solutions at 25 °C

C / mol L^{-1}	D / 10^{-5} cm^2 s^{-1}	
	this work	reference[44]
0.01	0.518 ± 0.007	0.520
0.10	0.503 ± 0.006	0.496
0.20	0.482 ± 0.008	0.470
0.27	0.458 ± 0.006	0.451
0.35	0.441 ± 0.005	0.430

Table 4-3 Binary interdiffusion coefficients of aqueous urea solutions at 25 °C

C / mol L^{-1}	D / 10^{-5} cm^2 s^{-1}	
	this work	reference[45]
0.25	1.36 ± 0.01	1.363
0.50	1.34 ± 0.01	1.344
1.00	1.33 ± 0.01	1.308

Table 4-4 Binary interdiffusion coefficients of aqueous tetrabutylammonium bromide solutions at 25 °C

C / mol L^{-1}	D / 10^{-5} cm^2 s^{-1}	
	this work	reference[46]
0.05	0.697 ± 0.009	0.687
0.10	0.616 ± 0.008	0.631
0.20	0.556 ± 0.006	0.554
0.30	0.494 ± 0.008	0.498
0.50	0.420 ± 0.005	0.418
0.80	0.330 ± 0.004	0.328

Table 4-5 Binary interdiffusion coefficients of aqueous potassium chloride solutions at 25 °C

C / mol L^{-1}	D / 10^{-5} cm^2 s^{-1}	
	this work	reference[47]
0.02	1.87 ± 0.01	1.888
0.04	1.86 ± 0.01	1.870
0.20	1.83 ± 0.01	1.838

Table 4-6 Ternary interdiffusion coefficients of aqueous solutions at 25 °C

(previously reported data in parentheses)

	C_1 / mol L^{-1}	C_2 / mol L^{-1}	$D_{11}/10^{-5}$ cm^2 s^{-1}	$D_{12}/10^{-5}$ cm^2 s^{-1}	$D_{21}/10^{-5}$ cm^2 s^{-1}	$D_{22}/10^{-5}$ cm^2 s^{-1}
Sucrose(1)-KCl(2)	0.088	0.805	0.507 ± 0.012 (0.497)[a]	0.004 ± 0.006 (0.004)[a]	0.24 ± 0.06 (0.314)[a]	1.77 ± 0.02 (1.775)[a]
LiCl(1)-KCl(2)	0.25	0.20	1.15 ± 0.01 (1.134)[b]	0.00 ± 0.03 (-0.001)[b]	0.20 ± 0.02 (0.215)[b]	1.80 ± 0.06 (1.811)[b]
Bu_4NBr(1)-KBr(2)	0.075	0.100	0.536 ± 0.008 (0.521)[c]	0.001 ± 0.006 (0.004)[c]	0.41 ± 0.11 (0.415)[c]	1.75 ± 0.02 (1.748)[c]
NaCl(1)-$MgCl_2$(2)	0.375	0.125	1.36 ± 0.01 (1.367)[d]	0.58 ± 0.05 (0.577)[d]	0.03 ± 0.02 (0.045)[d]	0.77 ± 0.02 (0.805)[d]

[a] ref.48; [b] ref. 49; [c] ref. 50; [d] ref. 51.

The small differences in composition ensure that the measured diffusion coefficients represent differential values at the composition of the flowing solution[39].

The output voltages from the refractometers are displayed on chart recorders and measured with a digital voltmeter (Hewlett-Packard model 34401A or 3478A) at accurately timed intervals. The voltage readings were collected and stored in a microcomputer. A switching unit (Hewlett-Packard model 3488A) controlled by the computer was used to connect the voltmeter to the different refractometers so that several different Taylor experiments could be run simultaneously.

In order to test the reliability of our Taylor dispersion equipment, diffusion coefficients measured for a number of solutions were compared with accurate values determined previously by Gouy and Rayleigh interferometry[44-51]. This check showed that the Taylor measurements are accurate within 1.0 - 1.5%, as shown in Tables 4-2 through 4-6.

4.4. References

1. B. Lindman, M.C. Puyal, N. Kamenka, B. Brun and G. Gunnarsson, *J. Phys. Chem.*, **86**, 1702 (1982)
2. B. Lindman and B. Brun, *J. Colloid Interface Sci.*, **43**, 388 (1973)
3. P. Stilbs, *J. Colloid Interface Sci.*, **87**, 385(1982); **89**, 547 (1982)
4. D. Langevin, *Annu. Rev. Phys. Chem.*, **43**, 341 (1992)
5. D. Stigter, R.J. Williams and B. Lindman, *J. Phys. Chem.*, **59**, 330 (1955)
6. H. Fabre, N. Kamenka and Lindman, *J. Phys. Chem.*, **85**, 3493 (1981)
7. A. Rohde and E. Sackmann, *J. Phys. Chem.*, **84**, 1598 (1980)
8. J. Briggs, D.F. Nicoli and R. Ciccolello, *Chem. Phys. Letters*, **73**, 149 (1980)
9. A. Rodhe and E. Sackmann, *J. Colloid Interface Sci.*, **70**, 494 (1979)
10. R.M. Mazo, *J. Chem. Phys.*, **43**, 8 (1965)
11. N.A. Mazer, G.B. Benedek and M.C. Carey, *J. Phys. Chem.*, **80**, 1075 (1976)
12. Robert M. Weinheimer, D.Fennell Evans and E.L. Cussler, *J. Colloid Interface Sci.*, **80**, 357 (1981)
13. D.G. Leaist, *J. Colloid Interface Sci.*, **111**, 230, 240 (1986)

14. D.F. Evans, S. Mukherjee, D.J. Mitchell and B.W. Ninham, *J. Colloid Interface Sci.*, **93**, 184 (1983)

15. L. Costantino, C. Della Volpe, O. Ortona and V. Vitagliano, *J. Chem. Soc. Faraday Trans.*, **88**, 61 (1992)

16. L. Costantino, C. Della Volpe, O. Ortona and V. Vitagliano, *J. Colloid Interface Sci.*, **148**, 72 (1992)

17. A.M. Cazabat, D. Langevin and A. Pouchelon, *J. Colloid Interface Sci.*, **73**, 1 (1980)

18. A.M. Cazabat and D. Langvin, *J. Chem. Phys.*, **74**, 3148 (1981)

19. A.C. Lam and R.S. Schechter, *J. Colloid Interface Sci.*, **120**, 42 (1987)

20. S.J. Chen, D.F. Evans and B.W. Ninham, *J. Phys. Chem.*, **88**, 1631 (1984)

21. E. Dayalan, S. Qutubuddin and J. Texter, *Electrochemistry in Colloids and Dispersions*, Chapter 10, R.A. Mackay and J. Texter eds., VCH Publishers, Inc., New York, 1992

22. S.I. Chou and D.O. Shah, *J. Colloid Interface Sci.*, **78**, 249 (1980)

23. B. Lindman, N. Kamenka, T.-M. Kathopoulis, B. Brun and P.-G. Nilsson, *J. Phys. Chem.*, **84**, 2485 (1980)

24. W.A. Wakeham, A. Nagashima and J.V. Sengers, *Measurement of Transport Properties of Fluids*, Chapter 9, Blackwell Scientific Publications, London, 1991

25. D.G. Leaist, *Can. J. Chem.*, **63**, 2933 (1985)

26. D.G. Leaist and P.A. Lyons, *J. Solution Chem.*, **13**, 77 (1984)

27. D.G. Leaist, *Can. J. Chem.*, **68**, 33 (1990)

28. R.A. Mackay, N.S. Dixit, C. Hermansky and A.S. Kertes, *Colloids Surf.*, **21**, 27 (1986)

29. J.P. Kratohvil and T.M. Aminabhavi, *J. Phys. Chem.*, **86**, 1254 (1982)

30. D.G. Miller and V. Vitagliano, *J. Phys. Chem.*, **90**, 1706 (1986)

31. P.L. Vitagliano, C. Della Volpe and V. Vitagliano, *J. Solution Chem.*, **13**, 549 (1984)

32. H.E. Huppert and J.S. Turner, *J. Fluid Mech.*, **106**, 299 (1981)

33. V. Vitagliano, A. Zagari, R. Sartorio, D. Spaduzzi and R. Laurentino, *J. Solution Chem.*, **6**, 671 (1977)

34. M.S. Bello, R. Rezzonico and P.G. Righetti, *Science*, **266**, 773 (1994)

35. D.G. Leaist and L. Hao, *J. Solution Chem.*, **22**, 263 (1993)

36. D.G. Leaist and L. Hao, *J. Chem. Soc. Faraday Trans.*, **89**, 515 (1993)

37. G. Taylor, *Proc. Roy. Soc.*, **A219**, 186(1953); **A223**, 446(1954); **A225**, 473 (1954)

38. R. Aris, *Proc. Roy. Soc.*, **A235**, 67 (1956)

39. A. Alizadeh, C.A. Nieto de Castro and W.A. Wakeham, *Int. J. of Thermophys.*, **1**, 243 (1980)

40. W.N. Gill and R. Sankarasubramanian, *Proc. Roy. Soc.*, **A316**, 341(1970)

41. D.G. Leaist, *J. Chem. Soc. Faraday Trans.*, **87**, 597 (1991)

42. W.E. Price, *J. Chem. Soc. Faraday Trans. 1*, **84**, 2431 (1988)

43. D.G. Leaist, *J. Phys. Chem.*, **94**, 5180 (1990)

44. L.J. Gosting and Morris, *J. Am. Chem. Soc.*, **71**, 1998 (1949)

45. L.J. Gosting and D.F. Akeley, *J. Am. Chem. Soc.*, **74**, 2058 (1952)

46. H. Kim, A. Revzin and L.J. Gosting, *J. Phys. Chem.*, **77**, 2567 (1973)

47. J.A. Rard and D.G. Miller, *J. Chem. Eng. Data*, **25**, 211 (1980)

48. E.L. Cussler and P.J. Dunlop, *J. Phys. Chem.*, **70**, 1880 (1966)

49. P.J. Dunlop and L.J. Gosting, *J. Am. Chem. Soc.*, **77**, 5238 (1955)

50. H. Kim, *J. Solution Chem.*, **3**, 149 (1974)

51. J.G. Albright, R. Mathew, D.G. Miller and J.A. Rard, *J. Phys. Chem.*, **93**, 2176 (1989)

Chapter 5

COMPARISON OF MULTICOMPONENT DIFFUSION COEFFICIENTS MEASURED BY LIGHT SCATTERING AND MACROSCOPIC GRADIENT TECHNIQUES. SODIUM DODECYLSULFATE MICELLES IN AQUEOUS SALT SOLUTIONS

Taylor dispersion is used to measure diffusion coefficients for sodium dodecylsulfate (SDS) micelles in aqueous sodium chloride solutions. The diffusion coefficient of the micelles suggested by quasi-elastic light scattering (QELS) spectroscopy is larger than the diffusion coefficient of SDS determined by the dispersion method. To clarify the apparent disagreement, an expression is developed for the spectrum of light scattered by the concentration fluctuations in a multicomponent solution. The spectrum shows that QELS gives the lower eigenvalue of the interdiffusion coefficient matrix for SDS/NaCl solutions. Because the cross-diffusion coefficients are not negligible, the measured eigenvalue is up to 15% larger than the diffusion coefficient of the micelles.

5.1. Introduction

Quasi-elastic light scattering (QELS) spectroscopy is widely used to study interdiffusion in liquids[1-3]. Although QELS can be used to study mixtures of small molecules[4-7], this versatile technique is more often applied to solutions of macromolecules[8-11], micelles[12-15], or microemulsions[16] which scatter light more efficiently. The theory behind QELS diffusion measurements is well understood for binary solutions[17]. In practice, however, the technique is frequently applied to multicomponent solutions. For example, considerable effort has been devoted to QELS studies of the diffusion of proteins and ionic micelles in multicomponent salt solutions or buffers[8-15]. The measured diffusion coefficients are assumed to represent the diffusion coefficients of the proteins or the micelles.

It has been known for many years, however, that interdiffusion in multicomponent solutions differs fundamentally from binary interdiffusion in two-component solutions. In particular, multicomponent interdiffusion is "coupled"[1,2]. It is not uncommon for a diffusing solute to produce fluxes of other solutes which exceed its own flux. The electric field generated by the diffusion of proteins or micelles together with mobile counterions can drive especially large coupled flows of supporting electrolytes[18-20]. It is not immediately obvious what effects, if any, coupled diffusion would have on QELS diffusion measurements.

When QELS is applied to micellar solutions, with or without added salt, it is generally believed that the measured diffusion coefficient represents the diffusion coefficient of the micelles[12-15]. By contrast, classical macroscopic gradient diffusion experiments[18,21-23], such as Taylor dispersion, give the interdiffusion coefficient of the total micellar component as defined by Fick's laws. The interdiffusion coefficient of the total micellar component is a weighted average of the diffusion coefficient of the rapidly equilibrating micelles and free surfactant monomers. The latter diffuse relatively rapidly, so the interdiffusion coefficient of the total micellar component is expected to be larger than the diffusion coefficient of the micelles determined by QELS[14].

In the present study, Taylor dispersion[1-3] is used to measure interdiffusion in aqueous solutions of sodium dodecylsulfate (SDS) micelles containing added sodium chloride. Taylor dispersion gives unambiguous interdiffusion coefficients of the total SDS and NaCl components. Surprisingly, the interdiffusion coefficient of SDS is found to be *smaller* than the diffusion coefficient indicated by QELS.

This unexpected result prompted the calculation of the spectrum of light scattered by the concentration fluctuations in a multicomponent solution. The spectrum shows that the diffusion coefficient determined by QELS for SDS/NaCl solutions is *not* the micelle diffusion coefficient or the diffusion coefficient of the total SDS component, but actually the lower eigenvalue of the multicomponent interdiffusion coefficient matrix. This distinction accounts for the apparent inconsistency of the Taylor and QELS data and may help to clarify the meaning of QELS diffusion measurements on multicomponent solutions.

5.2. Experimental Procedure

BDH "specially pure" SDS and reagent-grade NaCl were used as received. Solutions were prepared with distilled, deionized water in calibrated volumetric flasks. A Waters model 410 refractometer and a 3658-cm-long dispersion tube (inner radius 0.04335 cm) were used to make the diffusion measurements. At the start of each run 20 μL of solution of composition $\overline{C}_1 + \Delta C_1$, $\overline{C}_2 + \Delta C_2$ was injected into a carrier stream of composition $\overline{C}_1$, $\overline{C}_2$. Flow rates were adjusted to give retention times of about 10 000 s. Initial concentration differences were typically $\Delta C_1 = 0.01$ mol L^{-1} for SDS and $\Delta C_2 = 0.025$ mol L^{-1} for NaCl. The refractometer's output voltage was measured at 20-s intervals with a computer-controlled digital voltmeter. The diffusion coefficients were calculated by using nonlinear least squares to fit equation (4.20) to the measured refractometer voltages, as described in Chapter 4.

5.3. Theory

To account for possible differences between the diffusion coefficients from QELS and those from Taylor dispersion (or other macroscopic gradient techniques), it is helpful to develop an expression for the spectrum of light scattered from a multicomponent solution.

For the general case of a solution containing a solvent component plus N solute components, the N^2 interdiffusion coefficients are defined by the coupled Fick's equations[1-3]

$$J_i = -\sum_{k=1}^{N} D_{ik} \nabla C_k \qquad (i = 1, 2, ..., N) \tag{5.1}$$

J_i is the molar flux of solute component i in the volume-fixed reference frame, and C_k is the concentration of solute k in moles per unit volume.

Fick's equations are useful because they accurately describe the diffusion of any number of electrolyte or nonelectrolyte components in dilute or concentrated solutions. "Component" is used in the thermodynamic sense (*e.g.* total SDS or NaCl components,

but not micelles or Na^+, DS^-, Cl^- ions). Because these components are electrically neutral, explicit terms are not required for the diffusion-induced electric field.

Fick's equations can be used to describe the diffusion of associating solutes if the association/dissociation reactions are rapid enough to maintain local equilibrium[24]. This condition is satisfied for the vast majority of association reactions, including micellar aggregation[25,26]. Conveniently, it is not necessary to know the concentrations or the diffusion coefficients of the actual diffusing species.

The mathematics of multicomponent diffusion can always be simplified, without loss of generality or accuracy, by taking linear combinations of the concentrations and fluxes[27,28]

$$\mathcal{C}_i = \sum_{k=1}^{N} A_{ik} C_k \tag{5.2}$$

$$\mathcal{J}_i = \sum_{k=1}^{N} A_{ik} J_k \tag{5.3}$$

which reduce the diffusion equations to diagonal form:

$$\mathcal{J}_i = -\mathcal{D}_i \nabla \mathcal{C}_i \qquad (i = 1, 2, ..., N) \tag{5.4}$$

$\mathcal{D}_1, \mathcal{D}_2, ..., \mathcal{D}_N$ are the eigenvalues of the N by N matrix $\boldsymbol{D}$ of D_{ik} coefficients. The A_{ik} transformation coefficients are chosen so that the columns of matrix $\boldsymbol{A}^{-1}$ are independent eigenvectors of $\boldsymbol{D}$.

Correlation Functions from Light Scattering When a beam of light passes through a solution, the fluctuations $\delta\varepsilon(\mathbf{r},t)$ in the local dielectric constant scatter some of the incident light. The fluctuations in the dielectric constant are in turn caused by microscopic fluctuations in the temperature, pressure, and concentrations of the solutes[17,29]. In the present treatment, however, temperature and pressure fluctuations are ignored:

$$\delta\varepsilon(\mathbf{r},t) = \sum_i \frac{\partial \varepsilon}{\partial C_i} \delta C_i(\mathbf{r},t) \tag{5.5}$$

This approximation can be justified if the thermal diffusivity is much larger than the solute diffusivities and if the coupling between heat conduction and solute diffusion is weak. These conditions are satisfied for most solutions[5], except near critical points.

Statistically, the decay of microscopic concentration fluctuations is governed by the same equations that describe the decay of macroscopic concentration gradients[30,31].

$$\frac{\partial \delta C_i(\mathbf{r},t)}{\partial t} = \sum_{k=1}^{N} D_{ik} \nabla^2 \delta C_k(\mathbf{r},t) \tag{5.6}$$

The fluctuations in the concentration of solute i are coupled to the fluctuations in the concentration of solute k by cross-diffusion coefficient D_{ik} $(i \neq k)$. Mathematically, it is much easier to deal with the independent concentration fluctuations

$$\delta C'_i(\mathbf{r},t) = \sum_{k=1}^{N} A_{ik} \delta C_k(\mathbf{r},t) \tag{5.7}$$

which decay according to the pseudo-binary equations

$$\frac{\partial \delta C'_i(\mathbf{r},t)}{\partial t} = \Lambda_i \nabla^2 \delta C'_i(\mathbf{r},t) \tag{5.8}$$

The corresponding fluctuations in the local dielectric constant are

$$\delta\varepsilon(\mathbf{r},t) = \sum_{i=1}^{N} \frac{\partial \varepsilon}{\partial C'_i} \delta C'_i(\mathbf{r},t) \tag{5.9}$$

Mountain and Deutch[17] have calculated the spectrum of light scattered by the statistically independent modes of a binary solution. Neglecting temperature and pressure fluctuations, their exact treatment leads to

$$S(q,\omega) = \sum_{i=1}^{N} \left(\frac{\partial \varepsilon}{\partial C'_i} \right)^2 \frac{RT}{(\partial \mu'_i / \partial C'_i)} \frac{2\Lambda_i q^2}{(\Lambda_i q^2)^2 + \omega^2} \tag{5.10}$$

for the spectrum of light scattered by the concentration fluctuations in a multicomponent solution. q is the change in the wave vector, ω the change in the frequency of the scattered light, R the gas constant, and μ'_i the linear combination

$$\mu'_i = \sum_{k=1}^{N} A_{ik} \mu_k \tag{5.11}$$

of the chemical potentials μ_k of the solute components.

The Fourier transformation of $S(q,\omega)$ gives the field autocorrelation function

$$g^{(1)}(t) = \sum_{i=1}^{N}\left(\frac{\partial\varepsilon}{\partial\mathcal{C}_i}\right)^2 \frac{RT}{\left(\partial\mu_i'/\partial\mathcal{C}_i\right)}\exp(-q^2\mathcal{D}t) \tag{5.12}$$

measured in homodyne scattering experiments. In general $g^{(1)}(t)$ is a multi-exponential decay with time constants $1/q^2\mathcal{D}_1$, $1/q^2\mathcal{D}_2$, ..., $1/q^2\mathcal{D}_N$.

The intensity autocorrelation function

$$g^{(2)}(t) = 1 + \left|g^{(1)}(t)\right|^2 \tag{5.13}$$

measured in optical heterodyne experiments is a more complicated multi-exponential decay with time constants of the form $1/q^2(\mathcal{D}_i + \mathcal{D}_k)$. Fortunately there are many cases where the expressions for $g^{(1)}(t)$ and $g^{(2)}(t)$ simplify to only one or two exponential decays.

The expressions

$$\partial\varepsilon/\partial\mathcal{C}_i = \left[\sum_{k=1}^{N}\frac{A_{ik}}{\partial\varepsilon/\partial C_k}\right]^{-1} \tag{5.14}$$

$$\partial\mu_i'/\partial\mathcal{C}_k = \left\{\sum_{q=1}^{N} A_{kq}\left[\sum_{m=1}^{N} A_{im}\frac{\partial\mu_m}{\partial C_q}\right]^{-1}\right\}^{-1} \tag{5.15}$$

may be used to estimate the relative weights of the exponential decays from the measurable concentration derivatives of the dielectric constant and the solute chemical potentials. At optical frequencies the dielectric constant ε equals the square of the solution's refractive index, and therefore $\partial\varepsilon/\partial C_k = 2n(\partial n/\partial C_k)$.

Ternary Solutions (N + 1 = 3) In a solution containing solvent plus solute components 1 and 2 the fluctuations in the solute concentrations decay as

$$\frac{\partial\delta C_1}{\partial t} = -D_{11}\nabla^2\delta C_1 - D_{12}\nabla^2\delta C_2 \tag{5.16}$$

$$\frac{\partial\delta C_2}{\partial t} = -D_{21}\nabla^2\delta C_1 - D_{22}\nabla^2\delta C_2 \tag{5.17}$$

which transform to

$$\frac{\partial\delta\mathcal{C}_1}{\partial t} = \mathcal{D}\nabla^2\delta\mathcal{C}_1 \tag{5.18}$$

$$\frac{\partial \delta C_2}{\partial t} = \mathfrak{D}_2 \nabla^2 \delta C_2 \tag{5.19}$$

The eigenvalues are

$$\mathfrak{D}_1 = \frac{D_{11} + D_{22} + (D_{11} - D_{22})\left[1 + \dfrac{4D_{12}D_{21}}{(D_{11} - D_{22})^2}\right]^{1/2}}{2} \tag{5.20}$$

$$\mathfrak{D}_2 = \frac{D_{11} + D_{22} - (D_{11} - D_{22})\left[1 + \dfrac{4D_{12}D_{21}}{(D_{11} - D_{22})^2}\right]^{1/2}}{2} \tag{5.21}$$

It is easy to show that the A_{ik} coefficients

$$A_{11} = 1 \tag{5.22}$$

$$A_{12} = \frac{D_{12}}{D_{11} - \mathfrak{D}_2} \tag{5.23}$$

$$A_{21} = \frac{D_{21}}{D_{22} - \mathfrak{D}_1} \tag{5.24}$$

$$A_{22} = 1 \tag{5.25}$$

diagonalize the diffusion coefficient matrix:

$$\mathbf{ADA}^{-1} = \begin{pmatrix} \mathfrak{D}_1 & 0 \\ 0 & \mathfrak{D}_2 \end{pmatrix} \tag{5.26}$$

Dilute Nonelectrolyte Solutions Coupled diffusion is usually negligible for dilute solutions of non-associating nonelectrolytes[2]. In the limiting case where all of the cross-diffusion coefficients are zero: $\mathfrak{D}_i = D_{ii}$, $A_{ii} = 1$, A_{ik} $(i \neq k) = 0$, $C'_i = C_i$, and $\mu'_i = \mu_i$. Furthermore, if the solution is thermodynamically ideal, then $\mu_i = \mu_i^0 + RT \ln C_i$, $\partial \mu_i / \partial C_i = RT/C_i$, and the expression for the field autocorrelation function simplifies to[29,32]

$$g^{(1)}(t) = \sum_{i=1}^{N} \left(\frac{\partial \varepsilon}{\partial C_i}\right)^2 C_i \exp(-q^2 D_{ii} t) \tag{5.27}$$

It is well known that accurate diffusion coefficients can not be evaluated from multi-exponential decays if the D_{ii} values are similar in magnitude. But if solute 1 is

macromolecular polymer and the other solutes have much smaller molecular weights, the exponential in D_{11} will decay slowly owing to the slow diffusion of the polymer. Also, the pre-exponential factor $(\partial\varepsilon/\partial C_1')^2$ will be much larger than the corresponding factors for the other solutes. Under these conditions a reliable value for the diffusion coefficient D_{11} for the polymer can be extracted from the correlation functions.

5.4. Results and Discussion

Aqueous Na_nP (C_1)/NaCl (C_2) Solutions Coupled diffusion caused by long-range electrostatic forces is important for dilute electrolytes, even at submillimolar ionic strengths. Before considering the effects of coupled diffusion on the spectrum of light scattered from micellar solutions, we will first discuss the simpler problem of scattering from macroion P^{n-} in aqueous NaCl solutions. There are three diffusing solute species, P^{n-}, Cl^-, and Na^+, but only two solute components are independent in view of the electroneutrality restriction. Consequently, ternary diffusion equations (5.16)-(5.19) apply.

At low ionic strengths the limiting Nernst equations give

$$D_{11} = D_P + t_P(D_{Na} - D_P) \tag{5.28}$$

$$D_{12} = t_P(D_{Na} - D_{Cl})/n \tag{5.29}$$

$$D_{21} = nt_{Cl}(D_{Na} - D_P) \tag{5.30}$$

$$D_{22} = D_{Cl} + t_{Cl}(D_{Na} - D_{Cl}) \tag{5.31}$$

These equations may be used to estimate the interdiffusion coefficients of the $Na_nP(C_1')/NaCl(C_2')$ components from the diffusion coefficients D_P, D_{Cl}, and D_{Na} of the macroion and the chloride and sodium ions. n is the number of moles of sodium counterions per mole of macroion. t_P and t_{Cl} are the ionic transference numbers

$$t_i = c_i z_i^2 D_i \Big/ \sum_{k=1}^{3} c_k z_k^2 D_k \tag{5.32}$$

where $z_p = -n$, $z_{Cl} = -1$, $z_{Na} = +1$, $c_p = C_1$, $c_{Cl} = C_2$, and $c_{Na} = nC_1 + C_2$. At 25 °C the limiting diffusion coefficients[33] of the aqueous sodium and chloride ions are $D_{Na} = 1.33 \times 10^{-5}$ and $D_{Cl} = 2.03 \times 10^{-5}$ cm^2 s^{-1}.

The values $n = 10$ and $D_p = 0.075 \times 10^{-5}$ cm^2 s^{-1} will be used to model the diffusion of serum albumin (a water-soluble protein) in aqueous sodium chloride solutions at pH 7[22,23,34-36]. Figure 5-1 shows the interdiffusion coefficients calculated for solutions containing 0.000-0.010 mol L^{-1} $Na_{10}P(1)$ and 0.100 mol L^{-1} NaCl(2). When a gradient in the concentration of $Na_{10}P$ is formed, the electric field which is generated speeds up the macroion and slows down the mobile Na^+ ions to keep the solution electrically neutral. The electric field also causes cocurrent coupled diffusion of Cl^- ions as reflected by the large positive values for cross-coefficient D_{21}.

In order to estimate the light scattering correlation functions according to equation (5.15) and (5.16), the limiting expressions $\mu_1 = \mu_1^0 + RT\ln[C_1(10C_1 + C_2)^{10}]$ and $\mu_2 = \mu_2^0 + RT\ln[C_2(10C_1 + C_2)]$ may be used to evaluate the $\partial\mu_i/\partial C_k$ derivatives. Also, the molar refractivity of $Na_{10}P(1)$ may be assumed to be several hundred times larger than that for NaCl(2). The decay in $\mathcal{D}_1$ then completely dominates the correlation function: $g^{(1)}(t) = A_1 \exp(-q^2\mathcal{D}_1 t)$, so QELS diffusion measurements would give the eigenvalue $\mathcal{D}_1$.

In Figure 5-2 the interdiffusion coefficient D_{11} of the $Na_{10}P(1)$ component in 0.100 mol L^{-1} NaCl is compared with the eigenvalue $\mathcal{D}_1$. As the concentration of $Na_{10}P(1)$ is raised, $\mathcal{D}_1$ becomes increasingly larger than D_{11}. At 0.010 mol L^{-1} $Na_{10}P(1)$, the eigenvalue is 12% larger than the interdiffusion coefficient.

Owing to the electrostatic acceleration by the mobile Na^+ counterions, the interdiffusion coefficient of $Na_{10}P(1)$ is up to three times larger than the diffusion coefficient of the macroion, D_p.

The model calculations for $Na_{10}P(1)$/NaCl(2) solutions suggest that QELS would give the eigenvalue $\mathcal{D}_1$ which differs significantly from the interdiffusion coefficient D_{11} of the polyelectrolyte component and from the diffusion coefficient D_p of the polyion.

Figure 5-1 Calculated interdiffusion coefficients of $Na_{10}P(1)/NaCl(2)$ in solutions containing 0.100 mol L^{-1} NaCl and 0.000 - 0.010 mol L^{-1} $Na_{10}P$

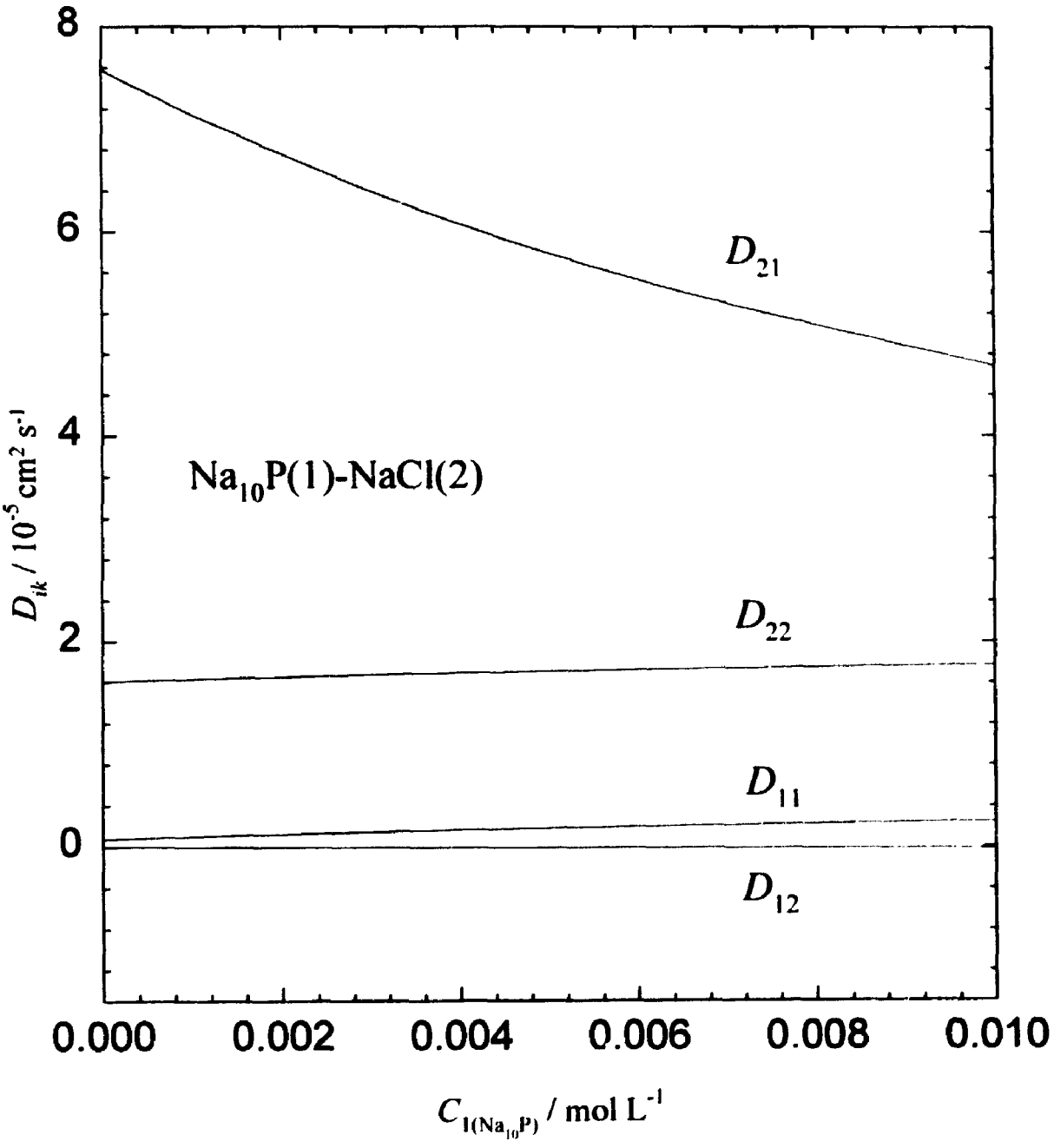
8
6
4
2
0
D_{ik} / 10^{-5} cm^2 s^{-1}
$Na_{10}P(1)$-NaCl(2)
D_{21}
D_{22}
D_{11}
D_{12}
0.000
0.002
0.004
0.006
0.008
0.010
$C_{1(Na_{10}P)}$ / mol L^{-1}

Figure 5-2 Calculated values of the interdiffusion coefficient D_{11} of the $Na_{10}P(1)$ component, eigenvalue $\mathfrak{D}_i$, and the polyion diffusion coefficient D_P for solutions containing 0.100 mol L^{-1} NaCl(2) and 0.000 - 0.010 mol L^{-1} $Na_{10}P(1)$

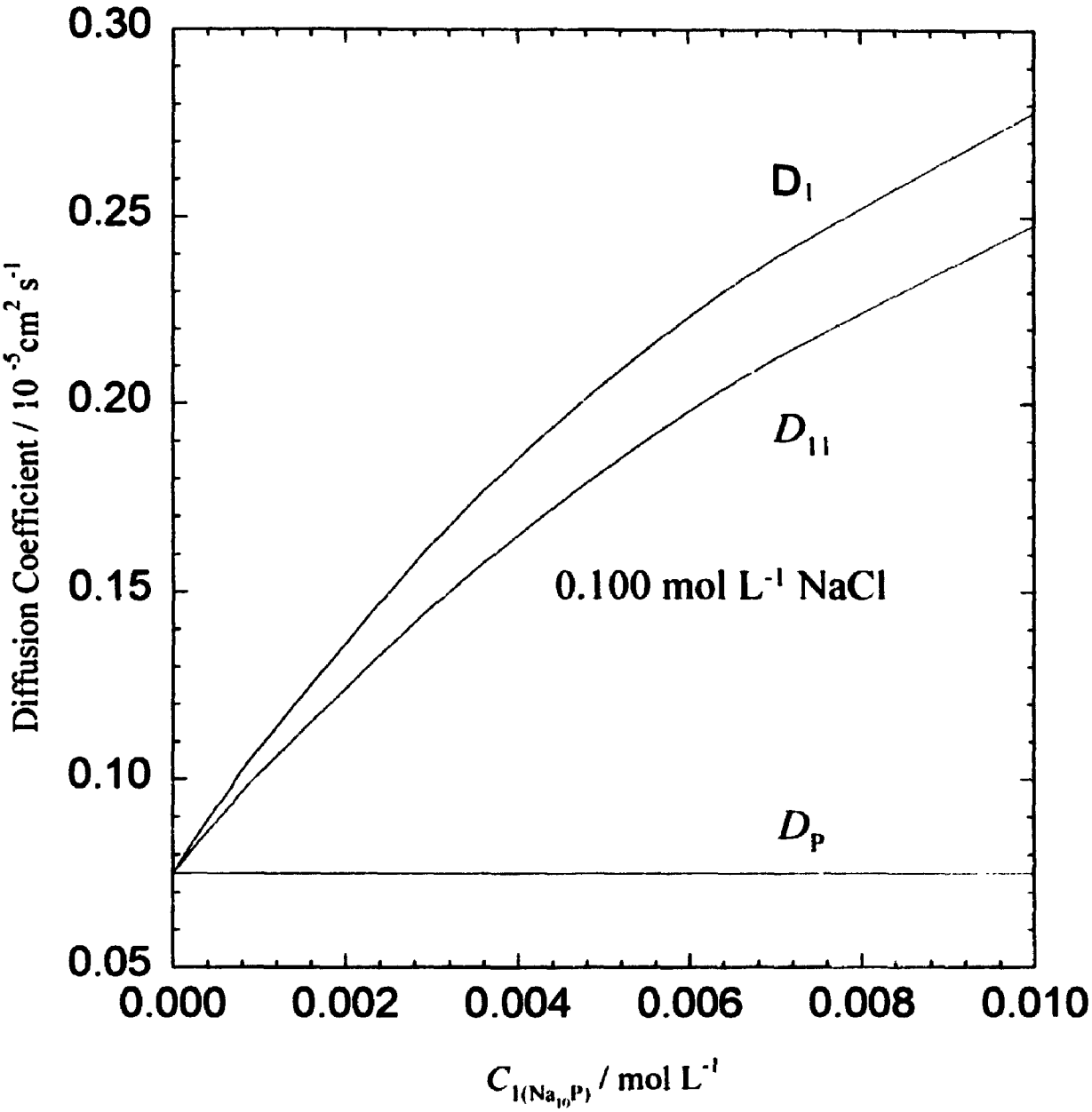
0.30
0.25
0.20
0.15
0.10
0.05
0.000
0.002
0.004
0.006
0.008
0.010
Diffusion Coefficient / 10 -5cm2 s-1
D1
D11
0.100 mol L-1 NaCl
DP
C1(Na10P) / mol L-1

Figure 5-3 Dispersion peaks measured against a carrier stream with $\overline{C_1} = 0.100$ mol L^{-1} SDS(1) and $\overline{C_2} = 0.100$ mol L^{-1} NaCl(2). SDS peak: $\Delta C_1 = 0.010$ mol L^{-1}, $\Delta C_2 = 0.000$ mol L^{-1}; NaCl peak: $\Delta C_1 = 0.000$ mol L^{-1}, $\Delta C_2 = 0.025$ mol L^{-1}

(a) Calculated contribution from the Gaussian in $\mathcal{D}_1$.

(b) Calculated contribution from the Gaussian in $\mathcal{D}_2$.

The peaks have been offset for clarity.

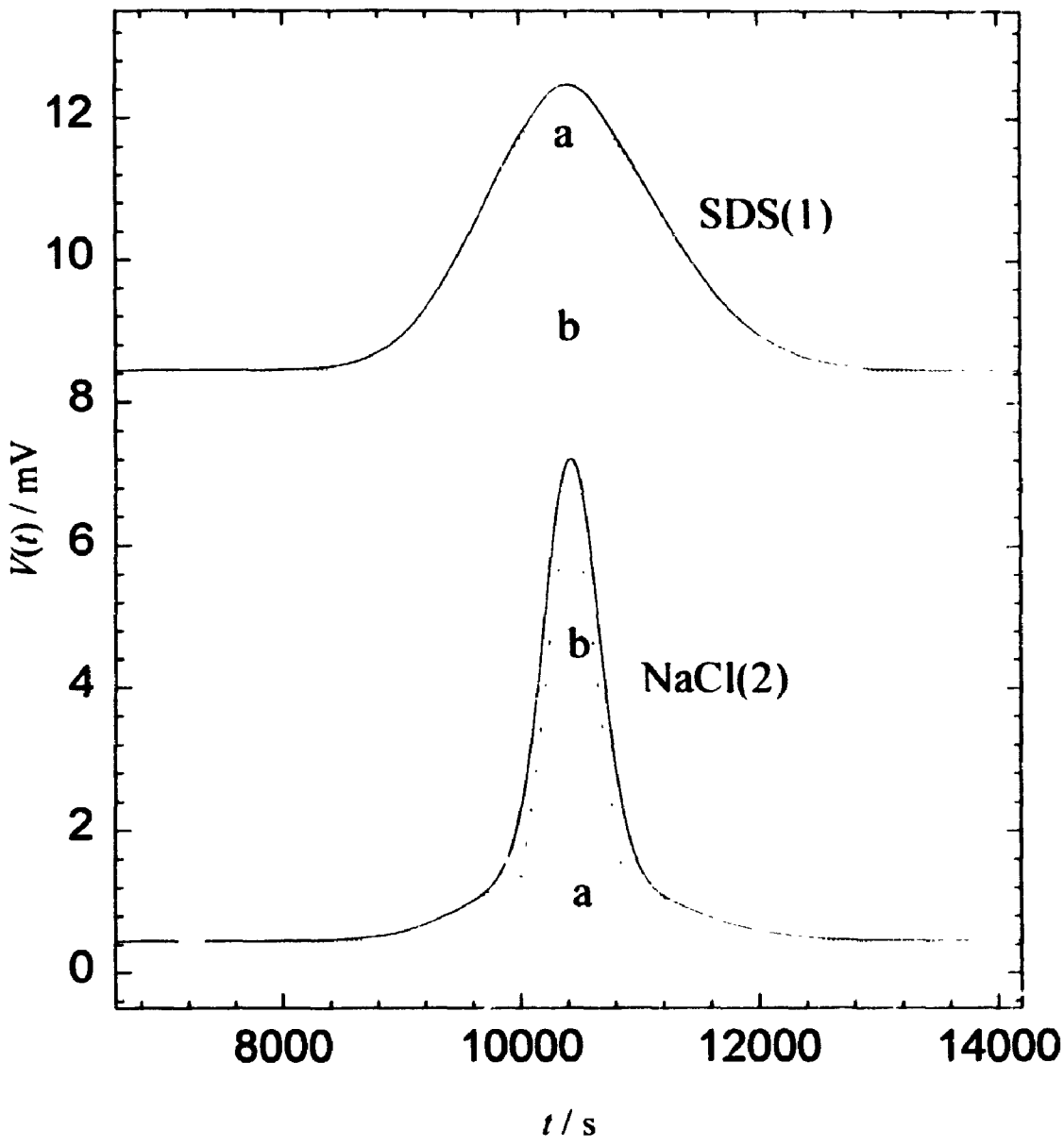
12
10
8
6
4
2
0
V(t) / mV
a
SDS(1)
b
b
NaCl(2)
a
8000
10000
12000
14000
t / s

Aqueous SDS(1)/NaCl(2) Solutions The interdiffusion coefficients of SDS(C_1)/NaCl(C_2) solutions were measured at eight different carrier-stream compositions. Figure 5-3 shows dispersed solute peaks for the injection of excess SDS or NaCl into a 0.100 mol L^{-1} SDS and 0.100 mol L^{-1} NaCl carrier stream. The NaCl peak consists of a relatively narrow peak superimposed on a broader base peak contributed by the relatively slow coupled diffusion of SDS.

SDS(1) diffuses about 10 times more slowly than NaCl. The eigenvalues $\mathcal{D}_1$ and $\mathcal{D}_2$ were therefore well separated, and the fitting procedure gave relatively precise diffusion coefficients. The average D_{ik} values listed in Table 5-1 were obtained by fitting equation (4.20) to four or five replicate pairs of peaks. Uncertainties are quoted as plus or minus two standard deviations. Because the refractive index change per mole of SDS is about three times larger than that for NaCl(2) ($R_1/R_2 = 3.45 \pm 0.03$), the coefficients D_{11} and D_{12} for SDS(1) could be determined more precisely than coefficients D_{21} and D_{22} for NaCl(2). The present results are in good agreement with the less precise diffusion coefficients measured previously by a conductimetric method[18].

In Table 5-2 the interdiffusion coefficient of the SDS component (D_{11}) is compared with the lower eigenvalue of the diffusion coefficient matrix ($\mathcal{D}_1$). At the compositions that were used, the eigenvalue is 7-14% larger than the interdiffusion coefficient.

Several QELS diffusion studies on aqueous SDS/NaCl solutions[12,13,15] have been reported. It is generally agreed, however, that the results obtained by Corti and Degiorgio[13] are the most reliable[14]. In Figure 5-4 their values for the diffusion coefficient of SDS micelles in 0.100 mol L^{-1} NaCl solutions are compared with the Taylor results. At low SDS concentrations the two sets of data are in reasonably good agreement. But as the concentration of SDS is raised (and coupled diffusion becomes more important) the diffusion coefficients from the Taylor method fall about 15% below the QELS values. The discrepancy is not large, but it does contradict the interpretation that QELS gives the diffusion coefficient of the micelle species. If the diffusion of the actual micelle species was measured, the QELS diffusion coefficients would certainly be lower than the interdiffusion coefficient D_{11} of the total SDS component (micellar plus rapidly diffusing free ions) measured by Taylor experiments.

Table 5-1 Ternary interdiffusion coefficients of aqueous SDS(1)/NaCl(2) solutions at 25 °C

C_1(SDS)	C_2(NaCl)	D_{11}	D_{12}	D_{21}	D_{22}
0.100	0.030	0.194 ± 0.005	-0.271 ± 0.008	0.118 ± 0.010	1.667 ± 0.007
0.150	0.030	0.239 ± 0.006	-0.315 ± 0.013	0.082 ± 0.013	1.712 ± 0.011
0.020	0.100	0.108 ± 0.006	-0.050 ± 0.008	0.194 ± 0.006	1.505 ± 0.008
0.050	0.100	0.110 ± 0.004	-0.099 ± 0.010	0.196 ± 0.020	1.545 ± 0.010
0.100	0.100	0.129 ± 0.005	-0.161 ± 0.005	0.165 ± 0.008	1.595 ± 0.008
0.120	0.100	0.138 ± 0.005	-0.178 ± 0.005	0.143 ± 0.006	1.647 ± 0.012
0.050	0.200	0.099 ± 0.003	-0.067 ± 0.008	0.233 ± 0.011	1.495 ± 0.007
0.050	0.300	0.086 ± 0.005	-0.043 ± 0.005	0.256 ± 0.008	1.483 ± 0.007

Units: C_i in mol L^{-1}; D_{ik} in 10^{-5} cm^2 s^{-1}.

Table 5-2 Interdiffusion coefficient, apparent diffusion coefficient and lower eigenvalue for SDS(1) in aqueous NaCl(2) solutions at 25 °C

C_1(SDS)	C_2(NaCl)	D_{11}	$\mathcal{D}_1$	$100\frac{\mathcal{D}_1 - D_{11}}{D_{11}}$	D_{app}	$100\frac{D_{app} - D_{11}}{D_{11}}$
0.100	0.030	0.194	0.216	11	0.226	16
0.150	0.030	0.239	0.257	7	0.271	13
0.020	0.100	0.108	0.115	7	0.131	21
0.050	0.100	0.110	0.124	12	0.135	23
0.100	0.100	0.129	0.147	14	0.155	20
0.120	0.100	0.138	0.155	12	0.171	24
0.050	0.200	0.009	0.110	11	0.123	24
0.050	0.300	0.086	0.094	9	0.109	27

Units: C_i in mol L^{-1}; D_{ik}, $\mathcal{D}_1$, and D_{app} in 10^{-5} cm^2 s^{-1}.

Figure 5-4 Comparison of diffusion coefficients for SDS(1) in 0.100 mol L^{-1} aqueous NaCl(2) solutions at 25 °C. ▲, QELS[13]; ●, interdiffusion coefficient D_{11} from Taylor dispersion (this work); ○, eigenvalue $\mathcal{D}_1$ calculated from Taylor dispersion data.

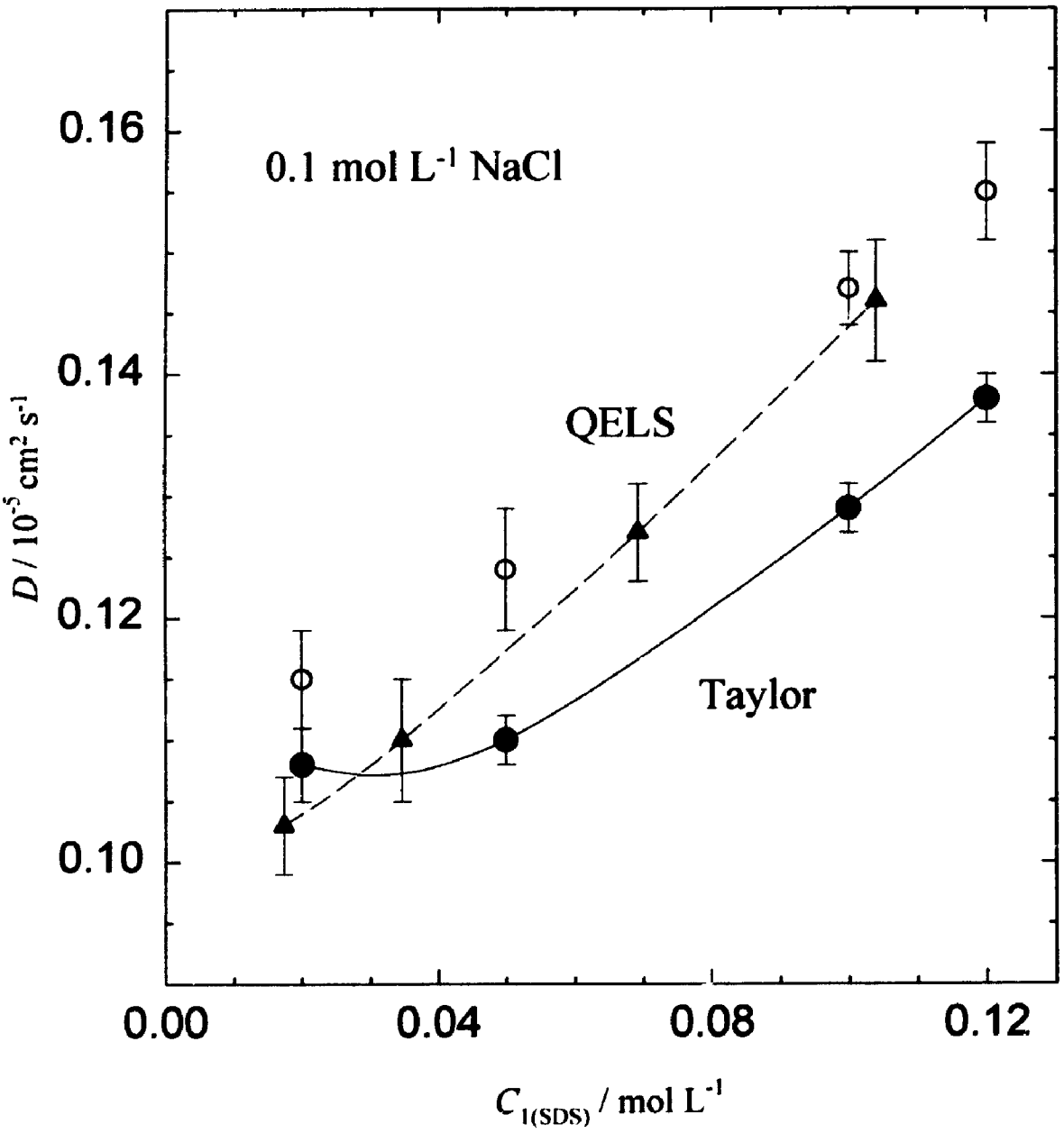
0.1 mol L-1 NaCl
QELS
Taylor
0.16
0.14
0.12
0.10
0.00
0.04
0.08
0.12
D / 10-5 cm2 s-1
C1(SDS) / mol L-1

The theory developed here suggests an explanation: the diffusion coefficient of SDS(1)/NaCl(2) solutions measured by QELS is actually the eigenvalue $\mathcal{D}_1$ of the interdiffusion coefficient matrix. To test this suggestion, the values of $\mathcal{D}_1$ calculated from the Taylor interdiffusion coefficient data are compared with the QELS coefficients in Figure 5-4. The rather good agreement supports the idea that QELS gives the lower eigenvalue of the diffusion coefficient matrix at higher concentration of SDS .

The refractivity ratio $R_1/R_2 = 3.45$ together with estimates of the chemical potential derivatives[18] were used to evaluate the relative weights of the terms in the correlation functions. The calculations confirmed that terms in $\mathcal{D}_1$ completely dominate the correlation functions. Therefore, in addition to the experimental evidence, theory also suggests that QELS diffusion measurements on SDS(1)/NaCl(2) solutions give the eigenvalue $\mathcal{D}_1$, not the diffusion coeffficient of the micelles or the diffusion coefficient D_{11} of the total SDS component.

If coupled diffusion is neglected in the analysis of the Taylor dispersion profiles for the SDS/NaCl solutions, this technique also gives apparent diffusion coefficients which were too high. A dispersion peak obtained by injecting excess SDS into a 0.100 mol L^{-1} SDS + 0.100 mol L^{-1} NaCl carrier stream is shown in Figure 5-3. Fitting the pseudo-binary dispersion equation

$$V(t) = a_0 + a_1 t + V_{max}(t_r/t)^{1/2} \exp[-12 D_{app}(t - t_r)^2 / r^2 t] \qquad (5.33)$$

to the peak gave $D_{app} = 0.155 \times 10^{-5}$ cm^2 s^{-1}, which is 20% higher than the interdiffusion coefficient of the SDS component at this composition.

5.5. Conclusions

The spectrum of light scattered by the concentration fluctuations in a multicomponent solution can be derived from the corresponding spectrum for a binary solution. In general, the QELS time-correlation functions for a multicomponent solution are multi-exponential decays with time constants governed by the eigenvalues of the interdiffusion coefficient matrix. In the favorable case of micelles dissolved in a salt solution, however, a single exponential decay dominates, and the lowest eigenvalue can

be determined. If the cross-diffusion coefficients can be safely neglected, the eigenvalue will equal the interdiffusion coefficient of the total micelle component (monomers + micelles). But in cases where cross-diffusion coefficients are not negligible, the measured eigenvalue will in general differ from the interdiffusion coefficient. For SDS micelles in aqueous NaCl solutions, the eigenvalue measured by QELS is up to 15% larger than the interdiffusion coefficient of the SDS component and the diffusion coefficient of the micelles.

5.6. References

1. P.J. Dunlop, K.R. Harris and D.J. Young, Experimental Methods for Studying Diffusion in Liquids. In *Physical Methods of Chemistry*, 2nd ed., vol.6, B. Rossiter, R.C. Baetzold, Eds., Wiley, New York, 1992, p. 229.
2. H.J.V. Tyrrell and K.R. Harris, *Diffusion in Liquids*, chapter 5, Butterworths, London, 1984.
3. J.N. Shaumeyer, R.W. Gammon and J.V. Sengers, In *Measurement of the Transport Properties of Fluids*, W.A. Wakeham, A. Nagashima, J.V. Sengers, Eds., Blackwell, London, 1991, p. 197.
4. K.J. Czworniak, H.J. Anderson and R. Pecora, *Chem. Phys.*, **11**, 451 (1975).
5. W. Krahn, G. Schweiger and K. Lucas, *J. Phys. Chem.* **87**, 4515 (1983).
6. E. Gulari, R.S. Brown and C. J. Pings, *AIChE J.*, **19**, 1196 (1973).
7. K. McKeigue and E. Gulari, *J. Phys. Chem.*, **88**, 3472 (1984).
8. T. Raj and W.H. Flygare, *Biochemistry*, **13**, 3336 (1974).
9. G.D.J. Phillies, G.B. Benedek and N.A. Mazer *J. Chem. Phys.*, **65**, 1883 (1976).
10. P. Doherty and G.B. Benedek, *J. Chem. Phys.*, **61**, 5426 (1974).
11. G.D. Neal, D. Purich and D.S. Cannell, *J. Chem. Phys.*, **80**, 3469 (1984).
12. N.A. Mazer, G.B. Benedek and M.C. Carey, *J. Phys. Chem.*, **80**, 1076 (1976).
13. M. Corti and V. Degiorgio, *J. Phys. Chem.*, **85**, 711 (1981).
14. J.P. Kratohvil and T.M. Aminabhavi, *J. Phys. Chem.*, **86**, 1254 (1982).
15. A. Rohde and E. Sackmann *J. Phys. Chem.*, **84**, 1598 (1980)

16. R. Finsey, A. Devriese and H.J. Lekkerker, *J. Chem. Soc., Faraday Trans. 2*, **76**, 767 (1980).

17. R.D. Mountain and J.M. Deutch, *J. Chem. Phys.*, **50**, 1103 (1969).

18. D.G. Leaist, *J. Colloid Interface Sci.*, **111**, 240 (1986).

19. D.G. Leaist, *J. Phys. Chem.*, **90**, 6600 (1986).

20. D.G. Leaist, *J. Phys. Chem.*, **93**, 474 (1989)

21. D.G. Leaist, *J. Colloid Interface Sci.*, **111**, 230 (1986).

22. R.M. Weinheimer, D.F. Evans and E.L. Cussler, *J. Colloid Interface Sci.*, **80**, 257 (1981).

23. D.F. Evans, S. Mukherjee, D.J. Mitchell and B.W. Ninham, *J. Colloid Interface Sci.*, **93**, 184 (1983).

24. W.H. Stockmayer, *J. Chem. Phys.*, **33**, 1291 (1960).

25. J. Lang, C. Tondre, R. Bauer, H. Hoffmann and W. Ulbricht, *J. Phys. Chem.*, **79**, 276 (1975).

26. E.A. Aniansson, S.N. Wall, M. Almgren, H. Hoffmann, I. Kielmann, W. Ulbricht, R. Zana, J. Lang and C. Tondre, *J. Phys. Chem.*, **80**, 905 (1976).

27. L. Onsager, *Ann. N.Y. Acad. Sci.*, **46**, 241 (1945).

28. H.L. Toor, *AEChE J.*, **10**, 448 (1964).

29. B.J. Berne and R. Pecora, *Dynamic Light Scattering*, Wiley, New York, 1976.

30. L. Onsager, *Phys. Rev.*, **37**, 405 (1931).

31. L. Onsager, *Phys. Rev.*, **28**, 2265 (1931).

32. D. McQuarrie, *Statistical Mechanics*, Harper and Row, New York, 1976, p. 567.

33. R. H. Robinson and R.H. Stokes, *Electrolyte Solutions*, 2nd ed., Academic, New York, 1959, p. 463.

34. C. Tanford, S.A. Swanson and W.S. Shore, *J. Am. Chem. Soc.*, **77**, 6414 (1955).

35. J.M. Creeth, *Biochem. J.*, **51**, 10 (1952).

36. I. Tinoco and P.A. Lyons, *J. Phys. Chem.*, **60**, 1342 (1956).

Chapter 6

A MODEL FOR INTERDIFFUSION OF IONIC MICELLES AND SOLUBILIZATES. AQUEOUS SOLUTIONS OF SODIUM DODECYLSULFATE AND *n*-ALCOHOLS

Taylor dispersion has been used to measure ternary interdiffusion coefficients for sodium dodecylsulfate (SDS)/*n*-hexanol/water and SDS/*n*-octanol/water. Surprisingly, the diffusion of solubilized octanol produces large *countercurrent* coupled flows of SDS. To help understand this result, Nernst-Planck equations are used to develop a model for the interdiffusion of solubilizates and ionic micelles. The model includes coupled transport of solubilizate driven by the electric field which is generated by the diffusion of the charged micelles and mobile counterions.

6.1. Introduction

Chapter 5 dealt with interdiffusion in solutions of ionic surfactants with added salt. In general, the diffusion of ionic surfactants and dissolved salts are strongly coupled by electrostatic interactions and by ion binding[1]. The present chapter is concerned with the ternary interdiffusion in solutions of SDS with added alcohols. The results provide new information about the coupled diffusion of ionic micelles and partially solubilized nonelectrolytes.

Oils and many other organic compounds that are almost insoluble in pure water can be solubilized in surfactant micelles[2,3] and transported into aqueous solutions where they would not otherwise be found. These processes have important practical applications related to detergency, petroleum recovery, biochemical separations, catalysis, digestion, and the controlled release of drugs and pesticides.

The diffusion of micelles and solubilizates has been extensively studied, mainly by NMR[2-6] and radioactive-tracer methods[7,8]. These techniques give *intradiffusion* coefficients[9-11] for the interchange of labelled and unlabelled species in solutions of

uniform chemical composition. An example would be the diffusion of a solution containing 0.100 mol L^{-1} SDS + 0.010 mol L^{-1} hexanol (tagged with ^{14}C) into a solution of 0.100 mol L^{-1} SDS + 0.010 mol L^{-1} hexanol (untagged). Intradiffusion is described by Fick's equation

$$j_i^* = -D_i^* \nabla C_i^* \qquad \text{(intradiffusion)} \qquad (6.1)$$

which relates the flux of labelled molecules (or ions) i to the gradient in the concentration of labelled species. Because the intradiffusion coefficient D_i^* of a partially solubilized molecule is the concentration-weighted average[13] of the diffusion coefficients of the unsolubilized and solubilized molecules, intradiffusion experiments provide valuable information about degrees of solubilization and micelle diffusion coefficients.

The work reported in this chapter is a study of a different kind of diffusion: chemical *interdiffusion*[9-11] of micelles and solubilizates. Interdiffusion (also called mutual diffusion) differs fundamentally from intradiffusion because there are gradients in chemical composition and coupled flows of chemical substances. An example would be the diffusion of a solution containing 0.100 mol L^{-1} SDS + 0.020 mol L^{-1} hexanol into a solution containing 0.100 mol L^{-1} SDS + 0.010 mol L^{-1} hexanol. Interdiffusion occurs in many physical and chemical processes, such as the attack and solubilization of oil droplets by surfactant micelles.

As described in Chapter 2, an accurate description of interdiffusion in three-component solutions of surfactant(1)/solubilizate(2)/solvent(0) should include two independent diffusional flows. Equations such as $J_1 = -D_1 \nabla C_1$ and $J_2 = -D_2 \nabla C_2$ are inadequate for this purpose because interactions between the flows of the components are neglected.

Interdiffusion in surfactant(1)/solubilizate(2)/solvent(0) solutions is described by the coupled Fick equations (2.46) and (2.47),

$$J_1 = -D_{11} \nabla C_1 - D_{12} \nabla C_2 \qquad (6.2)$$

(interdiffusion)

$$J_2 = -D_{21}\nabla C_1 - D_{22}\nabla C_2 \qquad (6.3)$$

This treatment is accurate because it includes two independent diffusional flows as well as cross-diffusion coefficients D_{12} and D_{21} to allow for the coupled flux of surfactant(1) caused by the gradient in solubilizate(2), and *vice versa*. If necessary, an expression for the flux of solvent (component 0, usually water) can be obtained from equations (6.2) and (6.3) by using the zero volume-flow constraint $J_1V_1 + J_2V_2 + J_0V_0 = 0$, where V_i is the partial molar volume of component i.

Coupled Fick equations are not abstract relations confined to advanced treatises on the theory of irreversible thermodynamics. In fact, equations (6.2) and (6.3) provide a practical description of diffusion in terms of well-defined concentrations and fluxes of total surfactant and total solubilizate components. Ideal-solution approximations are not required, and it is not necessary to make assumptions about the size, composition, polydispersity, or concentration of the micelles. Moreover, accurate D_{ik} coefficients can be measured by a variety of optical, conductimetric, diaphragm-cell, and flow techniques[8-10].

To illustrate these ideas, interdiffusion coefficients are reported here for aqueous solutions of sodium dodecylsulfate(SDS)/hexanol and SDS/octanol. Octanol, which is extensively solubilized in SDS micelles, was expected to carry significant amounts of SDS through the solutions. Yet diffusing octanol is found to produce large *countercurrent* coupled flows of SDS. A model for diffusion with solubilization is developed to provide a physical explanation for this surprising behaviour.

6.2. Experimental Procedure

Reagent-grade *n*-hexanol, *n*-octanol, and SDS ("specially pure") were used as received from BDH. Solutions were prepared in calibrated volumetric flasks with distilled, deionized water.

The ternary interdiffusion coefficients of SDS/hexanol/water and SDS/octanol/water solutions were measured by Taylor dispersion[9-13]. The dispersion tube used in this study was a 3334-cm-long Teflon capillary tube with an internal radius of 0.04738 cm. A metering pump maintained a steady flow of carrier solution through the tube at the flow

rates giving retention times of 7000-8000s. Samples of solution were introduced at the tube inlet through a low-pressure injection valve (Rheodyne model 50) fitted with a 20 μL sample loop. In most cases the injected solutions contained 0.010 mol L^{-1} excess SDS or excess alcohol relative to the carrier solution.

The broadened distribution of dispersed samples at the tube outlet was monitored by a deflection-type recording differential refractometer (Hewlett-Packard model 1047A). The refractometer output voltage $V(t)$ was measured with a digital voltmeter (Hewlett-Packard model 34401A) at accurately-timed 10-s intervals. The values of t and $V(t)$ were stored in a microcomputer. The least-squares method was used to fit equation (4.20) to pairs of peaks with initial gradients in SDS ($\alpha_1 = 1$) or alcohol ($\alpha_1 = 0$). Here α_1 is the fraction of the refractive index difference caused by the initial difference in the concentration of component 1, SDS. Diffusion coefficients D_{ik} were calculated according to the equations (4.23) to (4.26). The diffusion coefficients were measured 4-6 times at each carrier-stream composition and then averaged.

6.3. Results

Figure 6-1 shows dispersion profiles for aqueous SDS/octanol solutions. Peak 1 (initial gradient in SDS) was obtained by injecting a sample of 0.035 mol L^{-1} SDS + 0.005 mol L^{-1} octanol solution into a 0.025 mol L^{-1} SDS + 0.005 mol L^{-1} octanol carrier stream. For peak 2 (initial gradient in octanol), the injected solution contained 0.025 mol L^{-1} SDS + 0.015 mol L^{-1} octanol.

Dispersion profiles for non-interacting components resemble single-Gaussian peaks. Peak 2, however, is clearly not a single Gaussian. It consists of a negative Gaussian peak superimposed on a broader, positive Gaussian. This result shows that diffusing octanol produces a coupled flow of SDS.

The ternary diffusion coefficients measured in this study are summarized in Tables 6-2 and 6-3. In most cases the diffusion coefficients were reproducible within ± 0.01 x 10^{-5} cm^2 s^{-1}. Doubling the initial concentration differences did not change the results within the precision of the measurements. Hence the measured D_{ik} coefficients represent differential values at the composition of the carrier stream. Table 6-1 gives D_{ik} coefficients for aqueous

Figure 6-1 Dispersion profiles for a carrier stream containing 0.025 mol L^{-1} SDS(1) and 0.005 mol L^{-1} *n*-octanol(2):

Peak 1 (initial gradient in SDS(1)): ΔC_1 = 0.010 mol L^{-1}, ΔC_2 = 0.000 mol L^{-1};

Peak 2 (initial gradient in *n*-octanol(2)): ΔC_1 = 0.000 mol L^{-1}, ΔC_2 = 0.010 mol L^{-1}. Peak 2 has been offset for clarity.

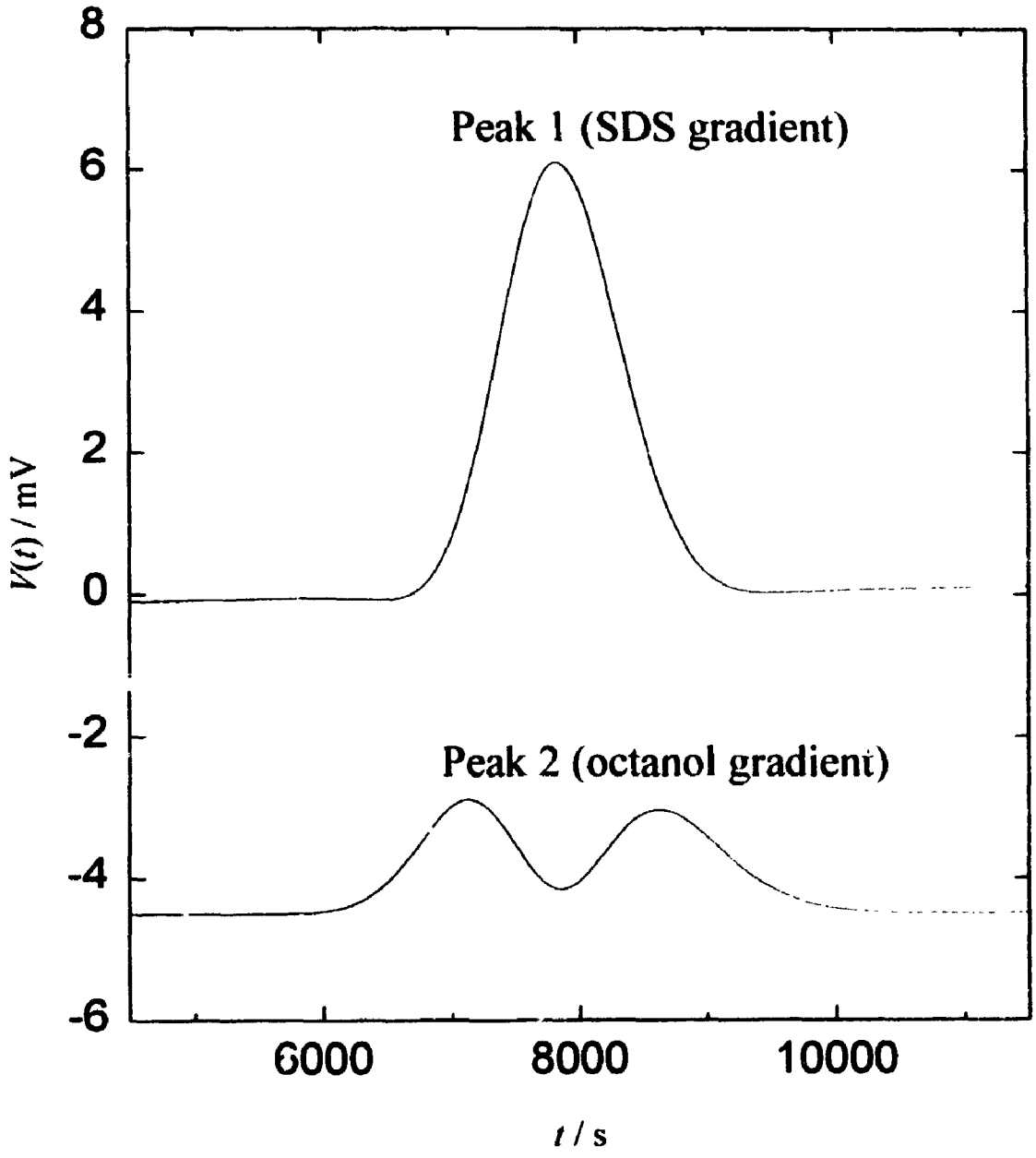
Peak 1 (SDS gradient)
Peak 2 (octanol gradient)
V(t) / mV
t / s
8
6
4
2
0
-2
-4
-6
6000
8000
10000

Table 6-1[a] Ternary interdiffusion coefficients of aqueous SDS(1)/*n*-butanol(2) solutions at 25 °C from ref. 14

(Predicted values in parentheses)

C_1	C_2	D_{11}	D_{12}	D_{21}	D_{22}
0.050	0.100	0.43(0.48)	0.04(0.02)	0.05(-0.12)	0.67(0.85)
0.100	0.050	0.47(0.52)	0.09(0.07)	0.02(-0.03)	0.63(0.76)
0.100	0.100	0.48(0.54)	0.12(0.07)	0.01(-0.06)	0.62(0.75)
0.100	0.200	0.46(0.59)	0.08(0.07)	0.01(-0.08)	0.68(0.73)
0.100	0.300	0.45(0.62)	0.07(0.07)	0.03(-0.06)	0.73(0.71)
0.200	0.100	0.51(0.58)	0.12(0.13)	0.09(-0.01)	0.59(0.63)
0.300	0.050	0.48(0.58)	0.12(0.18)	0.02(0.00)	0.54(0.53)
0.300	0.100	0.49(0.58)	0.17(0.18)	0.03(0.01)	0.57(0.53)
0.300	0.200	0.49(0.59)	0.13(0.17)	0.07(0.03)	0.58(0.53)
0.300	0.300	0.40(0.59)	0.12(0.16)	0.07(0.06)	0.58(0.53)

[a] Units: C_i in mol L^{-1}; D_{ik} in 10^{-5} cm^2 s^{-1}.

Table 6-2[a] Ternary interdiffusion coefficients of aqueous SDS(1)/*n*-hexanol(2) solutions at 25 °C

(Predicted values in parentheses)

C_1	C_2	D_{11}	D_{12}	D_{21}	D_{22}	R_2/R_1
0.025	0.000	0.29(0.30)	-0.08(-0.04)	0.00(0.00)	0.44(0.50)	0.33
0.050	0.000	0.41(0.40)	0.00(0.08)	-0.01(0.00)	0.30(0.34)	0.34
0.075	0.000	0.46(0.45)	0.05(0.15)	-0.01(0.00)	0.22(0.27)	0.34
0.100	0.000	0.50(0.49)	0.09(0.20)	-0.06(0.00)	0.17(0.23)	0.34
0.025	0.005	-0.06(-0.03)	0.33(0.34)	-0.04(-0.02)	0.42(0.47)	0.34
0.025	0.010	0.36(0.38)	-0.04(-0.01)	-0.05(-0.03)	0.39(0.44)	0.34
0.025	0.015	0.37(0.41)	0.00(0.00)	-0.04(-0.02)	0.32(0.42)	0.35
0.100	0.010	0.49(0.50)	0.12(0.20)	-0.01(0.02)	0.18(0.24)	0.35
0.100	0.030	0.45(0.51)	0.08(0.20)	0.12(0.08)	0.28(0.26)	0.34
0.100	0.050	0.42(0.51)	0.09(0.19)	0.21(0.14)	0.32(0.27)	0.34

[a] Units: C_i in mol L^{-1}; D_{ik} in 10^{-5} cm^2 s^{-1}.

Table 6-3[a] Ternary interdiffusion coefficients of aqueous SDS(1)/*n*-octanol(2) solutions at 25 °C

(Predicted values in parentheses)

C_1	C_2	D_{11}	D_{12}	D_{21}	D_{22}	R_2/R_1
0.015	0.000	0.21(0.23)	-0.39(-0.35)	0.00(0.00)	0.23(0.27)	0.42
0.025	0.000	0.28(0.30)	-0.22(-0.13)	0.00(0.00)	0.17(0.19)	0.45
0.050	0.000	0.40(0.40)	-0.06(0.07)	0.00(0.00)	0.13(0.14)	0.48
0.075	0.000	0.45(0.45)	-0.01(0.16)	0.00(0.00)	0.11(0.12)	0.46
0.100	0.000	0.48(0.49)	0.03(0.22)	0.00(0.00)	0.10(0.12)	0.47
0.025	0.005	0.35(0.38)	-0.14(-0.05)	0.04(0.04)	0.15(0.16)	0.46
0.025	0.010	0.40(0.42)	-0.11(0.00)	0.08(0.10)	0.14(0.17)	0.44
0.025	0.015	0.43(0.45)	-0.08(0.03)	0.15(0.17)	0.14(0.18)	0.44
0.100	0.010	0.48(0.50)	0.05(0.22)	0.03(0.04)	0.11(0.14)	0.48
0.100	0.030	0.48(0.50)	0.03(0.22)	0.10(0.12)	0.10(0.18)	0.46
0.100	0.050	0.49(0.50)	-0.06(0.21)	0.23(0.20)	0.06(0.21)	0.47

[a] Units: C_i in mol L^{-1}; D_{ik} in 10^{-5} cm^2 s^{-1}.

SDS/*n*-butanol solutions which were obtained in a previous study by using Harned restricted-diffusion conductivity cells[14].

A higher proportion of SDS diffuses in micellar form as the concentration of the surfactant is raised. Because micelles experience less frictional resistance than the equivalent amount of separate monomers[15], diffusion coefficient D_{11} for the total SDS(1) component increases with C_1. Increasing the concentration of SDS has the additional effect of solubilizing a higher proportion of alcohol (component 2). The transfer of free alcohol molecules to slower micelle species causes D_{22} to drop as the concentration of SDS is raised. Concentration gradients in SDS cannot produce coupled flows of alcohol in alcohol-free solution. Consequently, D_{21} drops to zero as $C_2/C_1 \rightarrow 0$. Similarly, $D_{12} \rightarrow 0$ as $C_1/C_2 \rightarrow 0$.

In the solutions studied here, *ca.* 40% of the butanol, 80% of the hexanol, and 90% of the octanol are solubilized by the SDS micelles[4]. The extensive solubilization led us to believe that diffusing SDS would carry significant amounts of alcohol through the solutions. Similarly, diffusing alcohol was expected to cotransport SDS. This mechanism, if correct, would lead to positive cross-diffusion coefficients. Table 6-1 shows that D_{12} and D_{21} are indeed positive for the SDS/butanol solutions.

Nearly all of the octanol is solubilized, so the largest cross-coefficients were anticipated for the SDS/octanol solutions. For this system, however, D_{12} is *negative* at most compositions. Thus diffusing octanol can produce counterflows of SDS. In some cases the magnitude of D_{12} exceeds that of D_{22}. This means that the counterflow of SDS produced by an octanol gradient can exceed the flow of octanol down its own gradient. The results for tracer diffusion of octanol ($C_2 = 0$) are interesting: D_{12} is negative at low SDS concentrations but it turns positive as the concentration of SDS is raised (see Table 6-3).

Table 6-2 shows that SDS/hexanol solutions also have negative cross-coefficients, but the values are smaller in magnitude than those of the SDS/octanol solutions.

6.4. Discussion

The interdiffusion coefficients presented in this chapter refer to flows of total SDS and total alcohol components. To help understand the results, a model for the interdiffusion

of micelles and solubilizates will be developed by relating the flows of components to the flows of micelles and other species that actually diffuse through the solutions. One of the goals is to provide an explanation for the counterflows of surfactant caused by diffusing solubilizates.

Relation Between the Diffusion Coefficients of the Components and Solution Species The SDS and alcohol components diffuse primarily as polydisperse $(Na^+)_q(DS\text{-})_n(ROH)_a^{q-n}$ mixed micelles consisting of associated dodecylsulfate ions, solubilized alcohol molecules, and bound sodium counterions. Smaller amounts of free aqueous dodecylsulfate ions, unbound sodium ions, and unsolubilized alcohol molecules are also present in the solutions.

If solution species s contains ν_{1s} dodecylsulfate ions, then the molar flux j_s of species s contributes $\nu_{1s}j_s$ to the total flux J_1 of the SDS(1) component. Species s also contributes $\nu_{2s}j_s$ to the flux of total alcohol(2), where ν_{2s} is the number of alcohol molecules carried by species s. Summing over all the solution species gives

$$J_1 \text{ (total SDS)} = \sum_s \nu_{1s} j_s \tag{6.4}$$

$$J_2 \text{ (total ROH)} = \sum_s \nu_{2s} j_s \tag{6.5}$$

In the following treatment the Nernst-Planck equations[16]

$$j_s \text{ (species s)} = -D_s \nabla c_s + \frac{F}{RT} z_s c_s D_s E \tag{6.6}$$

are used to estimate the fluxes of the species. The term $-D_s\nabla c_s$ is the "pure-diffusion" flux of species s down its concentration gradient. The term $(F/RT)z_sc_sD_sE$ is the flux of species s driven by the electric field E which is generated by the diffusion of charged species with unequal mobilities, such as ionic micelles and counterions. D_s and ∇c_s are the diffusion coefficient and the gradient in concentration of species s, F is the Faraday constant, R the gas constant, T the temperature, and z_s the charge number of species s.

Nernst-Planck equations are reliable for dilute solutions where interactions between the diffusing species are negligible, except for the electric field and rapid association/dissociation reactions. It might seem unnecessary to include electric-field terms

in a model for the transport of uncharged alcohols. In SDS solutions, however, most of the alcohol molecules are transported in charged micelles.

By combining the Nernst-Planck and coupled Fick equations, the interdiffusion coefficients can be decomposed[17]

$$D_{ik} = D_{ik(D)} + D_{ik(E)} \tag{6.7}$$

into the contribution $D_{ik(D)}$ from pure diffusion down concentration gradients

$$D_{ik(D)} = \sum_s \nu_{is} D_s \frac{\partial c_s}{\partial C_k} \tag{6.8}$$

and the contribution $D_{ik(E)}$

$$D_{ik(E)} = -\sum_q \sum_s \frac{\nu_{iq} t_q}{z_q} z_s D_s \frac{\partial c_s}{\partial C_k} \tag{6.9}$$

from the migration of charged species caused by the electric field. t_q is the transport number of species q.

$$t_q = z_q^2 c_q D_q \; / \; \sum_s z_s^2 c_s D_s \tag{6.10}$$

Equations (6.7)-(6.9) illustrate that interdiffusion coefficients are not concentration-weighted averages of the diffusing species. Coefficient D_{22} for the alcohol component, for example, is not the average diffusion coefficient $\Sigma \nu_{2s} c_s D_s / C_2$ of the alcohol-containing species.

Concentrations of the Solution Species Equations (6.7)-(6.9) can be used to predict surfactant-solubilizate interdiffusion coefficients from estimates of the concentrations and diffusion coefficients of the solution species. Because the exchange of ions and alcohol molecules between micelles is very rapid[2,18] compared to the timescale of Taylor dispersion and other macroscopic diffusion experiments, local equilibrium exists along the diffusion path. In particular, smaller micelles cannot diffuse ahead of the larger, slower micelles before exchange occurs. Time-averaging over the solution species allows the diffusion of polydisperse collection of $[(Na^+)_q(DS^-)_n(ROH)_a]^{q-n}$ micelles to be accurately approximated by the diffusion of monodisperse micelles of the same average size and composition[15]. Suppose that each micelle contains a fixed number (n) of dodecylsulphate ions. The number of bound counterions (q) and solubilized alcohol

molecules (a) per micelle are not constant[19-22]: added alcohol increases a. In addition, the insertion of alcohols into dodecylsulfate micelles reduces the charge density. This leads to a decrease in the number of bound counterions, and hence added alcohol decreases q.

In previous studies, ion association constants were used to calculate the concentrations of micelles, surfactant ions, and counterions in aqueous SDS solutions[1,15,22-25]. Unfortunately, it is difficult to extend this approach to the SDS/alcohol solutions studied here because association constants are not available for the formation of the numerous micelle species, such as ...., $[(Na^+)_{49}(DS^-)_n]^{49-n}$, $[(Na^+)_{49}(DS^-)_n(ROH)]^{49-n}$, $[(Na^+)_{49}(DS^-)_n(ROH)_2]^{49-n}$, ..., $[(Na^+)_{50}(DS^-)_n]^{50-n}$, $[(Na^+)_{50}(DS^-)_n(ROH)]^{50-n}$, $[(Na^+)_{50}(DS^-)_n(ROH)_2]^{50-n}$, ...

Instead, we will use phase partition equilibria to estimate the concentrations of the solution species. Consider first the distribution of alcohol molecules between aqueous and micelle pseudo-phases. According to the pseudo-phase model[13], the concentration of alcohol in the micelle phase divided by the concentration of free alcohol in the aqueous phase is constant.

$$K_a = \frac{n_{ROH}(mic)/V(mic)}{n_{ROH}(aq)/V(aq)} = \frac{\beta}{1-\beta}\,\frac{1 - nc_{mTOT}V_1 - \beta C'_2V_2}{nc_{mTOT}V_1 + \beta C'_2V_2} \qquad (6.11)$$

Here β is the fraction of the total alcohol that is solubilized and c_{mTOT} is the sum of the concentrations of the micelles. V_1 and V_2 are the respective molar volumes of surfactant and alcohol, and hence the volume fractions of the aqueous and micellar phases are $1 - nc_{mTOT}V_1 - \beta C'_2V_2$ and $nc_{mTOT}V_1 + \beta C'_2V_2$, respectively. The recommended values[1,4,16,24,25] $n \cong 60$ and $V_1 \cong 0.25$ L mol^{-1} will be used for the aggregation number and molar volume of dodecylsulphate ions. Molar volumes and partition coefficients for butanol, hexanol, and octanol are listed in Table 6-4. The molar ratio of micellar to aqueous dodecylsulphate ions is $nc_{mTOT}/(C_1 - nc_{mTOT})$, which gives

$$K_m = \frac{nc_{mTOT}}{C_1 - nc_{mTOT}}\,\frac{1 - nc_{mTOT}V_1 - \beta C'_2V_2}{nc_{mTOT}V_1 + \beta C'_2V_2} \qquad (6.12)$$

for the distribution of dodecylsulphate ions. At the critical micelle concentration of alcohol-free aqueous SDS solutions (0.008 mol L^{-1} at 25 °C)[26], we have $C_1 = 0.008$ mol L^{-1}, $C'_2 = 0$, $c_{mTOT} = 0$, and hence $K_m = 500$.

Given the concentrations C_1 and C_2 of total SDS(1) and total alcohol(2) components, equations (6.11) and (6.12) can be solved for c_{mTOT} and β. The concentrations of free dodecylsulphate ions and free alcohol molecules can then be calculated

$$c_{DS^-} = C_1 - n c_{mTOT} \tag{6.13}$$

$$c_{ROH} = (1 - \beta) C_2 \tag{6.14}$$

together with the average number of solubilized alcohol molecules per micelle

$$a_{AVG} = (C_2 - c_{ROH}) / c_{mTOT} \tag{6.15}$$

To allow for changes in the extents of solubilization and counterion binding, two micellar species will be included in the model: $(Na^+)_q(DS^-)_n(ROH)_{a-}$ and $(Na^+)_{q+}(DS^-)_n(ROH)_{a+}$. The number of alcohol molecules carried by the two micelles are a_- and a_+, the integers immediately below and above a_{AVG}. If a_{AVG} is 15.7, for instance, then a_- and a_+ are 15 and 16, respectively. The concentrations c_{m-} and c_{m+} of the micelles can be evaluated from mass balance.

$$C_1 = c_{DS^-} + n c_{m-} + n c_{m+} \tag{6.16}$$

$$C_2 = c_{ROH} + a_- c_{m-} + a_+ c_{m+} \tag{6.17}$$

A careful analysis of sodium-ion EMF data[19] indicates that the extent of counterion binding decreases with the mole fraction of alcohol in the micelles (x_a): $q/n = (q_0/n)(1 - x_a)/[1 - (q_0/n)x_a]$, where q_0 is the number of counterions bound to alcohol-free micelles (see Figure 6-2). Adapting this result to the problem at hand gives

$$q_- = q_0 \left(1 - \frac{a_-}{n + a_-}\right) / \left(1 - \frac{q_0}{n}\frac{a_-}{n + a_-}\right) \tag{6.18}$$

$$q_+ = q_0 \left(1 - \frac{a_+}{n + a_+}\right) / \left(1 - \frac{q_0}{n}\frac{a_+}{n + a_+}\right) \tag{6.19}$$

for the average number of sodium counterions bound to the micelles. Reported[23] extents of counterion binding suggest that q_0/n lies in the range from 0.78 to 0.86. We will use the values $q_0 = 50$ and $n = 60$ which correspond to 83% counterion binding to alcohol-free micelles.

Finally, the concentration c_{Na^+} of free counterions is calculated from the mass balance relation

Figure 6-2 Extent of counterion binding to $(Na^+)_q(DS^-)_n(ROH)_a^{q-n}$ mixed micelles plotted against the mole fraction of alcohol in the micelles.

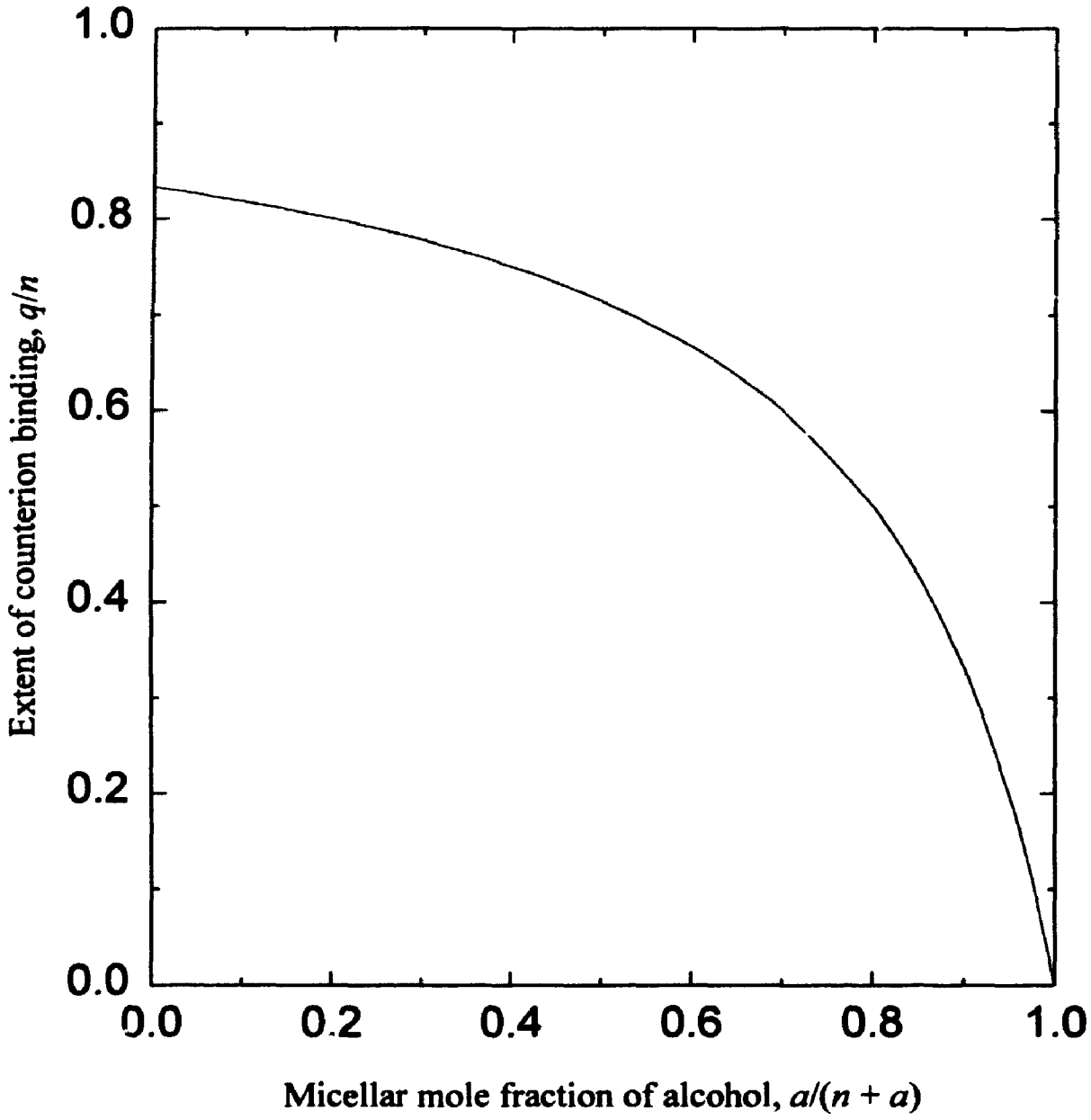
1.0
0.8
0.6
0.4
0.2
0.0
0.0
0.2
0.4
0.6
0.8
1.0
Extent of counterion binding, q/n
Micellar mole fraction of alcohol, a/(n + a)

Table 6-4 Diffusion coefficients, molar volumes, and partition coefficients of *n*-alcohols

alcohol	D / 10^{-5} cm^2 s^{-1}	V_2 / L mol^{-1}	K_a
butanol	0.97[a]	0.09	13[b]
hexanol	0.83	0.13	190[b]
octanol	0.59	0.16	1100[b]

[a]ref. 30; [b]ref. 4.

$$C_1 = c_{Na^+} + q_- c_{m-} + q_+ c_{m+} \tag{6.20}$$

Diffusion Coefficients of the Solution Species All that remains to complete the model of micelle-solubilizate interdiffusion is to estimate the diffusion coefficients of the solution species. For the free aqueous DS^- and Na^+ ions, the respective limiting diffusion coefficients[27,28] 0.61 x 10^{-5} and 1.33 x 10^{-5} $cm^2\ s^{-1}$ will be used. The limiting diffusion coefficients[30] of aqueous butanol, hexanol, and octanol molecules are listed in Table 6-4.

It is more difficult to estimate the diffusion coefficients of the micelles. For alcohol-free micelles ($a = 0$), we will use the diffusion coefficient $D_{m0} = 0.10$ x 10^{-5} $cm^2\ s^{-1}$ recommended in studies[15,23,24] of binary SDS/water solutions. For spherical micelles, Stoke's law suggests that the micelle diffusion coefficients are proportional to the reciprocal of the cube root of the micelle volume, and hence

$$D_{m-} = \left(\frac{nV_1}{nV_1 + a_- V_2}\right)^{1/3} D_{m0} \tag{6.21}$$

$$D_{m+} = \left(\frac{nV_1}{nV_1 + a_+ V_2}\right)^{1/3} D_{m0} \tag{6.22}$$

For computational purposes, the solution species were numbered: 1. $(Na^+)_{q-}(DS^-)_{60}(ROH)_{a-}$, 2. $(Na^+)_{q+}(D\ \ )_{60}(ROH)_{a+}$, 3. Na^+, 4. DS^-, 5. ROH, which defines the matrix of ν_{is} coefficients

$$\nu = \begin{pmatrix} 60 & 60 & 0 & 1 & 0 \\ a_- & a_+ & 0 & 0 & 1 \end{pmatrix} \tag{6.23}$$

and gives q_- - 60, q_+ - 60, 1, -1, and 0 for the charge numbers z_1 through z_5.

Predicted Interdiffusion Coefficients Measured and predicted interdiffusion coefficients for the SDS(1)/alcohol(2) solutions are compared in Tables 6-1, 6-2, and 6-3 . In most cases the predicted values are too large, probably because limiting diffusion coefficients and other dilute-solution approximations were used in model. Also, possible changes in the shape and structure[6,30,31] of micelles caused by solubilization are not included in the model.

Despite these limitations, the prediction of negative D_{12} values supports the puzzling experimental result that solubilizates can drive counterflows of surfactant. Also, trends in the diffusion behaviour are correctly predicted. For example, the model confirms that diffusing octanol cotransports SDS at high concentrations of the surfactant and countertransports SDS at low surfactant concentrations.

To explain how the diffusion of a solubilizate produces a counterflow of surfactant, consider what happens when a gradient in alcohol concentration is imposed on a dilute solution of SDS. These solutions contain relatively few micelles. When alcohol is added, solubilization of the alcohol molecules causes a significant drop in the activity of the surfactant in the micelle pseudo-phase. Equilibrium is regained by the transfer of aqueous surfactant ions to the micelle pseudo-phase. The formation of new micelles at the expense of free DS^- and Na^+ ions is reflected by the lowering of the critical micelle concentration and by the drop in electrical conductivity caused by added alcohol[121]. In fact, alcohols are frequently used as cosurfactants in preparation of microemulsions. Because a solution with a higher alcohol content is depleted in free Na^+ and DS^- ions, these relatively mobile ions will diffuse down their concentration gradients toward regions of higher alcohol concentration. The net result is a coupled flow of the SDS(1) up the alcohol gradient, and hence D_{12} is negative.

Figure 6-3 shows values of D_{12} predicted for solutions containing SDS and traces of octanol. In this case the octanol gradient is predicted to drive counterflows of SDS at concentrations of SDS below 0.040 mol L^{-1}. Here the largest contribution to D_{12} is made by the pure-diffusion term $D_{12(D)}$, which is also plotted in Figure 6-3. A term by term study of equation (6.8) showed that the coupled diffusion of DS^- ions makes the largest contribution to $D_{12(D)}$. In a solution containing 0.025 mol L^{-1} SDS, for example, the octanol gradient produces a substantial gradient of opposite sign in the concentration DS^- ions: $\partial c_{DS}/\partial C'_2$ = -0.248. The octanol gradient also produces counterdiffusion of free Na^+ ions ($\partial c_{Na}/\partial C'_2$ = -0.092) which makes an additional contribution to the counterflow of the total SDS component.

The model suggests a transition to different diffusion behaviour as the concentration of SDS is raised. Figure 6-3 shows that the electrical term $D_{12(E)}$ dominates D_{12} at higher

Figure 6-3 Predicted cross-diffusion coefficient D_{12} for aqueous solutions of SDS(1)/*n*-octanol(2) solutions containing trace amounts of *n*-octanol. Dashed curves: $D_{12(D)}$, contribution to D_{12} from pure diffusion; $D_{12(E)}$, contribution to D_{12} from the transport of charged species driven by the electric field.

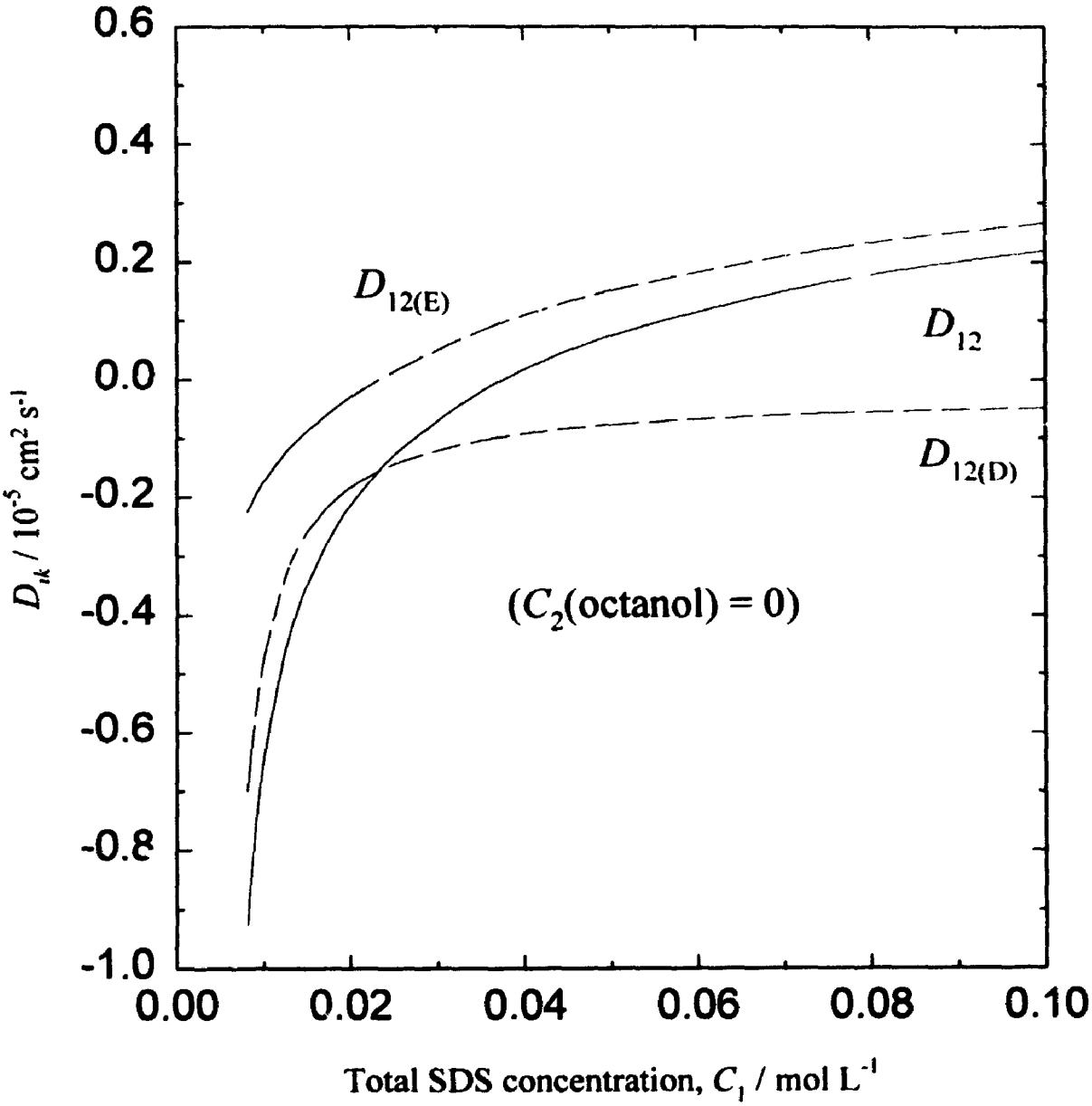
0.6
0.4
0.2
0.0
-0.2
-0.4
-0.6
-0.8
-1.0
0.00
0.02
0.04
0.06
0.08
0.10
$D_{12(E)}$
D_{12}
$D_{12(D)}$
(C_2(octanol) = 0)
D_{ik} / 10^{-5} cm^2 s^{-1}
Total SDS concentration, C_1 / mol L^{-1}

Figure 6-4 *n*-Octanol(2) interdiffusion coefficient D_{22} predicted for aqueous solutions containing 0.100 mol L^{-1} SDS(1). Dashed curves: $D_{22(D)}$, contribution to D_{22} from pure diffusion; $D_{22(E)}$, contribution to D_{22} from transport driven by the electric field.

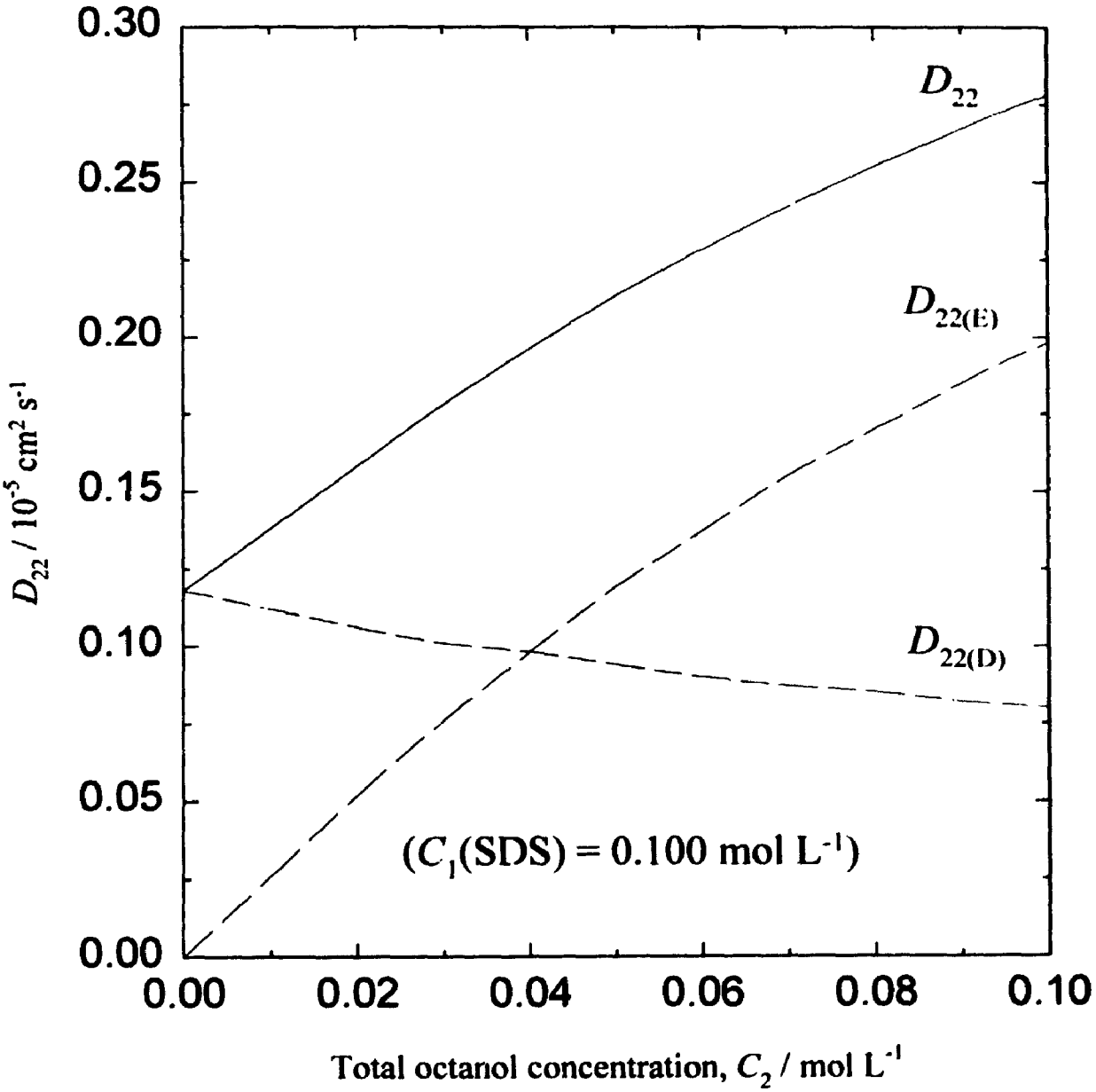
0.30
0.25
0.20
0.15
0.10
0.05
0.00
0.00
0.02
0.04
0.06
0.08
0.10
D_{22}
$D_{22(E)}$
$D_{22(D)}$
$(C_1(SDS) = 0.100$ mol $L^{-1})$
D_{22} / 10^{-5} cm^2 s^{-1}
Total octanol concentration, C_2 / mol L^{-1}

SDS concentrations. In these solutions solubilized alcohol releases bound sodium counterions from the micelles, as indicated by an increase in the electrical conductivity[20]. An electric field is generated to slow down the mobile Na^+ ions as they diffuse down the octanol gradient, thereby preventing charge separation. The field pulls negatively-charged micelles and DS^- ions along with the Na^+ ions. Octanol cotransports SDS by this electrostatic mechanism. For a 0.100 mol L^{-1} SDS solution, the model developed here gives $\partial c_{Na^+}/\partial C_2 = + 0.088$ and $\partial c_{DS^-}/\partial C_2 = - 0.053$, which illustrates that added alcohol leads to a net increase in the concentration of free ions.

In Figure 6-4, predicted values of the octanol diffusion coefficient, D_{22}, are plotted against the octanol concentration for solutions containing 0.100 mol L^{-1} SDS. The contributions to D_{22} from pure diffusion ($D_{22(D)}$) and migration in the electric field ($D_{22(E)}$) are also shown. Raising the concentration of octanol produces a small decrease in $D_{22(D)}$ because the micelles become swollen with solubilized alcohol and therefore diffuse more slowly. As mentioned above, gradients in octanol cause the diffusion of charged micelles and sodium counterions, which in turn generates an electric field. As a result, the pure diffusion of octanol down its concentration gradient is augmented by the migration of solubilized octanol in the electric field. At octanol concentrations above 0.040 mol L^{-1}, $D_{22(E)}$ is predicted to exceed $D_{22(D)}$ which suggests that the flux of octanol driven by the electric field can exceed the pure-diffusion flux of octanol down its concentration gradient.

6.5. Conclusions

Interdiffusion coefficients, including cross-coefficients, for ionic surfactants and solubilizates, can be determined by the Taylor dispersion technique. The results for aqueous SDS/*n*-alcohol solutions indicate strong coupling between the diffusing components. In some cases the cross-coefficients are larger than the main interdiffusion coefficients.

A model for the interdiffusion of surfactants and solubilizates can be developed by using Nernst-Planck equations to relate the flows of surfactant and solubilizate components to the flows of micelles, counterions, and other solution species. Quantitative agreement with experiment is not obtained. Nevertheless, the model provides physical explanations

for the measured diffusion properties, including the countertransport of surfactant caused by the diffusion of solubilizate. Also, the model shows that the electric field generated by the diffusion of free counterions and charged micelles makes an important contribution to transport of neutral solubilizates. Other important features are the release of bound counterions and the lowering of the critical micelle concentration caused by solubilization.

6.6. References

1. D. G. Leaist, *J. Colloid Interface Sci.*, **111**, 240 (1986)
2. D. Langevin, *Annu. Rev. Phys. Chem.*, **43**, 341 (1992)
3. B. Lindman and P. Stilbs in *Surfactants in Solution*, eds. K. L. Mittal and B. Lindman, Plenum, New York, 1984, vol. 3, p. 1651
4. P. Stilbs, *J. Colloid Interface Sci.*, **87**, 385 (1982)
5. B. Lindman and B. Brun, *J. Colloid Interface Sci.*, **43**, 388 (1973)
6. P. Stilbs, *J. Colloid Interface Sci.*, **89**, 547 (1982)
7. D. Stigter, R. J. Williams and K. J. Mysels, *J. Phys. Chem.*, **59**, 330 (1955)
8. H. Fabre, N. Kamenka and B. Lindman, *J. Phys. Chem.*, **85**, 3493 (1981)
9. P. J. Dunlop, K. R. Harris and D. J. Young, Experimental Methods for Studying Diffusion in Liquids. In *Physical Methods of Chemistry*, eds. B. Rossiter and R. C. Baetzold, Wiley, New York, 2nd edn., 1992, vol. 6
10. H. J. V. Tyrrell and K. R. Harris, *Diffusion in Liquids*, Butterworths, London, 1984
11. *Measurement of the Transport Properties of Fluids*, eds. W. A. Wakeham, A. Nagashima and J. V. Sengers, Blackwell, London, 1991
12. K. C. Pratt and W. A. Wakeham, *Proc. Roy. Soc. London Ser. A*, **342**, 401 (1975)
13. A. Alizadeh, C. A. Nieto de Castro and W. A. Wakeham, *Int. J. Thermophys.*, **1**, 243 (1980)
14. D. G. Leaist, *Can. J. Chem.*, **68**, 33 (1990)
15. D. G. Leaist, *J. Colloid Interface Sci.*, **111**, 230 (1986)
16. J. S. Newman, *Electrochemical Systems*, Prentice Hall, Englewood Cliffs, 1973
17. D. G. Leaist and L. Hao, *J. Chem. Soc. Faraday Trans.*, **89**, 2775 (1993)

18. E. A. G. Aniansson, S. N. Wall, M. Almgren, H. Hoffman, I. Kielmann, W. Ulbricht, R. Zana, J. Lang, and C. Tondre, *J. Phys. Chem.*, **80**, 905 (1976)

19. D. G. Hall and T. J. Price, *J. Chem. Soc., Faraday Trans. 1*, **80**, 1193 (1984)

20. M. Manabe, H. Kawamura, A. Yamashita and S. Tokunaga, *J. Colloid Interface Sci.*, **115**, 147 (1987)

21. S. Backlund and K. Lundt, *Acta Chem. Scand. A*, **34**, 433 (1980)

22. J. F. Rathman and J. F. Scamehorn, *J. Phys. Chem.*, **88**, 5807 (1984)

23. R. M. Weinheimer, D. F. Evans and E. L. Cussler, *J. Colloid Interface Sci.*, **80**, 357 (1981)

24. D. F. Evans, S. Mukherjee, D. J. Mitchell and B. W. Ninham, *J. Colloid Interface Sci.*, **93**, 184 (1983)

25. D. G. Leaist and L. Hao, *J. Phys. Chem.*, **87**, 7763 (1993)

26. P. Mukerjee and K. J. Mysels, *Critical Micelle Concentrations of Aqueous Surfactant Solutions*, Natl. Stand. Ref. Data Ser., Natl. Bur. Stand. (U. S.), Washington, 1971

27. R. A. Robinson and R. H. Stokes, *Electrolyte Solutions*, Academic, New York, 2nd edn., 1959

28. G. D. Parfitt and A. L. Smith, *J. Phys. Chem.*, **66**, 942 (1962)

29. D. G. Leaist, *J. Solution Chem.*, **20**, 175 (1991)

30. I. Vikholm, G. Douheret, S. Backlund and H. Høiland, *J. Colloid Interface Sci.* , **116**, 582 (1987)

31. H. Høiland, A. M. Bolkhus, O. J. Kvammen and S. Backlund, *J. Colloid Interface Sci.* **107**, 576 (1985)

Chapter 7

INTERDIFFUSION IN AQUEOUS SOLUTIONS OF SODIUM CHOLATE

This chapter is concerned with diffusion in aqueous solutions of sodium cholate (SC), an important biosurfactant. The results are used to estimate the critical micelle concentration (cmc) and the aggregation number of SC micelles. In addition, ternary interdiffusion coefficients for aqueous solutions of SC(1)/*n*-decanol(2) and SC(1)/*n*-octanol(2) are reported. The results suggest that the diffusion of SC and solubilizates is similar to the diffusion of sodium dodecylsulfate (SDS)/solubilizate systems (Chapter 6), although coupled diffusion in the SC solutions is stronger. The ternary diffusion coefficients predicted by the model developed in chapter 6 are in reasonably good agreement with the experimental results despite the polydispersity of SC micelles.

7.1. Introduction

Sodium cholate (SC) plays a vital role as a surfactant in biological systems, particularly in fat digestion, cholesterol solubilization, and drug absorption[1,2]. The properties of aqueous sodium cholate solution have been studied intensively by a number of techniques, including light scattering[3-5], NMR[6-8], surface tension measurements[9-12], ESR[13-15], fluorescence spectroscopy[13-16], microcalorimetry[17], ultrasonic absorption[18], potentiometry[19,20], osmometry[21-25], density measurements[18,26-28], X-ray diffraction[8,29], solubilization measurements[30-35], phase partitioning[36], and refractive index measurements[19,37]. The transport properties of aqueous SC solutions have also been studied, including viscosity[7,27,38], conductivity[9,26,39], and intradiffusion measurements[40-43]. It appears, however, that chemical interdiffusion in SC solutions has not been studied.

Interdiffusion in surfactant solutions has been most thoroughly studied for aqueous solutions of sodium dodecylsulfate (SDS). SDS, a long-chain anionic surfactant, forms relatively large micelles (aggregation number ~60). By contrast, SC, a polycyclic anionic surfactant (see Figure 7-1), forms relatively small micelles[44]. Moreover, cholate micelles are polydisperse, without a well defined cmc[45]. Reported aggregation numbers, degrees of

Figure 7-1 Chemical structure of sodium cholate

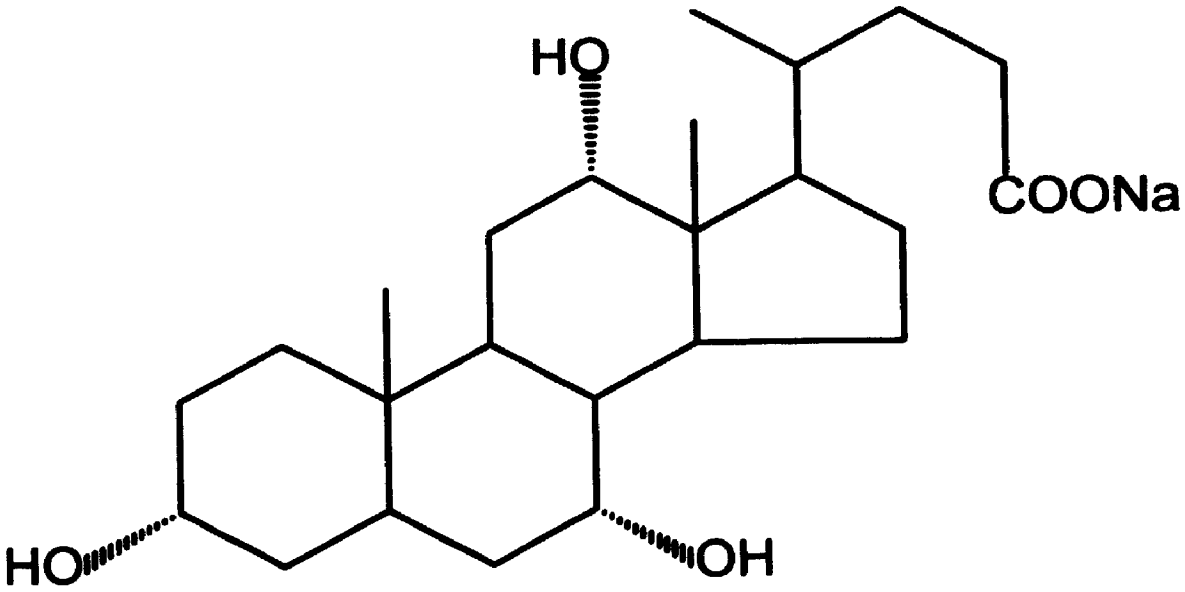
HO
COONa
HO
OH

bound counterions and cmc's for aqueous SC solutions range from 3 to 16, 0.04 to 0.70, and 0.003 to 0.018 mol L^{-1}, respectively[3,10,16,20,24,32,39,45]. Because of these inconsistencies, the intriguing properties of SC solutions are still under active investigation. In this chapter interdiffusion coefficients are reported for aqueous SC solutions. The results are compared with previously reported intradiffusion coefficients for aqueous SC solutions. In addition, ternary interdiffusion coefficients are reported for aqueous SC(1)/decanol(2) and SC(1)/octanol(2) solutions. These results provide new information on the interaction between solubilizates and SC.

7.2. Experimental Procedure

Reagent-grade (> 99% purity) sodium cholate (Sigma), *n*-decanol, *n*-octanol and sodium dodecylsulfate (BDH) were used as received. Solutions were prepared in calibrated volumetric flasks with distilled, deionized water.

Taylor dispersion was used to measure the binary interdiffusion coefficient of aqueous SC solutions and the ternary interdiffusion coefficients of aqueous SC/decanol and SC/octanol at 25 °C. For comparison with the results for binary aqueous SC solutions, a few diffusion measurements were made for binary aqueous SDS solution. The experimental procedure and the least-squares analysis of the dispersion profiles are described in Chapters 4 and 6. The injected solutions typically contained 0.005 mol L^{-1} excess SC, 0.015 mol L^{-1} excess octanol, or 0.010 mol L^{-1} excess decanol relative to the carrier solutions.

7.3. Results and Discussion

Binary Interdiffusion Coefficients of Sodium Cholate Solutions The binary interdiffusion coefficient of aqueous sodium cholate was measured at 14 different SC concentrations, from 0.001 to 0.100 mol L^{-1}. The results are summarized in Table 7-1. The reproducibility of measured diffusion coefficients was better than ± 0.5%. In Figure 7-2, the values of the interdiffusion coefficient of aqueous SC are plotted against the concentration of the surfactant. For comparison, previously reported interdiffusion

Table 7-1 Binary interdiffusion coefficients of aqueous SC solutions at 25 °C

C	*D*	*C*	*D*	*C*	*D*
0.001	0.681	0.016	0.569	0.040	0.487
0.004	0.672	0.020	0.529	0.050	0.482
0.008	0.655	0.024	0.505	0.075	0.440
0.010	0.639	0.028	0.498	0.100	0.439
0.012	0.620	0.032	0.492		

Units: C in mol L^{-1}; D in 10^{-5} cm^2 s^{-1}.

Figure 7-2 Diffusion coefficients of aqueous surfactant solutions plotted against the concentration of surfactant at 25 °C: ◇, interdiffusion coefficient of SDS (ref. 46); O, interdiffusion coefficient of SDS (this work); ●, interdiffusion coefficient of SC (this work); ▲, intradiffusion coefficient of cholate ions in aqueous SC solutions (ref. 40); ▼, intradiffusion coefficient of sodium ions in aqueous SC solutions (ref. 40)

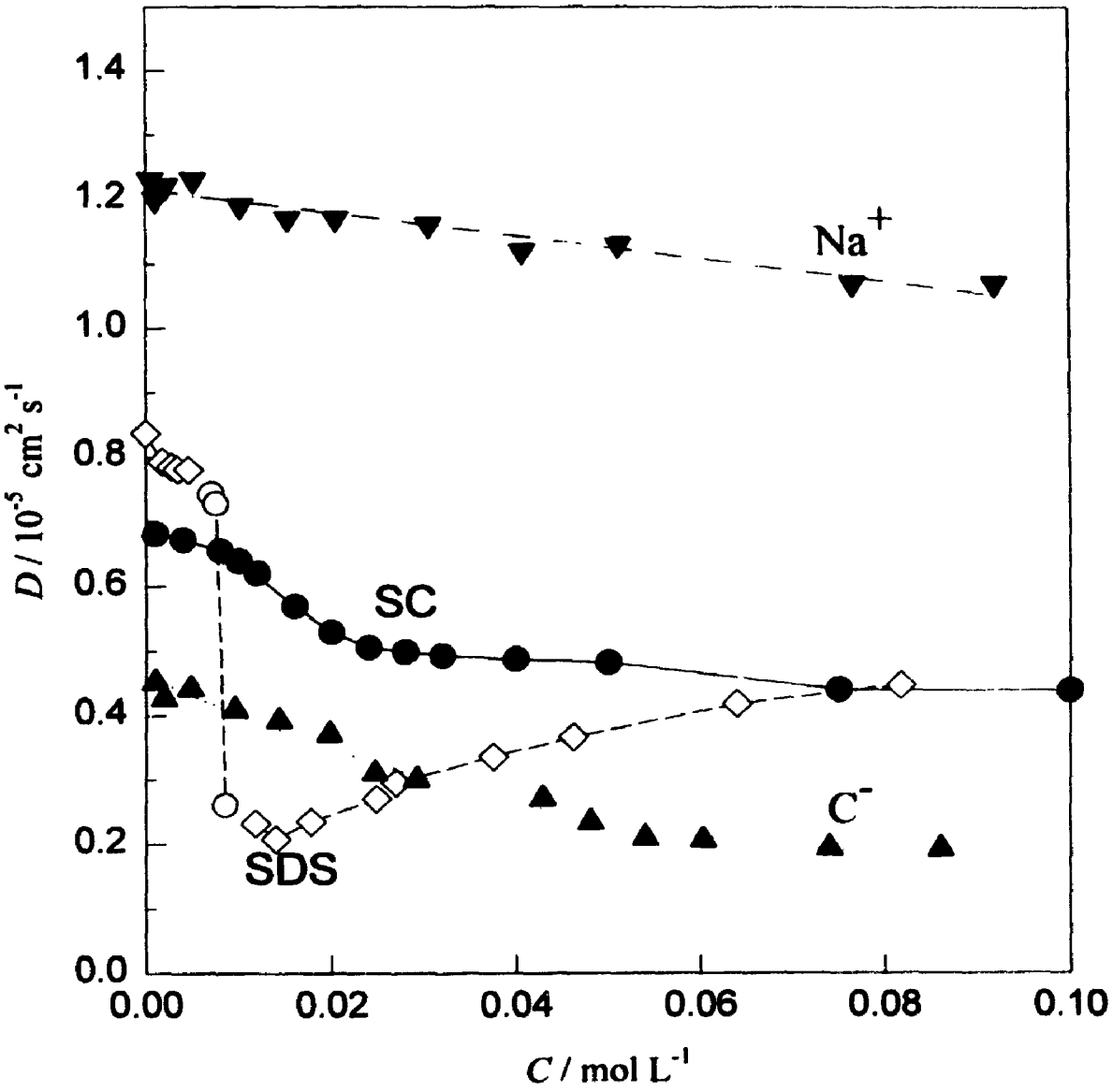
1.4
1.2
1.0
0.8
0.6
0.4
0.2
0.0
0.00
0.02
0.04
0.06
0.08
0.10
D / 10^-5 cm^2 s^-1
C / mol L^-1
Na+
SC
SDS
C-

coefficients for aqueous SDS solutions[46] are also plotted, together with intradiffusion coefficients[40] for the sodium ion and cholate ion in aqueous SC solutions.

It is evident from Figure 7-2 that the interdiffusion coefficient of aqueous SDS changes slowly as the concentration is raised until a sudden drop near 0.008 mol L^{-1}, the accepted cmc of this surfactant. As the concentration of SDS increases from 0.0075 to 0.0085 mol L^{-1}, a difference of only 0.001 mol L^{-1}, D plunges by ~ 65%, from 0.73×10^{-5} to 0.26×10^{-5} cm^2 s^{-1}. The precipitous drop in the diffusion coefficient of SDS at the cmc results from the substantial decrease in the free energy gradient caused by ion association[46]. The diffusion coefficient of SDS passes through a minimum just above the cmc, then rises steadily with concentration. The increase in the rate of diffusion above the cmc has been attributed to the significant increase in the mobility of the associated electrolyte[46]. According to Stokes Law, the frictional force acting on a diffusing aggregate of N monomers should increase approximately as $N^{1/3}$, i.e., directly proportional to the radius of the aggregate. However, each aggregate transports N monomers, so the frictional resistance per mole of monomer decreases with N approximately as $N^{1/3}/N = N^{-2/3}$.

In contrast to the behaviour of SDS, the interdiffusion coefficient of aqueous SC drops relatively slowly as the concentration increases. This result suggests that cholate ions undergo continuous self-association, even at very low concentrations. Premicellar association was also observed by Kawamura *et al.*[15] using ESR spectroscopy. Precise evaluation of the cmc is difficult in cases of premicellar association. It is evident from Figure 7-2, however, that the binary diffusion coefficient of aqueous SC drops most rapidly at concentrations from 0.010 mol L^{-1} to 0.020 mol L^{-1}, which suggests that the cmc of aqueous SC is 0.015 (± 0.005) mol L^{-1}. This qualitative value is consistent with previously reported cmc's for aqueous SC[5,10-12,15,18,20,39,40,45]: 0.010 to 0.019 mol L^{-1}.

The concentration dependence of D suggests that SC micelles grow progressively as the concentration of SC increases until the concentration reaches about 0.030 mol L^{-1}. Above 0.030 mol L^{-1}, D drops only slightly as the concentration is raised. Unlike aqueous SDS, a minimum in the diffusion coefficient of aqueous SC is not observed. This implies that the contribution to D from the thermodynamic effect outweighs the increase in mobility caused by the association of the cholate ions.

Extrapolation of the measured D values to zero SC concentration gives the limiting diffusion coefficient of aqueous SC: $D^0 = 0.68 \times 10^{-5}$ cm^2 s^{-1}. Using the Nernst relation $D^0 = 2D^0_{Na}D^0_C / (D^0_{Na} + D^0_C)$ and the limiting diffusion coefficient of sodium ion[47], $D_{Na}{}^0 = 1.33 \times 10^{-5}$ cm^2 s^{-1}, the limiting diffusion coefficient $D_C{}^0 = 0.46 \times 10^{-5}$ cm^2 s^{-1} is obtained for the cholate ion. This value is in excellent agreement with the limiting intradiffusion coefficient of the cholate ion, 0.459×10^{-5} cm^2 s^{-1}, determined by Lindman *et al.*[40] by using the open-ended capillary tube method with radioactive tracers.

As shown in Figure 7-2, the intradiffusion coefficients of sodium and cholate ions reported by Lindman *et al.*[40] decrease smoothly as the concentration of SC is raised. Thus, intradiffusion coefficients cannot provide information on the cmc of aqueous SC. It is also evident from Figure 7-2 that the interdiffusion coefficient of SC is not a simple average of the intradiffusion coefficients of the Na^+ and C^- ions.

Ternary Interdiffusion Coefficients for Aqueous SC/Decanol and SC/Octanol Solutions Diffusion in aqueous SC/octanol and SC/decanol solutions was measured at six and eight different carrier-stream compositions, respectively. Dispersion profiles obtained by injecting excess SC or excess decanol into a 0.050 mol L^{-1} SC + 0.005 mol L^{-1} decanol carrier stream are shown in Figure 7-3. The profile obtained by injecting excess decanol consists of two overlapping Gaussian peaks: a relatively narrow negative peak (caused by rapid coupled diffusion of SC) superimposed on a broader positive peak (from the slower diffusion of decanol). This result shows that diffusing decanol interacts strongly with SC; the dispersion of non-interacting decanol would generate a single Gaussian peak.

The ternary interdiffusion coefficients of aqueous SC(1)/decanol(2) and SC(1)/octanol(2) solutions are summarized in Tables 7-2 and 7-3, respectively. The average D_{ik} values for each carrier-stream composition were obtained by fitting equation (4.20) to 4 - 6 replicate pairs of peaks. Uncertainties, which are quoted as ± two standard deviations, indicate that the diffusion coefficients were reproducible within ± 0.01×10^{-5} cm^2 s^{-1}. The results were not affected by doubling the initial concentration differences, so the measured D_{ik} values represent differential values at the composition of the carrier stream. It is evident from Tables 7-2 and 7-3 that SC diffuses about twice as rapidly as decanol or octanol. As a result, the eigenvalues of the D_{ik} matrix are well separated, and

Figure 7-3 Dispersion profiles for a carrier stream containing 0.050 mol L^{-1} SC(1) and 0.005 mol L^{-1} *n*-decanol. Peak 1 (initial gradient in SC): ΔC_1 = -0.005 mol L^{-1}, ΔC_2 = 0.000 mol L^{-1}; Peak 2 (initial gradient in *n*-decanol): ΔC_1 = 0.000 mol L^{-1}, ΔC_2 = 0.010 mol L^{-1}. Peak 1 has been offset for clarity.

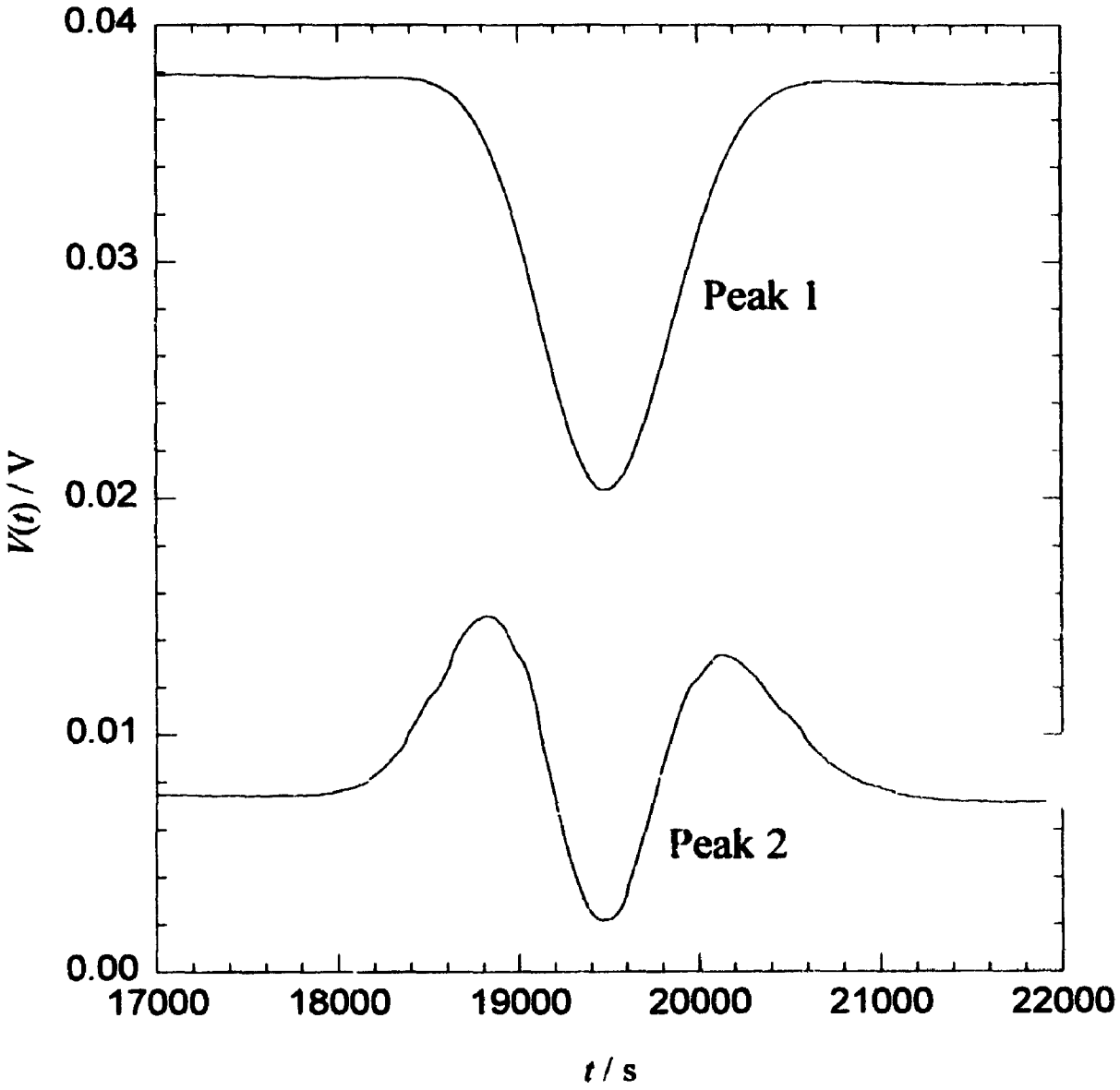
0.04
0.03
0.02
0.01
0.00
V(t) / V
Peak 1
Peak 2
17000
18000
19000
20000
21000
22000
t / s

the fitting procedure gives relatively precise diffusion coefficients. Tables 7-1 and 7-2 also show that the refractive index change per mole of SC(1) is at least three times larger than that for decanol(2), and at least four times larger than that for octanol(2). Coefficients D_{11} and D_{12} for SC(1) were therefore determined more precisely than D_{21} and D_{22} for decanol(2) and octanol(2).

Concentration gradients in SC cannot produce coupled flows of alcohol in alcohol-free solutions, so D_{21} approaches zero as $C_2/C_1 \rightarrow 0$. In this limit D_{11} is equivalent to the binary diffusion coefficient of aqueous SC (Table 7-1). The accuracy of the ternary diffusion coefficients can therefore be checked by using the identities $D_{21} = 0$ and $D_{11} = D$ in the limit $C_2/C_1 \rightarrow 0$. The present results are consistent with these limiting values within the suggested experimental precision, $\pm 0.01 \times 10^{-5}$ cm^2 s^{-1}.

Because the solubility of decanol in water[48] is very low, 3.14×10^{-4} mol L^{-1} at 25 °C, it is reasonable to assume that decanol is completely solubilized in the SC micelles. Consequently, the tracer diffusion coefficient for decanol in aqueous SC solutions is approximately equal to the diffusion coefficient of the SC micelles, D_m. In the present study, we will use the value $D_m = 0.225 \times 10^{-5}$ cm^2 s^{-1} for the diffusion coefficient of SC micelles. This value equals the tracer interdiffusion coefficient (Table 7-2) measured for decanol in 0.025 mol L^{-1} aqueous SC, which lies in the middle of the SC concentration range used here. We believe 0.225×10^{-5} cm^2 s^{-1} is a more reasonable value than the value 0.150×10^{-5} cm^2 s^{-1} determined from the intradiffusion of decanol in SC solutions in a previous study[41]. In the intradiffusion studies, the concentration of decanol was sufficiently high (*ca.* 0.001 mol L^{-1}) to slow down the diffusion of the micelles. The effect of added decanol is evident in Table 7-2: the values of D_{22} for decanol in 0.050 mol L^{-1} SC solutions are 15-30% smaller than those for the tracer diffusion of decanol in decanol-free SC solutions.

It has been shown[41] that aggregates of cholate ions are nearly spherical at low concentrations. The average size of SC micelles can therefore be estimated by using the Stokes-Einstein equation: $D_m = kT/6\pi r_m \eta$. Using $D_m = 0.225 \times 10^{-5}$ cm^2 s^{-1}, the average radius of micelles is estimated to be 10.9 Å. This value is in good agreement with the result

Table 7-2 Ternary interdiffusion coefficients of aqueous SC(1)/*n*-decanol(2) solutions at 25 °C

C_1	C_2	D_{11}	D_{12}	D_{21}	D_{22}	R_2 / R_1
0.025	0.000	0.506 ± 0.008	-0.662 ± 0.005	-0.002 ± 0.003	0.225 ± 0.004	0.302 ± 0.004
0.040	0.000	0.502 ± 0.003	-0.516 ± 0.004	0.002 ± 0.001	0.214 ± 0.003	0.299 ± 0.003
0.050	0.000	0.482 ± 0.002	-0.355 ± 0.001	-0.009 ± 0.002	0.209 ± 0.003	0.299 ± 0.009
0.050	0.005	0.533 ± 0.003	-0.264 ± 0.002	0.027 ± 0.004	0.181 ± 0.004	0.287 ± 0.008
0.050	0.010	0.541 ± 0.002	-0.190 ± 0.006	0.070 ± 0.005	0.149 ± 0.008	0.276 ± 0.008
0.050	0.015	0.519 ± 0.003	-0.072 ± 0.000	0.111 ± 0.008	0.151 ± 0.004	0.195 ± 0.006

Units: C_i in mol L^{-1}; D_{ik} in 10^{-5} cm^2 s^{-1}

Table 7-3 Ternary interdiffusion coefficients of aqueous SC(1)/*n*-octanol(2) solutions at 25 °C

C_1	C_2	D_{11}	D_{12}	D_{21}	D_{22}	R_2 / R_1
0.025	0.000	0.514 ± 0.005	-0.237 ± 0.002	-0.007 ± 0.006	0.444 ± 0.006	0.214 ± 0.005
0.040	0.000	0.489 ± 0.001	-0.245 ± 0.002	-0.011 ± 0.004	0.329 ± 0.003	0.204 ±0.001
0.050	0.000	0.482 ± 0.002	-0.223 ± 0.001	-0.010 ± 0.002	0.308 ± 0.002	0.201 ± 0.001
0.050	0.005	0.517 ± 0.006	-0.182 ± 0.003	0.011 ± 0.004	0.282 ± 0.005	0.214 ± 0.006
0.050	0.010	0.520 ± 0.001	-0.147 ± 0.002	0.025 ± 0.003	0.246 ± 0.003	0.209 ± 0.001
0.050	0.015	0.527 ± 0.001	-0.120 ± 0.001	0.063 ± 0.003	0.229 ± 0.001	0.180 ± 0.004
0.050	0.020	0.521 ± 0.002	-0.105 ± 0.005	0.068 ± 0.012	0.212 ± 0.003	0.186 ± 0.008
0.050	0.025	0.515 ± 0.001	-0.074 ± 0.002	0.118 ± 0.014	0.155 ± 0.004	0.169 ± 0.004

Units: C_i in mol L^{-1}; D_{ik} in 10^{-5} cm^2 s^{-1}.

(11 Å) measured by QELS[44]. Taking counterion binding into account, we are able to calculate the aggregation number of the cholate micelles by using the following formula,

$$n = \frac{r_m^3}{r_C^3 + \beta r_{Na}^3} \qquad (7.1)$$

where n represents the number of SC monomers per micelle, β is the degree of counterion binding, and r_m, r_C and r_{Na} the radii of the micelles, cholate and sodium ions, respectively. The effective radii of the cholate and sodium ions in aqueous solution are estimated by using the Stokes - Einstein equation: r_C = 5.33 Å and r_{Na} = 1.84 Å. Measurements[41,45] with Na^+ ion selective electrodes have shown that the counterion binding is quite low (β < 0.1) for SC micelles at concentrations below 0.10 mol L^{-1}. Adopting the value[45] 0.07 for β leads to the approximate value n = 13 for the aggregation number of the SC micelles. This value is consistent with previously reported values which range from 3 to 16[5,41,45].

Since the solubilities of decanol[48] and octanol[49] in pure water are low (3.14×10^{-4} and 4.53×10^{-3} mol L^{-1}, respectively), most of the decanol or octanol dissolved in aqueous SC solutions is solubilized by cholate micelles. Diffusing SC might be expected to cotransport alcohol, and *vice versa*. This behaviour, if correct, would lead to positive cross-diffusion coefficients. Positive D_{21} values are indeed observed for aqueous SC(1)/decanol(2) or SC(1)/octanol(2). The amount of decanol or octanol solubilized by SC micelles increases as the molar ratio C_2:C_1 of decanol or octanol to SC increases. As a result, D_{21} increases with the C_2:C_1 ratio, as shown in Tables 7-2 and 7-3. It is also understandable that D_{21} values for SC(1)/decanol(2) are generally larger than those for SC(1)/octanol(2) bacause more decanol is solubilized relative to octanol.

It is interesting, however, that negative values of D_{12} are observed at all compositions. This means that diffusing decanol or octanol countertransports SC. Moreover, the coupled diffusion is much stronger than that reported in Chapter 6 for SDS/octanol solutions. The larger values of D_{12} for SC/alcohol solutions might result from the lower degree of sodium counterion binding in SC solutions, which in turn leads to a stronger electric field along SC concentration gradients.

To describe the interdiffusion behaviour of SC(1)/decanol(2) or octanol(2) by using the model established in Chapter 6, it is necessary to estimate: 1) the partition coefficients

K_a for the equilibrium distribution of the alcohols between the aqueous and SC micellar phases, and 2) the distribution constants K_m of cholate ions between aqueous and SC micellar phases.

K_a can be estimated by using the following equation

$$K_a = \frac{C_{2mic}}{C_{2aq}} \approx \frac{C_{2s}^{\bullet}(V_{aq}/V_{mic})}{C_2^{\bullet}} \qquad (7.2)$$

where C_{2mic} and C_{2aq} denote the concentrations of alcohol in the micellar phase and the aqueous phase, $C_{2s}^{\bullet}$ and $C_2^{\bullet}$ are the solubilities of alcohol in the SC solution and pure water, and V_{aq} and V_{mic} are the volumes of aqueous phase and micellar phase. $C_{2s}^{\bullet}$ for decanol and octanol in 0.050 mol L^{-1} SC solution are determined to be 0.017 and 0.029 mol L^{-1}, respectively. The value $V_1 = 0.37$ L mol^{-1} was used for the molar volume of SC[26]. Linear extrapolation of the molar volumes of alcohols presented in Table 6-4 gives 0.19 L mol^{-1} for the molar volume of decanol. Consequently, the values of K_a for SC(1)/decanol(2) and SC(1)/octanol(2) are estimated to be 2400 and 270.

The distribution constant for cholate ions is expressed by equation (6.12). For alcohol-free SC solutions, $C_2 = 0$ and $V_2 = 0$, in which case equation (6.12) simplifies to

$$K_m = \frac{1 - nc_{mTOT}V_1}{(C_1 - nc_{mTOT})V_1} \qquad (7.3)$$

Lindman *et al.*[41] have determined that the fraction of cholate ions in aggregated form is about 0.56 for 0.050 mol L^{-1} aqueous SC solution. As a result, nc_{mTOT} is 0.028 mol L^{-1}. Substituting $nc_{mTOT} = 0.028$ mol L^{-1}, $C_1 = 0.050$ mol L^{-1} and $V_1 = 0.37$ L mol^{-1} into equation (7.3) gives 122 for the value of K_m.

In Figures 7-4 and 7-5, the predicted D_{ik} (lines) and measured D_{ik} (symbols) are plotted against the concentration of decanol or octanol in 0.050 mol L^{-1} SC solution. It is evident that the values predicted by using the model proposed in Chapter 6 are in reasonably good agreement with the diffusion coefficients measured by the Taylor dispersion technique. The predicted values of D_{21} and D_{22} are very close to the measured values. Although the measured and predicted D_{12} values are in poorer agreement, trends in the variation of D_{12} with concentration are correctly predicted. For instance, the

Figure 7-4 Ternary interdiffusion coefficients plotted against the concentration of *n*-decanol(2) in 0.050 mol L^{-1} SC(1) solution at 25 °C: symbols, measured diffusion coefficients; curves, predicted values.

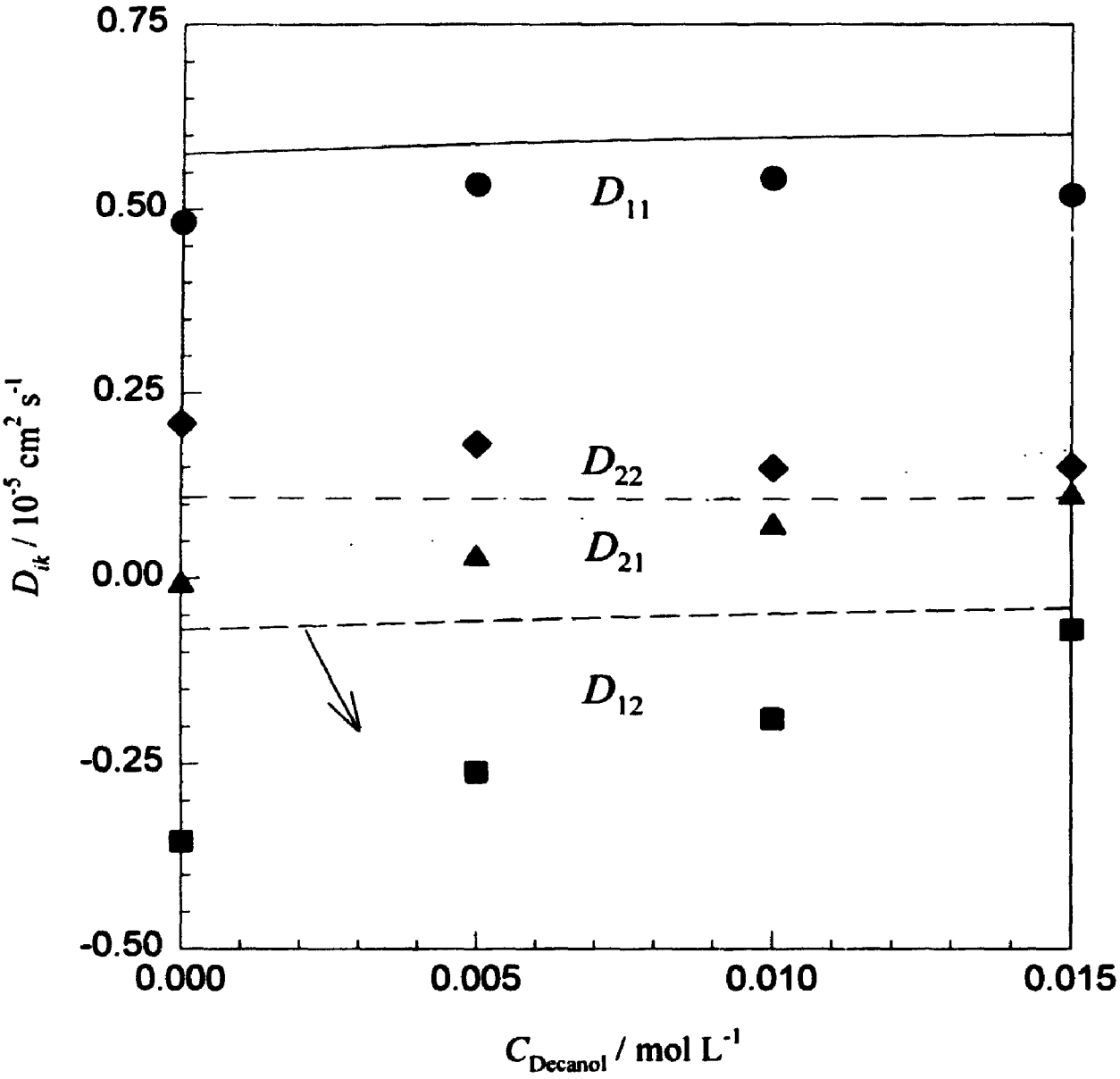
0.75
0.50
0.25
0.00
-0.25
-0.50
0.000
0.005
0.010
0.015
D_{ik} / 10^{-5} cm^2 s^{-1}
$C_{Decanol}$ / mol L^{-1}
D_{11}
D_{22}
D_{21}
D_{12}

Figure 7-5 Ternary interdiffusion coefficients plotted against the concentration of *n*-octanol(2) in 0.050 mol L^{-1} SC(1) solution at 25 °C: symbols, measured diffusion coefficients; curves, predicted values.

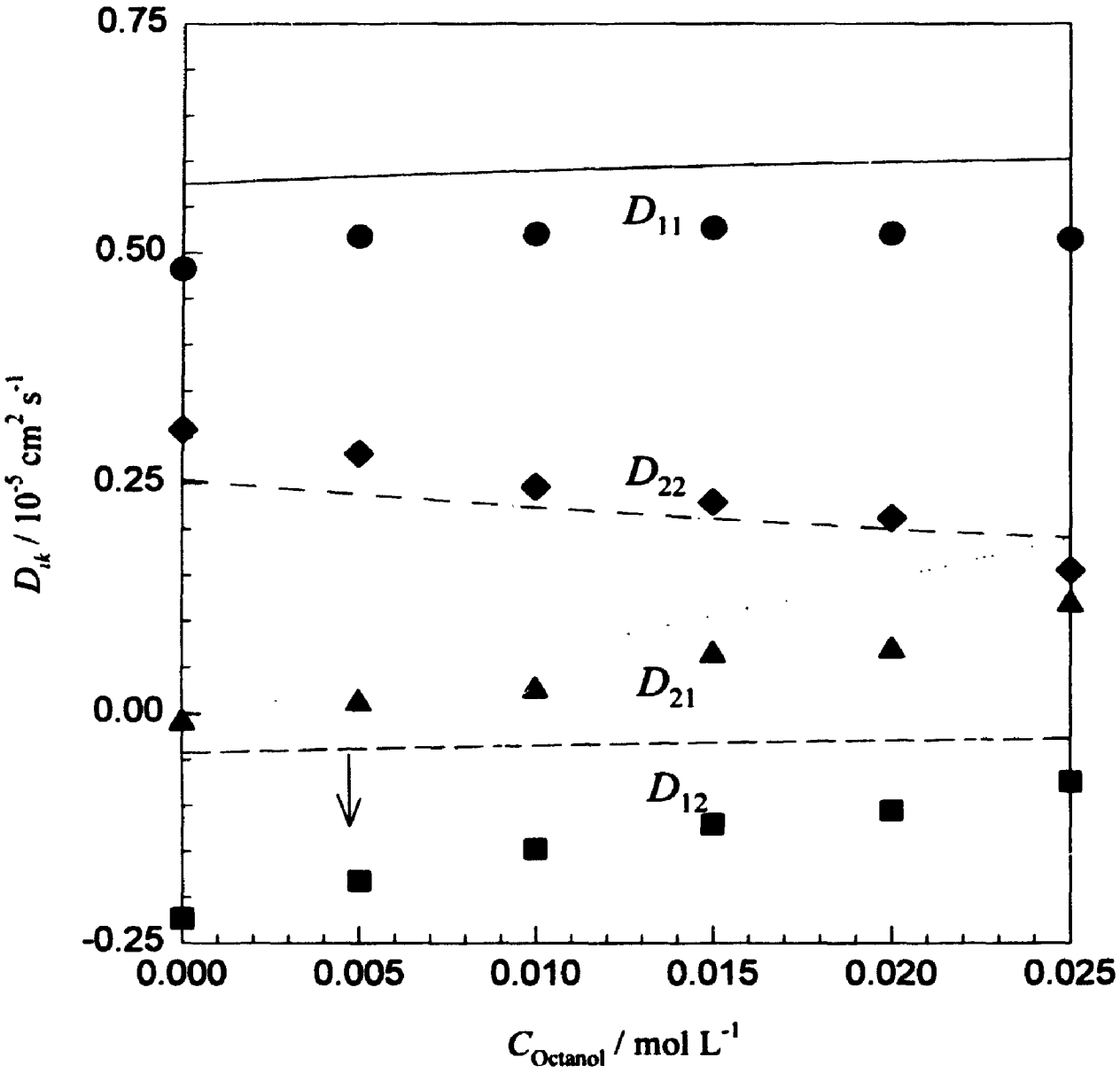
0.75
0.50
0.25
0.00
-0.25
D_{ik} / 10^{-5} cm^2 s^{-1}
D_{11}
D_{22}
D_{21}
D_{12}
0.000
0.005
0.010
0.015
0.020
0.025
$C_{Octanol}$ / mol L^{-1}

counterflow of SC decreases as the concentration of solubilizates(2) increases. In contrast, the predicted values of D_{21} are positive and increase as the concentration of solubilizate(2) is raised.

According to equations (6.7) through (6.9), each interdiffusion coefficient can be divided into the contribution $D_{ik(D)}$ from pure diffusion and the contribution $D_{ik(E)}$ from the migration of charged species in the electric field.

The predicted values of $D_{ik(D)}$ and $D_{ik(E)}$ are presented in Tables 7-4 and 7-5. $D_{11(E)}$ is about three times larger than $D_{11(D)}$, which suggests that the electric field produced by the diffusing ions plays a major role in the transport of SC. This is understandable because the degree of counterion binding to SC micelles is quite low, $\beta < 0.1$. The lower the degree of counterion binding, the higher is the charge on the micelles. In contrast, the effect of the diffusion-induced electric field on the transport of SDS (Chapter 6) is relatively small because the extent of counterion binding is much larger, about 0.8[146,50,51].

For comparison, the predicted values of $D_{ik(D)}$ and $D_{ik(E)}$ for aqueous SDS(1)/octanol(2) solutions are given in Table 7-6. For this system the values of $D_{11(D)}$ are twice as large as the $D_{11(E)}$ values for SDS(1)/octanol(2) solutions. For SC(1)/octanol(2), in contrast, the values of $D_{11(E)}$ are more than three times larger than $D_{11(D)}$.

The decanol and octanol concentration gradients are predicted to drive counterflows of SC. This prediction is consistent with the experimental results, as illustrated in Figures 7-4 and 7-5. The largest contribution to D_{12} is made by the pure-diffusion term, $D_{12(D)}$.

$D_{21(E)}$ is much larger than $D_{21(D)}$ according to the results presented in Tables 7-4 and 7-5. Moreover, $D_{21(E)}$ increases with the concentration of alcohol solubilizate more rapidly than $D_{21(D)}$. This means that the coupled flow of alcohol solubilizates in SC micellar solutions is caused primarily by the electric field generated by the diffusion of charged micelles and sodium counterions, even though the alcohol molecules are electrically neutral. It appears, however, that each alcohol is transported down its own concentration gradient mainly by pure diffusion, because $D_{22(D)} >> D_{22(E)}$. In Tables 7-4 and 7-5, for example, the values of $D_{22(D)}$ for both SC(1)/decanol(2) and SC(1)/octanol(2) solutions are about one order of magnitude larger than the corresponding values of $D_{22(E)}$. $D_{22(D)}$ drops with the increase in concentration of decanol or octanol, while $D_{22(E)}$ increases as the alcohol

Table 7-4 Contributions to the interdiffusion coefficients of aqueous SC(1)/*n*-decanol(2) solutions from pure diffusion ($D_{ik(D)}$) and migration in the diffusion-induced electric field ($D_{ik(E)}$)

C_1	C_2	$D_{11(D)}$	$D_{12(D)}$	$D_{21(D)}$	$D_{22(D)}$	$D_{11(E)}$	$D_{12(E)}$	$D_{21(E)}$	$D_{22(E)}$
0.050	0.005	0.115	-0.124	0.000	0.099	0.474	0.065	0.061	0.008
0.050	0.010	0.124	-0.102	0.000	0.095	0.473	0.054	0.119	0.014
0.050	0.015	0.130	-0.088	0.000	0.092	0.472	0.048	0.175	0.018

Units: C_i in mol L^{-1}; D_{ik} in 10^{-5} cm^2 s^{-1}.

Table 7-5 Contributions to the interdiffusion coefficients of aqueous SC(1)/*n*-octanol(2) solutions from pure diffusion ($D_{ik(D)}$) and migration in the diffusion-induced electric field ($D_{ik(E)}$)

C_1	C_2	$D_{11(D)}$	$D_{12(D)}$	$D_{21(D)}$	$D_{22(D)}$	$D_{11(E)}$	$D_{12(E)}$	$D_{21(E)}$	$D_{22(E)}$
0.050	0.005	0.107	-0.090	-0.018	0.233	0.476	0.052	0.048	0.005
0.050	0.010	0.114	-0.080	-0.031	0.214	0.476	0.045	0.097	0.009
0.050	0.015	0.120	-0.073	-0.040	0.199	0.476	0.041	0.145	0.013
0.050	0.020	0.124	-0.066	-0.047	0.186	0.476	0.036	0.194	0.015
0.050	0.025	0.126	-0.060	-0.052	0.174	0.477	0.032	0.242	0.017

Units: C_i in mol L^{-1}; D_{ik} in 10^{-5} cm^2 s^{-1}.

Table 7-6 Contributions to the interdiffusion coefficients of aqueous SDS(1)/*n*-octanol(2) solutions from pure diffusion ($D_{ik(D)}$) and migration in the diffusion-induced electric field ($D_{ik(E)}$)

C_1	C_2	$D_{11(D)}$	$D_{12(D)}$	$D_{21(D)}$	$D_{22(D)}$	$D_{11(E)}$	$D_{12(E)}$	$D_{21(E)}$	$D_{22(E)}$
0.050	0.005	0.345	0.033	-0.003	0.161	0.173	0.087	0.038	0.019
0.050	0.010	0.354	0.044	-0.005	0.152	0.181	0.092	0.080	0.040
0.050	0.015	0.361	0.051	-0.006	0.144	0.187	0.094	0.123	0.062
0.050	0.020	0.367	0.058	-0.006	0.138	0.190	0.094	0.168	0.083
0.050	0.025	0.372	0.062	-0.005	0.132	0.191	0.093	0.213	0.103

Units: C_i in mol L^{-1}; D_{ik} in 10^{-5} cm^2 s^{-1}.

concentration increases. These trends are consistent with those discussed in Chapter 6 for octanol in aqueous SDS solutions.

7.4. Conclusions

The binary interdiffusion coefficient of aqueous sodium cholate and the ternary interdiffusion coefficients of aqueous SC(1)/decanol(2) and SC(1)/octanol(2) solutions have been measured by the Taylor dispersion technique. The cmc determined from the binary diffusion measurements is about 0.015 mol L^{-1}, and the estimated aggregation number of SC micelles is 13. The ternary results show that the interdiffusion behaviour of aqueous SC/decanol or SC/octanol solutions is similar to that of aqueous SDS/solubilizate solutions reported in Chapter 6, but coupled diffusion in the SC solutions is stronger than that in SDS solutions. In spite of the polydispersity of SC micelles, the diffusion coefficients predicted by the model developed in chapter 6 are in reasonably good agreement with the measured diffusion coefficients. This result suggests that the model developed in chapter 6 will apply to a wide range of surfactant-solubilizate systems.

7.5. References

1. D.M. Small, *The Bile Acids: Chemistry, Physiology and Metabolism*, P.P. Nair and D. Kritevsky eds., Vol. 1, Plenum Press, New York, 1971, p. 266
2. M.C. Carey and D.M. Small, *Am. J. Med.*, **49**, 590 (1970)
3. D.M. Small, *Adv. Chem. Ser.*, **84**, 31 (1968)
4. Y. Chang and J.R., *J. Pharm. Sci.*, **67**, 174 (1978)
5. J.M. Roe and B.W. Barry, *J. Colloid Interface Sci.*, **94**, 580 (1983); **107**, 398 (1985)
6. H. Gustavsson and B. Lindman, *J. Am. Chem. Soc.*, **97**, 3923 (1975)
7. W.B. Smith and G.D. Barnard, *Can. J. Chem.*, **59**, 1602 (1981)
8. J. Zakrzewska, V. Markovic, D. Vucelic, L. Feigin, A. Dembro and L. Mogilevsky, *J. Phys. Chem.*, **94**, 5078 (1990)
9. A.J.H. Rains and N. Crawford, *Nature*, **171**, 829 (1953)
10. P. Mukerjee, Y. Moroi, M. Murata and A.Y.S. Yang, *Hepatology*, **4**, S61 (1984)

11. C.J. O'Connor, B.T. Ch'ng and R.G. Wallace, *J. Colloid Interface Sci.*, **95**, 410 (1983)

12. A. Roda, A.F. Hoffman and K.J. Mysels, *J. Biol. Chem.*, **258**, 6362 (1983)

13. L. Fisher and D. Oakenfull, *Aust. J. Chem.*, **32**, 31 (1979)

14. H. Kawamura, M. Manabe, T. Narikiyo, H. Igimi, Y. Murata, G. Sugihara and M. Tanaka, *J. Solution Chem.*, **16**, 433 (1987)

15. H. Kawamura, Y. Murata, T. Yamaguchi, H. Igimi, G. Sugihara, M. Tanaka and J.P. Kratohvil, *J. Phys. Chem.*, **93**, 3321 (1989)

16. R. Zana and D.E. Güveli, *J. Phys. Chem.*, **89**, 1687 (1985)

17. N. Rajajopalan, M. Vadnere and S. Lindenbaum, *J. Solution Chem.*, **11**, 785 (1981)

18. A. Djavanbakht, K.M. Kale and R. Zana, *J. Colloid Interface Sci.*, **59**, 139 (1977)

19. P. Ekwall, A. Sten and A. Norman, *Acta Chem. Scand.*,**10**, 681 (1956)

20. P. Ekwall, K. Fontell and A. Norman, *Acta Chem. Scand.*, **11**, 590 (1957)

21. R.R. Roepke and H.L. Mason, *J. Biol. Chem.*, **133**, 103 (1940)

22. E.W. Moore and J.M. Dietschy, *Am. J. Physiol.*, **206**, 1111 (1964)

23. E.L. Cussler and C.L. Duncan, *J. Solution Chem.*, **1**, 269 (1972)

24. P. Carpenter and S. Lindenbaum, *J. Solution Chem.*, **8**, 347 (1979)

25. J.M. Beckerdite and E.T. Adams, *Biophys. Chem.*, **21**, 103 (1985)

26. D.G. Oakenfull and L.R. Fisher, *J. Phys. Chem.*, **81**, 1838 (1977); **82**, 2443 (1978)

27. D.E. Güveli, *J. Chim. Phys.*, **83**, 123 (1986)

28. M. Vadnere, R. Natarajan and S. Lindenbaum, *J. Phys. Chem.*, **84**, 1900 (1980)

29. P. Ekwall, K. Fontell and A. Morman, *Acta Chem. Scand.*, **11**, 190 (1957)

30. A. Norman, *Acta Chem. Scand.*, **14**, 1295 (1960)

31. P. Mukerjee and J.R. Cardinal, *J. Pharm. Sci.*, **65**, 882 (1976)

32. G. Sugihara, K. Yamakawa, Y. Murata and M. Tanaka, *J. Phys. Chem.*, **86**, 2784 (1982)

33. C.H. Spink and S. Colgan, *J. Colloid Interface Sci.*, **97**, 41 (1984)

34. E. Kolehmainen, *J. Colloid Interface Sci.*, **105**, 273(1985); **127**, 301 (1989)

35. P. Ekwall, *J. Colloid Interface Sci.*, **9**(Suppl.1), 66 (1954)

36. M. Vadnere and S. Lindenbaum, *J. Pharm. Sci.*, **71**, 875 (1982)

37. D.E. Güveli, *Colloid Polym. Sci.*, **264**, 707 (1986)

38. B.W. Barry and G.M.T. Gray, *J. Colloid Interface Sci.*, **52**, 327 (1975)

39. A. Norman, *Acta Chem. Scand.*, **14**, 1300 (1960)

40. B. Lindman, N. Kamenka and B. Brun, *J. Colloid Interface Sci.*, **56**, 328 (1976)

41. B. Lindman, N. Kamenka, H. Fabre, J. Ulmius and T. Wieloch, *J. Colloid Interface Sci.*, **73**, 556 (1980)

42. B. Lindman, *Hepatology*, **4**, S103 (1984)

43. B. Lindman, M.C. Puyal, N. Kamenka, R. Rynden and P. Stilbs, *J. Phys. Chem.*, **88**, 5048 (1984)

44. N.A. Mazer, M.C. Carey, R.F. Kwasnick and G. B. Benedek, *Biochemistry*, **18**, 3064 (1979)

45. A. Coello, F. Meijide, E. Rodríguez Núñez and J. Vázquez Tato, *J. Phys. Chem.*, **97**, 10186 (1993)

46. D.G. Leaist, *J. Colloid Interface Science*, **111**, 230 (1986)

47. R.H. Robinson and R.H. Stokes, *Electrolyte solutions*, 2nd ed., Academic Press, New York, 1959, p.463

48. R.S. Stearns, H. Oppenheimer, E. Simon and W.D. Harkins, *J. Chem. Phys.*, **15**, 496 (1947)

49. J.W. McBain and P.H. Richards, *Ind. Eng. Chem.*, **38**, 642 (1946)

50. D.F. Evans, S. Mukherjee, D.J. Mitchell and B.W. Ninham, *J. Colloid Interface Sci.*, **93**, 184 (1983)

51. K.M. Kale, E.L. Cussler and D.F. Evans, *J. Phys. Chem.*, **84**, 583 (1980)

Chapter 8

TERNARY INTERDIFFUSION IN WATER/AOT/*n*-HEPTANE WATER-IN-OIL MICROEMULSIONS

Ternary interdiffusion coefficients for water/AOT (sodium bis(2-ethylhexyl) sulfosuccinate)/heptane water-in-oil microemulsions have been measured by Taylor dispersion. Although water and AOT diffuse together through the heptane-continuous medium as surfactant-coated water droplets, the diffusion coefficient of AOT is three times larger than the diffusion coefficient of water. Also, concentration gradients in AOT produce cocurrent coupled flows of water, but gradients in water produce counterflows of AOT. This unexpected behaviour is attributed to changes in the average droplet size along the diffusion path. The analysis confirms the experimental result that the diffusion of water and surfactant in a microemulsion produces two distinct diffusional relaxation times, even in cases of negligible droplet polydispersity.

8.1. Introduction

Large amounts of oil can be dispersed in water by using surfactants to coat and stabilize nanometer-sized droplets of oil. These systems are called "oil-in-water" microemulsions. Similarly, "water-in-oil" microemulsions can be prepared by stabilizing nanodroplets of water in an oil-continuous phase. The microstructure of microemulsions is responsible for a number of interesting properties[1,2] as well as important practical applications[2,3] related to petroleum recovery, cleaning processes, digestion, targetted drug delivery, and the production of lubricants, paints, and food products.

Certain surfactants can form water-in-oil (w/o) microemulsions containing large amounts of water without the help of added cosurfactant, such as alcohols[2]. A good example is the surfactant sodium bis(2-ethylhexyl) sulfosuccinate (AOT). AOT has two alkyl chains and a relatively small hydrophilic head group, as shown in Figure 8-1. This structure allows AOT to form reverse micelles without the addition of cosurfactant, which greatly simplifies the properties of the system.

Figure 8-1 Chemical structure of sodium bis(2-ethylhexyl) sulfosuccinate (AOT)

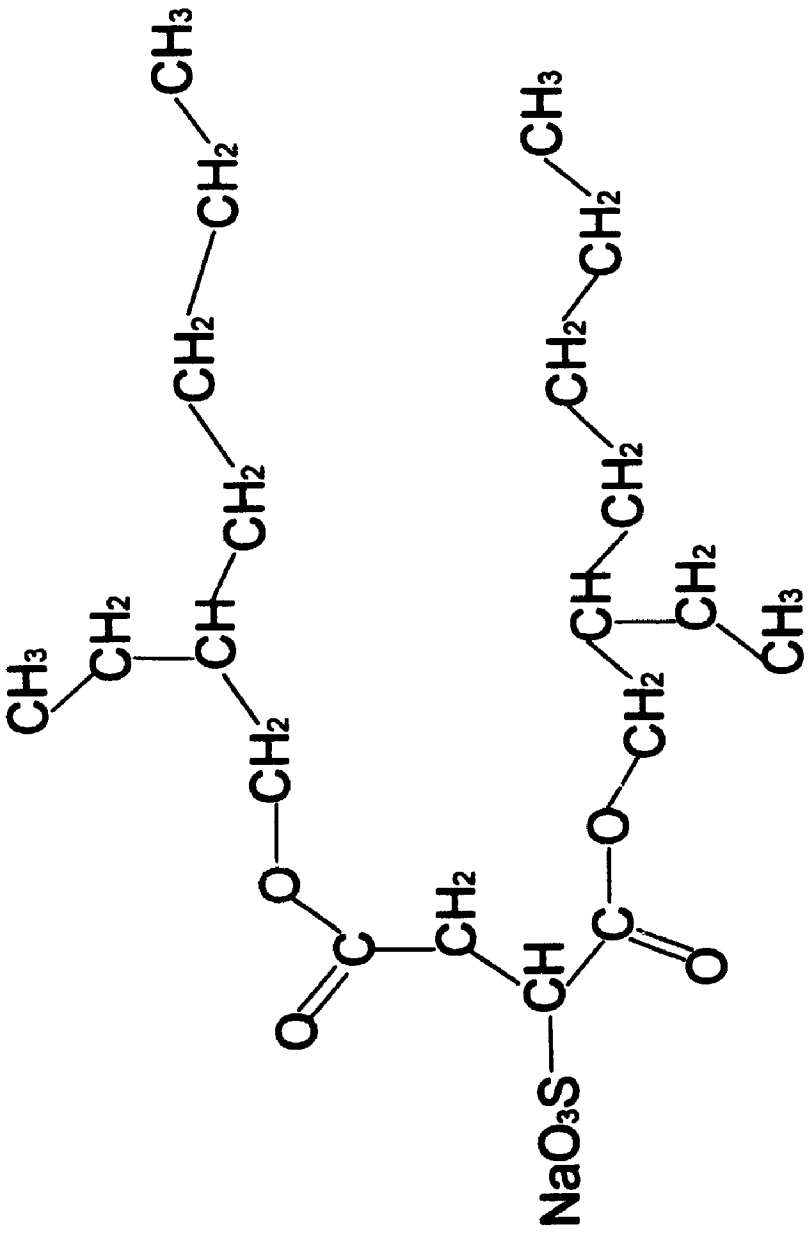
CH3
CH2
CH2
CH2
CH2
CH
CH3
CH2
CH2
O
C
O
CH2
CH
C
O
NaO3S
CH2
CH
CH2
CH2
CH3
CH2
CH2
CH3

AOT micelles and microemulsions have received increasing interest in the past few years. In addition to practical applications, AOT microemulsions have been studied extensively to provide fundamental information about these systems. Phase equilibria[2], densities[4], refractive indexes[5], compressibilities[6], vapor pressures[2], and viscosities[6] have been reported. In addition, the size and mean average aggregation number of the microemulsion droplets have been determined by a variety of techniques such as ultracentrifugation[7], light scattering[8-13], small-angle neutron scattering[14-19], small-angle X-ray scattering[20-22], and time-resolved luminescence methods[23-25]. Studies of diffusion in water/AOT/oil microemulsions have focused on measurements of intradiffusion, mainly by NMR techniques[9,26-28]. As mentioned in the preceding chapters, there are no gradients in chemical composition in intradiffusion experiments.

Interdiffusion, on the other hand, entails gradients in chemical composition and net flows of chemical substances. Only a few studies of interdiffusion in microemulsions have been reported[29-32]. Vitagliano *et al.*[31,32], for example, have used Gouy interferometry to study interdiffusion in water/AOT/heptane microemulsions. In one study, they treated water/AOT/heptane microemulsions as a pseudo-binary system at constant molar ratios of water to AOT. This approximation was justified because the size of microemulsion droplets is constant if C_1/C_2 is constant along the diffusion path. If the water and surfactant components migrate together through the oil as surfactant-coated water droplets, it seems reasonable to use Fick's binary diffusion equation

$$J = -D\nabla C \qquad \text{(constant AOT/water ratio)} \qquad (8.1)$$

to relate the droplet flux J to the gradient ∇C in droplet concentration. D is a "pseudo-binary" microemulsion diffusion coefficient. Measured values of D have been used to estimate the sizes of microemulsion droplets[31].

The pseudo-binary treatment of microemulsion diffusion appears to be well suited to water/AOT/heptane water-in-oil microemulsions: the lifetime of the droplets is much longer than the time between droplet collisions[33], and the droplet polydispersity is limited[15,34]. Because the solubility of water in hydrocarbons is negligible, virtually all of the water is transported in the droplets. The cmc of AOT in *n*-heptane is very low, so hardly any AOT monomers exist.

Although there is some justification for the pseudo-binary treatments of microemulsion diffusion, it should be noted that water/AOT/heptane is a ternary system. Moreover, a constant ratio of water to AOT is not a general feature of the system; the concentrations of water and AOT are independent variables. In general, chemical interdiffusion in three-component mixtures produces two independent diffusional flows. Although water and AOT diffuse together as AOT-coated water droplets, it is still possible to have independent flows of these components. Microemulsion droplets are dynamic entities. They collide and exchange both surfactant and water molecules on a microsecond timescale, which is very rapid compared to diffusion experiments. Suppose the concentration of total surfactant is fixed, but one region of the system contains a higher concentration of water. In this case water molecules can move down their concentration gradient by hopping from one droplet to another during droplet-droplet collisions. This will allow water to diffuse through the system without a corresponding flow of surfactant. Similarly, rapid exchange of surfactant between droplets will allow surfactant to diffuse down its gradient, independently of water.

These considerations suggest that a more complete description of interdiffusion in water(1)/surfactant(2)/oil systems might be offered by the ternary Fick equations

$$J_1 = -D_{11}\nabla C_1 - D_{12}\nabla C_2 \tag{8.2}$$

$$J_2 = -D_{21}\nabla C_1 - D_{22}\nabla C_2 \tag{8.3}$$

which relate the independent molar fluxes of water(1) and surfactant(2) to the gradients in concentration of these components. Interdiffusion coefficients[8] D_{11} and D_{22} give the fluxes of the components down their own concentration gradients. Cross-coefficients D_{12} and D_{21} are included to allow for the coupled flux of water caused by the gradient in surfactant, and *vice versa*. The concentrations C_1 and C_2 in equations (8.2) and (8.3) are well-defined stoichiometric concentrations of total water and total surfactant components. Equations (8.2) and (8.3), unlike the pseudo-binary equation (8.1), provide an unambiguous description of microemulsion diffusion because assumptions about the size, composition, or polydispersity of the microemulsion droplets are not required.

Following their study of pseudo-binary diffusion in the water/AOT/heptane sytem, Vitagliano *et al.*[32] used the Gouy optical technique to measure ternary interdiffusion

coefficients for a water/AOT/heptane microemulsion. The diffusion of AOT was found to produce a coupled-flow of water. In fact, the water cross-diffusion coefficient D_{12} was much larger than its main diffusion coefficient D_{11}. This indicates that strong interactions exist between water and AOT. Unfortunately, Gouy studies of microemulsion diffusion proved to be difficult because of gravitational instabilities in the diffusion boundaries (discussed in Chapter 4). In fact, diffusion coefficients were reported for only one microemulsion composition. The effects of changes in the concentrations of surfactant and water were not studied.

The shortage of microemulsion interdiffusion data prompted us to perform a more extensive investigation of the ternary diffusion behaviour of the water/AOT/heptane system. We used the Taylor dispersion technique which is not prone to errors from convection, including gravitational instabilities. The Taylor results show that AOT diffuses several times more rapidly than water in water/AOT/heptane microemulsions. Although AOT cotransports water, diffusing water produces countercurrent coupled flows of AOT. A simple model for microemulsion diffusion is developed to help understand the surprising results.

8.2. Experimental Procedure

Water was purified by distillation and ion exchange. Reagent grade AOT (Fisher) was dried in a vacuum oven at 80 °C. The residual water content (< 0.5%) was determined by Karl Fischer titrations. *n*-Heptane (BDH, > 99% purity) was used as supplied. Solutions were prepared in calibrated volumetric flasks.

Ternary interdiffusion coefficients of water(1)/AOT(2)/*n*-heptane(0) microemulsions were measured by the Taylor dispersion method. The dispersion tube employed in this study was a 3115-cm-long Teflon capillary (internal diameter 0.09030 cm). A metering pump maintained a steady flow of carrier solution through the tube, giving retention times of about 11,000 s. At the start of each run a 20 μL sample of solution was injected into the carrier stream through a low-pressure injection valve at the tube inlet. The injected samples contained 0.10-0.20 mol L^{-1} excess water or 0.005-0.010 mol L^{-1} excess AOT relative to the carrier solution.

8.3. Results

Dispersion Profiles Figure 8-2 shows dispersion profiles obtained by injecting excess water (peak 1) or excess AOT (peak 2) into a microemulsion carrier stream containing 0.108 mol L^{-1} water and 0.200 mol L^{-1} AOT.

Peak 1 shows that an initial concentration gradient in water(1) does not decay as a single Gaussian. Instead, peak 1 resembles a narrow Gaussian superimposed on a second, broader Gaussian. This result is important because it provides clear experimental evidence for two independent diffusional flows in a water/AOT/heptane microemulsion. Peak 1 also shows that a gradient in the concentration of water produces a coupled flow of AOT.

Ternary Interdiffusion Coefficients The D_{ik} coefficients were measured at 11 different compositions of the water(1)/AOT(2)/heptane system. In most cases the coefficients were evaluated by fitting pairs of peaks with initial gradients in water ($\alpha_1 = 1$) or AOT ($\alpha_1 = 0$). The coefficients were measured four or five times at each composition and then averaged. The results are summarized in Table 8-1.

Table 8-1 includes ratios of the molar refractive index increments for water(1) and AOT(2). The R_1/R_2 values were calculated by taking ratios of peak areas generated per mole of excess water or AOT in the injected samples. The relatively large values of R_2 allowed the dispersion of AOT to be followed more precisely than the dispersion of water. Consequently, diffusion coefficients D_{21} and D_{22} for the AOT component were determined more precisely than coefficients D_{11} and D_{12} for water (see Table 8-1).

Identical results were obtained when the initial concentration differences were changed by a factor of two. This check indicated that the measured diffusion coefficients represented differential values at the composition of the carrier solution.

Significantly different values were obtained for diffusion coefficient D_{22} of the AOT component and coefficient D_{11} of the water component. In some cases D_{22} is three times larger than D_{11}. This result is surprising at first glance. Because water and AOT diffuse together as water-AOT aggregates, nearly identical values of D_{11} and D_{22} were anticipated. This point will be discussed later.

Figure 8-2 Dispersion peaks (refractometer voltage plotted against time) for a carrier stream containing 0.108 mol L^{-1} water(1) and 0.200 mol L^{-1} AOT(2).
Peak 1: $\Delta C'_1 = 0.100$ mol L^{-1}, $\Delta C'_2 = 0.000$ mol L^{-1}; Peak 2: $\Delta C'_1 = 0.000$ mol L^{-1}, $\Delta C'_2 = 0.005$ mol L^{-1}.

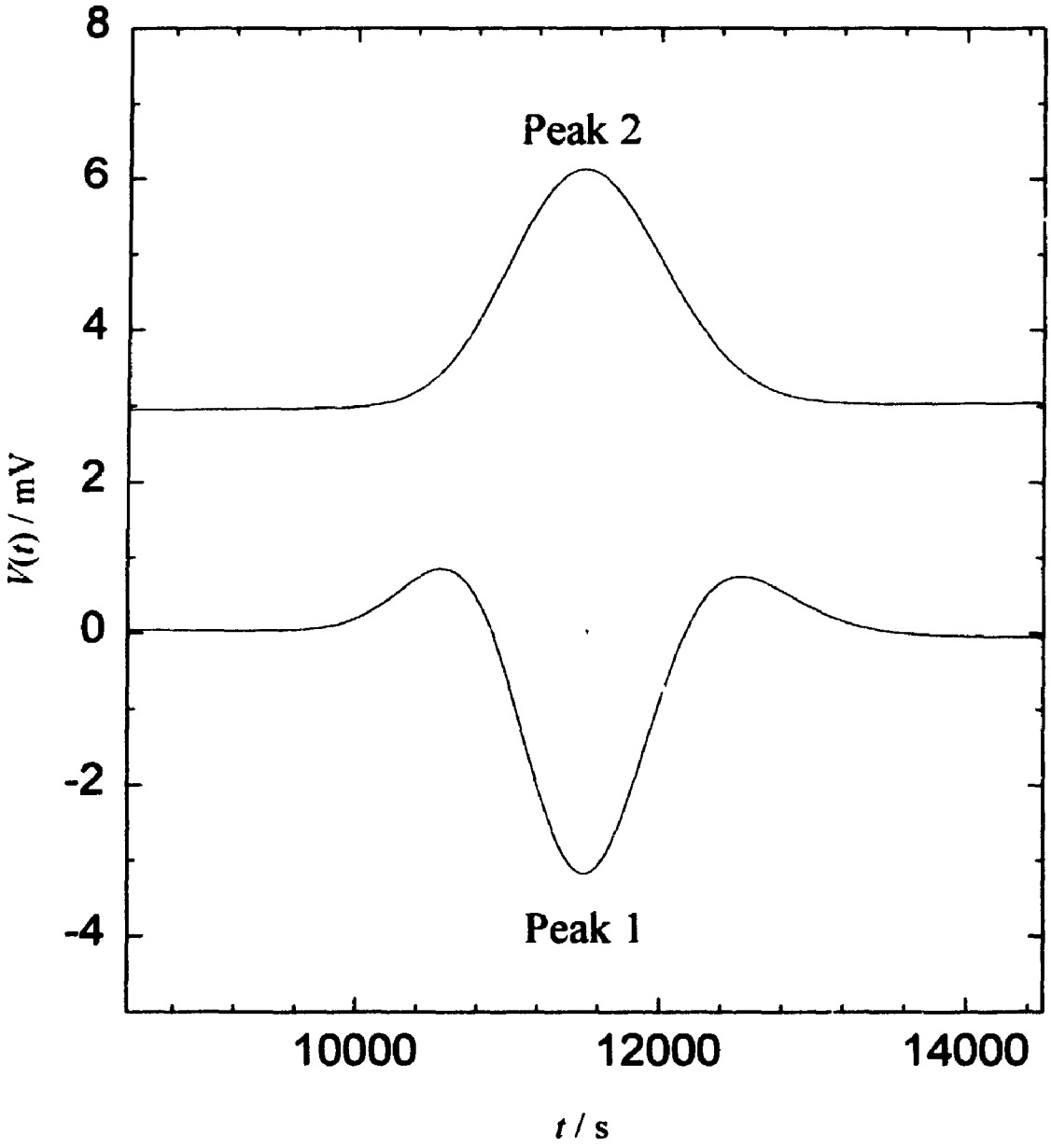
8
6
4
2
0
-2
-4
V(t) / mV
Peak 2
Peak 1
10000
12000
14000
t / s

Table 8-1[a] Ternary interdiffusion coefficients of water(1)/AOT(2)/*n*-heptane(0) at 25 °C

(Predicted values in parentheses)

C_1	C_2	D_{11} [± 0.03]	D_{12} [± 0.04]	D_{21} [±0.005]	D_{22} [± 0.005]	R_1/R_2
0.0135	0.025	0.52(0.35)	-0.02(0.028)	-0.026(-0.099)	0.384(0.45)	-0.022
0.027	0.050	0.48(0.35)	-0.05(0.028)	-0.028(-0.099)	0.388(0.45)	-0.024
0.054	0.100	0.40(0.35)	-0.02(0.028)	-0.029(-0.099)	0.380(0.45)	-0.023
0.108	0.200	0.30(0.35)	0.03(0.028)	-0.019(-0.099)	0.392(0.45)	-0.023
0.025	0.025	0.49(0.30)	0.00(0.063)	-0.029(-0.064)	0.363(0.43)	-0.022
0.125	0.025	0.19(0.15)	0.22(0.44)	-0.017(-0.018)	0.335(0.33)	-0.024
0.252	0.025	0.13(0.092)	0.34(0.88)	-0.007(-0.009)	0.257(0.27)	-0.027
0.504	0.050	0.11(0.094)	0.44(0.[illegible])	-0.007(-0.009)	0.245(0.27)	-0.026
1.008	0.100	0.09(0.092)	0.30(0.88)	-0.006(-0.009)	0.213(0.27)	-0.027
2.016	0.200	0.08(0.092)	0.45(0.88)	-0.003(-0.009)	0.172(0.27)	-0.022
0.503	0.025	0.06(0.046)	0.54(1.54)	-0.003(-0.004)	0.194(0.20)	-0.033

[a]Units: C_i in mol L^{-1}; D_{ik} in 10^{-5} cm^2 s^{-1}.

Cross-coefficient D_{12} is large and positive for microemulsions with high water:AOT ratios. In some cases D_{12} is 2-3 times larger than D_{22}, which means that each mole of diffusing AOT can cotransport several moles of water. A similar observation was reported in Vitagliano *et al.*'s study[32]. This result appears to be reasonable: a surrounding shell of diffusing AOT may carry along a core of emulsified water. On the other hand, the negative D_{21} values indicate that diffusing water produces a countercurrent coupled flow of AOT. The explanation for this surprising behaviour is not obvious.

8.4. Discussion

Molecular Interpretation of Microemulsion Interdiffusion Coefficients The D_{ik} coefficients reported in this chapter give the fluxes of total water and AOT components produced by macroscopic concentration gradients. To develop a molecular interpretation of the diffusion behaviour, water and AOT will be assumed to diffuse through a heptane-continuous solvent as a collection of associated $(H_2O)_m(AOT)_n$ species[35]. This simplified picture of a water-in-oil microemulsion is valid at low volume fractions of water and AOT.

The flux of each $(H_2O)_m(AOT)_n$ species will be represented by

$$j_m = -D_m \nabla c_m \qquad (m = 0, 1, 2, 3, \ldots) \tag{8.4}$$

where D_m and ∇c_m are the diffusion coefficient and the gradient in concentration of the mth species. Equation (8.4) is an accurate approximation at low concentrations where the interactions between the diffusing species (other than rapid association equilibria) are negligible.

Each mole of the mth species carries m moles of water(1) and, on average, $n(m)$ moles of AOT(2). Hence, the species flux j_m contributes mj_m to the molar flux J_1 of the total water component, and $n(m)j_m$ to the flux J_2 of the total AOT component:

$$J_1 = \sum_m m j_m = -\sum_m m D_m \nabla c_m \tag{8.5}$$

$$J_2 = \sum_m n(m) j_m = -\sum_m n(m) D_m \nabla c_m \tag{8.6}$$

The chain rule can be used to express the concentration gradients for the species in terms of the concentration gradients in the water(1) and AOT(2) components.

$$J_1 = -\sum_m mD_m[\frac{\partial c_m}{\partial C_1}\nabla C_1 + \frac{\partial c_m}{\partial C_2}\nabla C_2] \quad (8.7)$$

$$J_2 = -\sum_m n(m)D_m[\frac{\partial c_m}{\partial C_1}\nabla C_1 + \frac{\partial c_m}{\partial C_2}\nabla C_2] \quad (8.8)$$

Comparison of equations (8.7) and (8.8) with the ternary Fick equations (equations (8.2) and (8.3)) shows that the diffusion coefficients of the species (D_m) are related to the interdiffusion coefficients of the components (D_{ik}) as follows

$$D_{11} = \sum_m mD_m \partial c_m/\partial C_1 \quad (8.9)$$

$$D_{12} = \sum_m mD_m \partial c_m/\partial C_2 \quad (8.10)$$

$$D_{21} = \sum_m n(m)D_m \partial c_m/\partial C_1 \quad (8.11)$$

$$D_{22} = \sum_m n(m)D_m \partial c_m/\partial C_2 \quad (8.12)$$

It is important to notice that the interdiffusion coefficients are not simple concentration-weighted averages of the diffusing species (*e.g.*, mc_m/C_1 is the fraction of total water carried by species m, but $D_{11} \neq \Sigma mc_mD_m/C_1$). This means that coefficients D_{11} and D_{22} for the water and AOT components are not average diffusion coefficients of the microemulsion droplets.

Equations (8.9)-(8.12) suggest that a model for diffusion in microemulsions requires estimates of: i) the composition of the microemulsion droplets (m, n); ii) the diffusion coefficients of the droplets (D_m); iii) the changes in the concentrations of the droplets caused by changes in the concentrations of total water(1) and surfactant(2) components ($\partial c_m/\partial C_1$, $\partial c_m/\partial C_2$).

In the treatment developed here, each $(H_2O)_m(AOT)_n$ species is assumed to consist of a spherical water core (radius $r_{m(core)}$) surrounded by a monolayer skin of AOT (thickness r_{skin}). The radius of the mth droplet is therefore $r_m = r_{skin} + r_{m(core)}$. The number of water molecules in the droplet is obtained by dividing the core volume by the molecular volume of water, v_{H_2O}.

$$m = (4/3)\pi r^3_{m(core)} / v_{H_2O} \quad (8.13)$$

Similarly, the average number of AOT molecules carried by droplet m is obtained by dividing the skin volume $(4/3)\pi(r^3_m - r^3_{m(core)})$ by the molecular volume of AOT:

$$n(m) = (4/3)\pi[r_m^3 - (3mv_{H_2O}/4\pi)]/v_{AOT} \quad (8.14)$$

The diffusion coefficients of the droplets can be estimated by using the Stokes-Einstein equation: $D_m = kT/6\pi\eta r_m$, where k is Boltzmann's constant, T the temperature, and η the viscosity of pure heptane. At 25 °C the expression for D_m simplifies to

$$D_m / \text{cm}^2\ \text{s}^{-1} = \frac{5.66 \times 10^{-13}}{r_m / \text{cm}} \quad (8.15)$$

Microemulsion droplets are constantly colliding and reforming on a microsecond timescale, which is very rapid compared to macroscopic diffusion processes. It is useful and meaningful, therefore, to estimate the average size and composition of the droplets. Equations (8.13) and (8.14) can be used together with the mass balance requirement

$$\bar{n} = (C_2/C_1)\bar{m} \quad (8.16)$$

to obtain

$$\bar{r}_{core} = \frac{r_{skin}}{[1 + (C_2 v_{AOT}/C_1 v_{H_2O})]^{1/3} - 1} \quad (8.17)$$

for the average core radius and hence

$$\bar{m} = (4/3)\pi\bar{r}^3_{core}/v_{H_2O} \quad (8.18)$$

for the average value of m.

Given the concentrations C_1 and C_2 of the total water(1) and AOT(2) components, equations (8.15)-(8.18) can be used to estimate the average size, composition, and diffusion coefficient of the microemulsion droplets. Table 8-2 lists average values of m, n, r_m, and D_m obtained in this manner. The values[31] $r_{skin} = 10 \times 10^{-8}$ cm, $v_{H_2O} = 3.00 \times 10^{-24}$ cm^3, and $v_{AOT} = 649 \times 10^{-24}$ cm^3 were used in the calculations. The average size of the droplets increases sharply with the molar ratio $R = C_1{:}C_2$ of water to AOT.

Two-Droplet Model of Microemulsion Diffusion To simplify the analysis, we will assume initially that the microemulsion droplets are almost monodisperse. A given microemulsion will be assumed to contain only two droplet species designated by m_- and

Table 8-2 Calculated average compositions, sizes, and diffusion coefficients of $(H_2O)_m(AOT)_n$ microemulsion droplets

$R = C_1/C_2$	m	n	r_m / nm	D_m / 10^{-5} cm^2 s^{-1}
0.0	0.0	6.5	10.0	0.566
0.5	8.54	13.9	13.9	0.406
1.0	22.8	22.8	15.5	0.366
2.0	66.8	33.4	17.8	0.318
5.0	334	66.9	23.4	0.242
10.0	1360	136	31.3	0.181
20.0	6550	327	46.0	0.123
30.0	17800	593	60.3	0.094

m_+, where m_- and m_+ are the integers immediately above and below the average value . The concentration of the two species can be evaluated by solving the mass balance requirements

$$C_1 = m_- c_{m-} + m_+ c_{m+} \quad (8.19)$$

$$C_2 = n_- c_{m-} + n_+ c_{m+} \quad (8.20)$$

As a particular example, consider the water-in-heptane microemulsion containing $C_1 = 0.108$ mol L^{-1} water and $C_2 = 0.200$ mol L^{-1} AOT. At this composition the average number of water and AOT molecules per droplet are 9.48 and 17.56, respectively, the average droplet radius is $r_m = 14.07$ nm, and the average droplet diffusion coefficient is $D_m = 0.402 \times 10^{-5}$ cm^2 s^{-1}. In this case m_- is 9, m_+ is 10, and the average number of AOT molecules carried by the two species calculated from equation (8.14) is $n_- = 17.31$ and $n_+ = 17.82$. The concentrations of the $(H_2O)_9(AOT)_{17.31}$ and $(H_2O)_{10}(AOT)_{17.82}$ species are $c_9 = 0.00592$ mol L^{-1} and $c_{10} = 0.00548$ mol L^{-1}, and their respective diffusion coefficients are $D_9 = 0.404 \times 10^{-5}$ cm^2 s^{-1} and $D_{10} = 0.400 \times 10^{-5}$ cm^2 s^{-1}.

In this way the concentrations and diffusion coefficients of the microemulsion droplets can be estimated for different overall concentrations of the total water and AOT components. Equations (8.9)-(8.12) can then be used to predict the ternary D_{ik} coefficients.

In Figure 8-3 the predicted ternary diffusion coefficients are plotted against R, the molar ratio of water:AOT. The predictions are encouraging, especially the large, positive D_{12} values and small, negative D_{21} values which agree qualitatively with the experimental results. Also, the two-droplet model supports the experimental result that diffusion coefficient D_{22} for the AOT component can be significantly larger than D_{11} for the water component. At $R = 25$, for example, D_{22} is predicted to be five times larger than D_{11}: $D_{11} = 0.035 \times 10^{-5}$ and $D_{22} = 0.178 \times 10^{-5}$ cm^2 s^{-1}. In this case the diffusion coefficients of the droplet species, $D_{11274} = 0.10641 \times 10^{-5}$ and $D_{11275} = 0.10640 \times 10^{-5}$ cm^2 s^{-1}, differ by less than 0.01%. This example demonstrates clearly that a nearly monodisperse collection of microemulsion droplets can have two distinct diffusional relaxation times. Moreover, AOT appears to "break the speed limit" because its diffusion coefficient is about 70% larger than the diffusion coefficients of the AOT-containing species that actually transport the AOT component through the heptane solvent!

Figure 8-3 Ternary diffusion coefficients of water(1)/AOT(2)/*n*-heptane(0) water-in-oil microemulsions predicted by the two-droplet model plotted against the molar water:AOT ratio. Solid curves: D_{ik} values; Dashed curve: average droplet diffusion coefficient D_m.

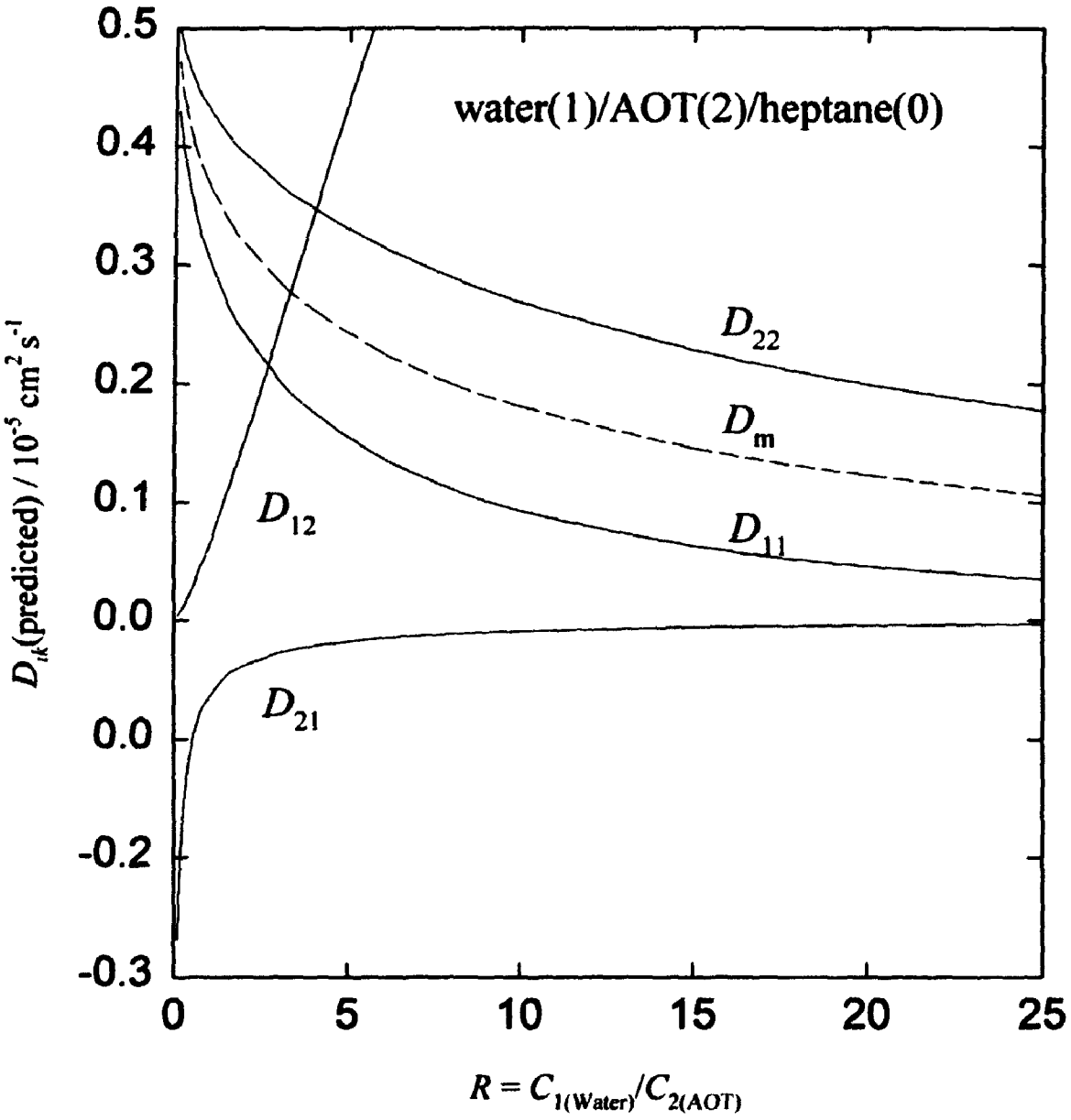
water(1)/AOT(2)/heptane(0)
D_{22}
D_m
D_{11}
D_{12}
D_{21}
D_{ik}(predicted) / 10^{-5} cm^2 s^{-1}
$R = C_{1(Water)}/C_{2(AOT)}$
0.5
0.4
0.3
0.2
0.1
0.0
0.0
-0.2
-0.3
0
5
10
15
20
25

The key to understanding this seemingly paradoxical behavior is the fact that an increase in the concentration of AOT produces a larger number of droplets, which in turn increases the droplet concentration gradients that drive the diffusion of the droplets. Conversely, an increase in the concentration of water produces fewer droplets and smaller droplet concentration gradients.

To put these ideas on a firmer footing, Figure 8-4 shows droplet concentration gradients produced by a gradient in the concentration of the total AOT(2) component. (The concentration of the total water(1) component is held constant.) This example shows that the concentration of the smaller $(H_2O)_9(AOT)_{17.3}$ droplets clearly increases with the concentration of AOT, while the concentration of the larger $(H_2O)_{10}(AOT)_{17.8}$ droplets decreases. More precisely, we find: $\partial c_9/\partial C_2 = 0.782$ and $\partial c_{10}/\partial C_2 = -0.703$. The $(H_2O)_9(AOT)_{17.3}$ droplets have a larger concentration gradient and a larger diffusion coefficient than the $(H_2O)_{10}(AOT)_{17.8}$ droplets. These two factors combine to move the smaller droplets down the AOT gradient more rapidly than the larger droplets move up the AOT gradient. The extra flux of water transported by the smaller droplets produces a net flux of water down the AOT gradient, as reflected by the positive D_{12} values.

Figure 8-5 shows droplet concentration gradients produced by a gradient in the concentration of the total water component(1) (In this case the concentration of total AOT(2) is fixed.). As mentioned earlier, increasing the concentration of water favors the formation of the larger droplets: $\partial c_9/\partial C_1 = -1.39$ and $\partial c_{10}/\partial C_1 = 1.35$. Because the gradient in the concentration of the smaller droplet ($m = 9$) is negative and larger in magnitude than the gradient in concentration of the larger droplet ($m = 10$), the flux of $(H_2O)_9(AOT)_{17.3}$ up the water gradient exceeds the flux of $(H_2O)_{10}(AOT)_{17.8}$ down the water gradient. The net flux of AOT transported up the water gradient appears as a countercurrent coupled flow of AOT, and hence cross-coefficient D_{21} is negative.

The measured and predicted D_{ik} values are compared in Table 8-1. The agreement is reasonable in view of the simplicity of the two-droplet model. Nevertheless, there is room for improvement. For example, the magnitude of cross-coefficient D_{21} is overestimated. Better agreement might be obtained by including interactions between the

Figure 8-4 Gradients in the concentrations of microemulsion droplet species $(H_2O)_9(AOT)_{17.3}$ and $(H_2O)_{10}(AOT)_{17.8}$ produced by a linear gradient in C'_2, the concentration of the total AOT(2) component. The concentration of water(2) is fixed at 0.108 mol L^{-1}.

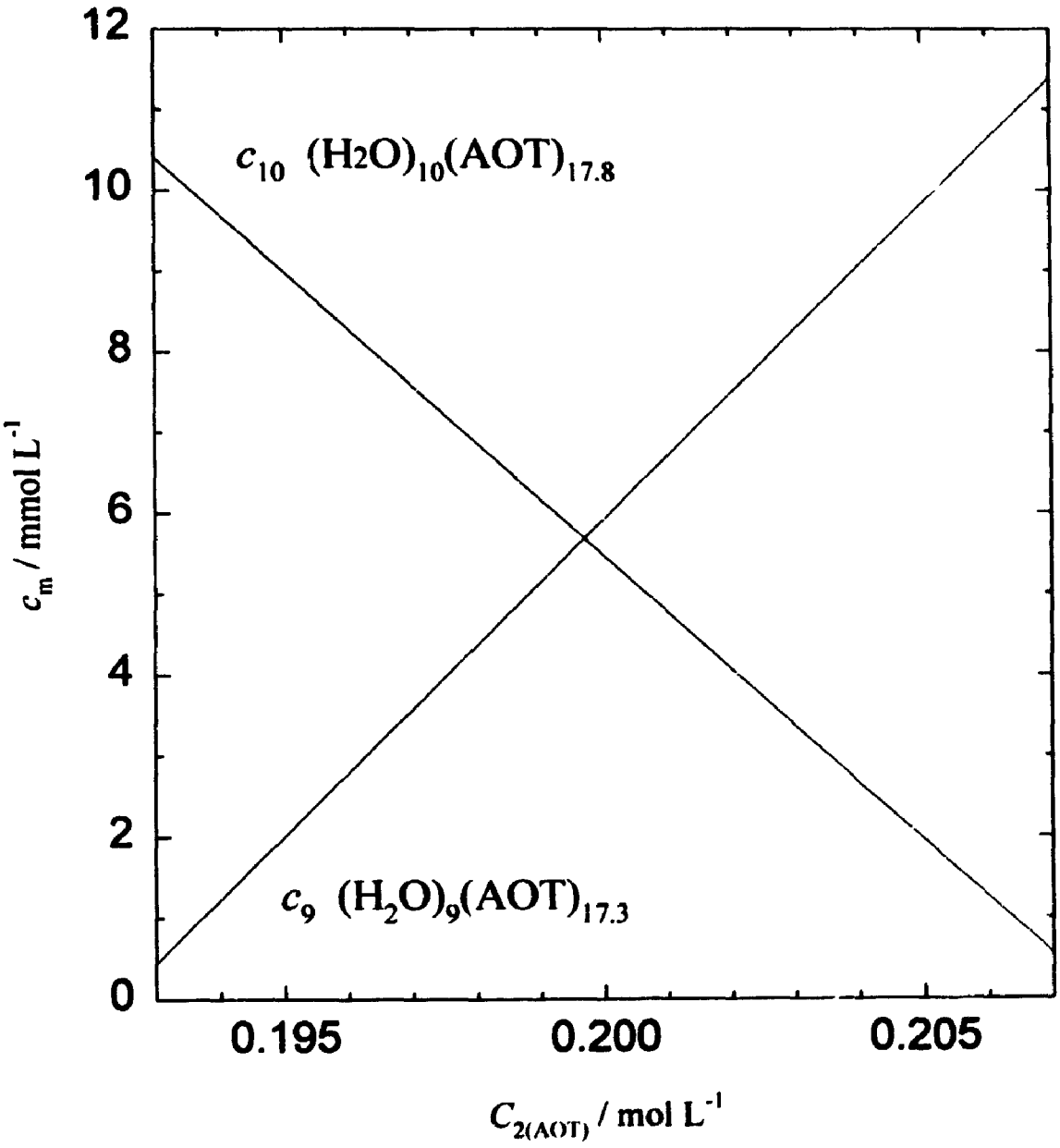
12
10
8
6
4
2
0
c_m / mmol L^{-1}
c_{10} $(H_2O)_{10}(AOT)_{17.8}$
c_9 $(H_2O)_9(AOT)_{17.3}$
0.195
0.200
0.205
$C_{2(AOT)}$ / mol L^{-1}

Figure 8-5 Gradients in the concentrations of microemulsion droplet species $(H_2O)_9(AOT)_{17.3}$ and $(H_2O)_{10}(AOT)_{17.8}$ produced by a linear gradient in C_1, the concentration of the total water(1) component. The concentration of AOT(2) is fixed at 0.200 mol L^{-1}.

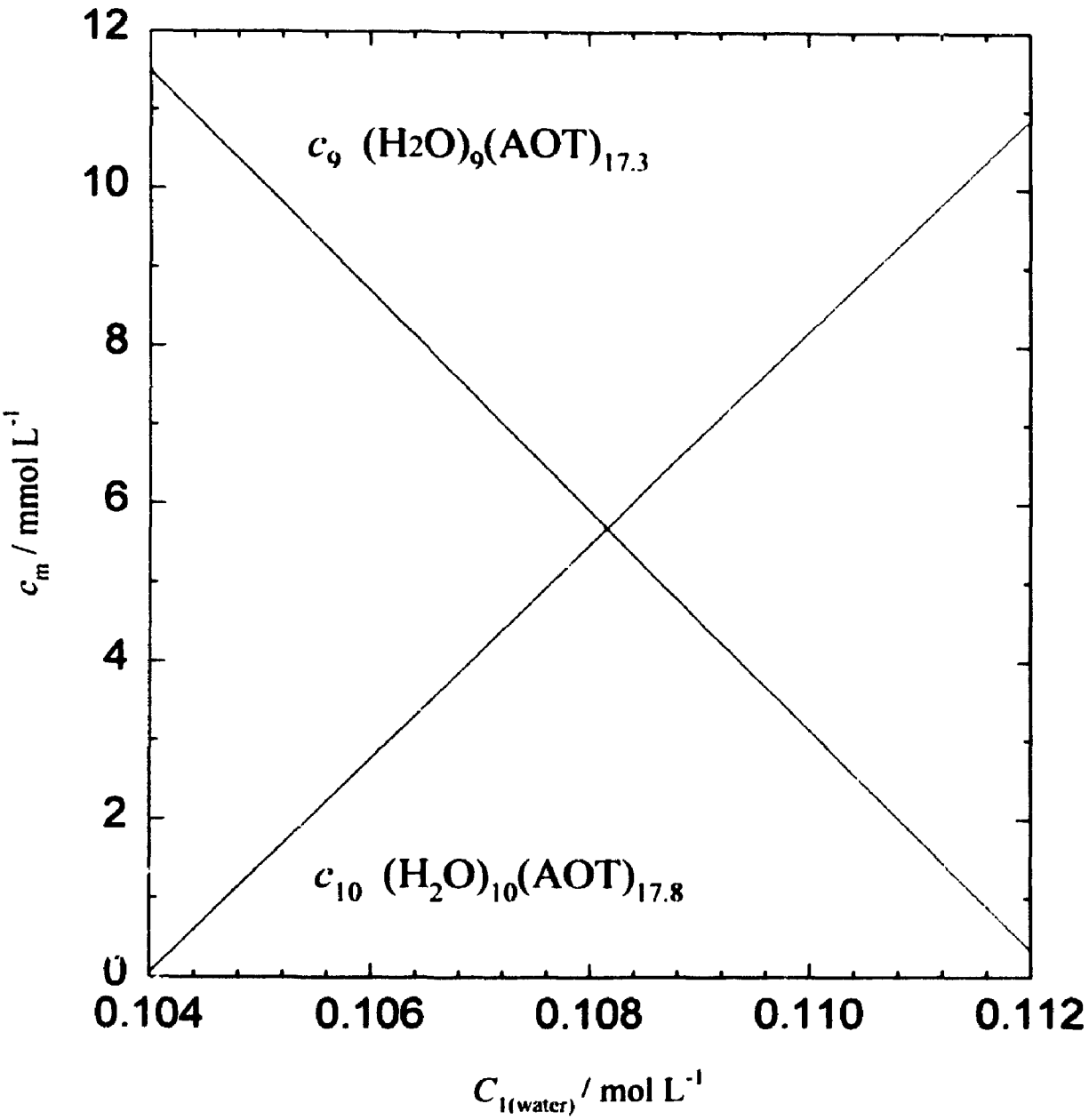
12
10
8
6
4
2
0
0.104
0.106
0.108
0.110
0.112
c_m / mmol L^{-1}
$C_{1(water)}$ / mol L^{-1}
c_9 $(H_2O)_9(AOT)_{17.3}$
c_{10} $(H_2O)_{10}(AOT)_{17.8}$

droplet species or by using a larger number of droplet species to represent the polydispersity.

Gaussian Distribution Model To check whether the two-droplet approximation is too severe, droplet concentrations were recalculated from the Gaussian distribution

$$\frac{mc_m}{C_1} = \frac{A}{\sqrt{2\pi}\sigma_m}\exp[-\frac{(m-\bar{m})^2}{2\sigma_m^2}] \tag{8.21}$$

The standard deviation σ_m was arbitrarily set equal to 0.1 or 0.2. A is a normalization factor to allow for the fact that the distribution is not continuous.

The ternary diffusion coefficients calculated from the Gaussian and two-droplet distributions differed by only a few percent, which is not significant in view of the approximations made in the model. The two-droplet distribution is preferred because of its greater simplicity.

Pseudo-Binary Microemulsion Diffusion Coefficients If the concentration gradients are adjusted to maintain a fixed ratio of water:AOT at each point along the diffusion path, the composition and sizes of the microemulsion droplets will be nearly constant throughout the system. Vitagliano *et al.*[31] pointed out that the pseudo-binary treatment of microemulsion diffusion is a good approximation under these conditions.

If the ratio $R = C_1(\text{water})/C_2(\text{AOT})$ is constant, then $\nabla C_2 = R^{-1}\nabla C_1$ can be substituted into equation (8.2) to obtain

$$J_1 = -(D_{11} + R^{-1}D_{12})\nabla C_1 = -D_{1(\text{bin})}\nabla C_1 \tag{8.22}$$

Similarly, $\nabla C_1 = R\nabla C_2$ can be substituted into equation (8.3) to obtain

$$J_2 = -(D_{22} + RD_{21})\nabla C_2 = -D_{2(\text{bin})}\nabla C_2 \tag{8.23}$$

Equations (8.22) and (8.23) relate the diffusional flows to single concentration gradients, which defines the pseudo-binary diffusion coefficient in terms of the ternary diffusion coefficients as follows

$$D_{1(\text{bin})} = D_{11} + R^{-1}D_{12} \tag{8.24}$$

$$D_{2(\text{bin})} = D_{22} + RD_{21} \tag{8.25}$$

Table 8-3[a] Pseudo-binary diffusion coefficients of water(1)/AOT(2)/*n*-heptane(0) at 25 °C (Predicted values in parentheses)

C_1	C_2	R	$D_{11} + R^{-1}D_{12}$	$D_{22} + RD_{21}$	D(Taylor)	D(Gouy)[b]
0.0135	0.025	0.54	0.48 ± 0.10 (0.40)	0.37 ± 0.01 (0.40)	0.37	0.37
0.027	0.050	0.54	0.39 ± 0.10 (0.40)	0.37 ± 0.01 (0.40)	0.37	0.37
0.054	0.100	0.54	0.36 ± 0.10 (0.40)	0.36 ± 0.01 (0.40)	0.36	0.35
0.108	0.200	0.54	0.36 ± 0.10 (0.40)	0.38 ± 0.01 (0.40)	0.36	-
0.025	0.025	1.00	0.49 ± 0.07 (0.37)	0.33 ± 0.01 (0.37)	0.36	-
0.125	0.025	5.00	0.23 ± 0.04 (0.24)	0.25 ± 0.03 (0.24)	0.24	-
0.252	0.025	10.1	0.16 ± 0.04 (0.18)	0.19 ± 0.05 (0.18)	0.19	0.16
0.504	0.050	10.1	0.15 ± 0.05 (0.18)	0.17 ± 0.02 (0.18)	0.19	-
0.503	0.025	20.1	0.09 ± 0 03 (0.12)	0.13 ± 0.10 (0.12)	0.16	0.12

[a]Units: C_i in mol L^{-1}; D_{ik} and D in 10^{-5} cm^2 s^{-1}.

[b]ref. 31

Table 8-3 gives values the pseudo-binary diffusion coefficients calculated from the measured D_{ik} values. Taking into account the relatively large experimental uncertainties in $D_{11} + R^{-1}D_{12}$, the values of $D_{1(bin)}$ and $D_{2(bin)}$ calculated from equations (8.24) and (8.25) are in good agreement at each composition.

Table 8-3 includes the pseudo-binary diffusion coefficients predicted by the two-droplet model. Identical values of $D_{1(bin)}$ and $D_{2(bin)}$ are predicted at each composition. This result shows that the model for microemulsion diffusion developed in this chapter contains pseudo-binary diffusion as a special case (constant water:AOT ratio along the diffusion path).

For comparison, pseudo-binary diffusion coefficients (D) measured by Vitagliano *et al.*[31] by the Gouy optical interference method are also listed in Table 8-3. The good agreement of the D values with the measured and predicted values of $D_{11} + R^{-1}D_{12}$ and $D_{22} + RD_{21}$ serves as an independent check of the Taylor data and the two-droplet model developed in this chapter.

As an additional check, we measured pseudo-binary diffusion coefficients by the Taylor method. In these runs the concentrations of water and AOT in the injected solutions differed from the corresponding concentrations in the carrier solutions, but the ratios of water:AOT in the two solutions were identical. The results were analyzed by fitting the binary dispersion equation (4.9) to the peaks. In Table 8-3 the pseudo-binary D values obtained by the Taylor method are compared with the Gouy values. The agreement is excellent at compositions where the cross-diffusion coefficients are negligible and the pseudo-binary approximation is valid. Small differences (up to 0.04×10^{-5} cm^2 s^{-1}) between the Gouy and Taylor D values are observed at other compositions.

8.5. Conclusions

Taylor dispersion can provide detailed information about chemical interdiffusion in microemulsions. The ternary interdiffusion coefficients measured for water/AOT/heptane show that water and surfactant diffuse independently in water-in-oil microemulsions. At compositions with high ratios of water:AOT, for example, the diffusion of water is

significantly slower than the diffusion of AOT. As a result, gradients in composition in this system decay with two distinct diffusional relaxation times.

Cross-diffusion is important for the water/AOT/heptane system: a gradient in the concentration of AOT produces a coupled flow of water, and *vice versa*. The inclusion of coupled diffusion provides a more complete picture of microemulsion diffusion than reported previous studies.

A simple model for microemulsion diffusion can be developed by taking into account the changes in size and composition of the microemulsion droplets caused by changes in the concentration of the water and surfactant. The model supports the Taylor results, and it accounts for the two different diffusional relaxation times, even in cases of negligible polydispersity.

8.6. References

1. M. Kahlweit, R. Strey, D. Haase, H. Kunieda, T. Schmeling, B. Faulhaber, M. Borkovec, H.F. Eicke, G. Busse, F. Eggers, T. Funck, H. Richmann, L. Magid, O. Soderman, P. Stilbs, J. Winkler, A. Dittrich and W. Jahn, *J. Colloid Interface Sci.* **118**, 436 (1987).
2. O. Ghosh and C.A. Miller, *J. Phys. Chem.* **91**, 4528 (1987).
3. F. Candau, Y.S. Leong, G. Pouyet and S. Candau, *J. Colloid Interface Sci.* **101**, 167 (1984).
4. A. D'Aprano, G. D'Arrigo, A. Paparelli, M. Goffredi and T. Liveri, *J. Phys. Chem.* **97**, 3616 (1993).
5. V. Goffredi, T. Liveri and G. Vassallo, *J. Solution Chem.* **22**, 941 (1993).
6. G. D'Arrigo, A. Paparelli, A. D'Aprano, I.D. Donato, M. Goffredi and V.T. Liveri, *J. Phys. Chem.* **93**, 8367 (1989).
7. B.H. Robinson, D.C. Steyler and R.D. Tack, *J. Chem. Soc Faraday Trans. 1*, **75**, 481 (1979)
8. M. Zulauf and H.F. Eicke, *J. Phys. Chem.*, **83**, 480 (1979)
9. J.D. Nicholson and J.H.R. Clarke, *Surfactants in Solution*, Vol.3, K.L. Mittal and B. Lindman eds., Plenum, New York, 1984, p.1663

10. E. Sein, J.R. Lalanne, J. Buchert and S. Kielich, *J. Colloid Interface Sci.*, **72**, 363 (1979)

11. R.A. Day, B.H. Robinson, J.H.R. Clarke and J.V. Doherty, *J. Chem. Soc. Faraday Trans. 1*, **75**, 132 (1979)

12. E. Gulari, B. Bedwell and S.J. Alkhafaji, *J. Colloid Interface Sci.*, **77**, 202 (1980)

13. J.H.R. Clarke, J.D. Nicholson and K.N. Regan, *J. Chem. Soc. Faraday Trans.1*, **81**, 1173 (1985)

14. C. Cabos and P. Delord, *J. Appl. Crystallogr.*, **12**, 502 (1979)

15. B.H. Robinson, C. Toprakcioglu, J.C. Dore and P. Chieux, *J. Chem. Soc. Faraday Trans. 1*, **80**, 13 (1984)

16. C. Toprakcioglu, J.C. Dore, B.H. Robinson and A. Howe, *J. Chem. Soc. Faraday Trans. 1*, **80**, 413 (1984)

17. M. Kotlarchyk, S.H. Chen and J.S. Huang, *J. Phys. Chem.*, **86**, 3273 (1982)

18. M. Kotlarchyk, S.H. Chen, J.S. Huang and M.W. Kim, *Phys. Rev.*, **A29**, 2054 (1984)

19. M. Kotlarchyk, J.S. Huang and S.H. Chen, *J. Phys. Chem.*, **89**, 4382 (1985)

20. T. Assih, F. Larché and P. Delord, *J. Colloid Interface Sci.*, **89**, 35 (1982)

21. C. Cabos and J. Marignan, *J. Phys. Lett.*, **46**, L-267 (1985)

22. M.P. Pileni, T. Zemb and C. Petit, *Chem. Phys. Lett.*, **118**, 414 (1985)

23. S.S. Atik and J.K. Thomas, *J. Am. Chem. Soc.*, **103**, 3543 (1981)

24. N.J. Bridge and P.D.I. Fletcher, *J. Chem. Soc. Faraday Trans. 1*, **79**, 2161 (1983)

25. A.M. Ganz and B.E. Boeger, *J. Colloid Interface Sci.*, **109**, 504 (1986)

26. A. Maita, *J. Phys. Chem.*, **88**, 5122 (1984)

27. T. Wärnheim, E. Sjöblom, U. Henriksson and P. Stilbs, *J. Phys. Chem.*, **88**, 5420 (1984)

28. P. Guéring and B Lindman, *Langmuir*, **1**, 464 (1985)

29. A.C. Lam and R.S. Schechter, *J. Colloid Interface Sci.*, **120**, 56 (1987)

30. R.A. Mackay, N.S. Dixit and C. Hermansky, *Colloids Surf.*, **21**, 27 (1986)

31. L. Costantino, C. Della Volpe, O. Ortona and V. Vitagliano, *J. Colloid Interface Sci.*, **148**, 72 (1992)

32. L. Costantino, C. Della Volpe, O. Ortona and V. Vitagliano, *J. Chem. Soc. Faraday Trans.*, **88**, 61 (1992)

33. P.D.I. Fletcher, A.M. Howe, N.M. Perrins, B.H. Robinson, C. Toprakcioglu and J.C. Dore, *Surfactants in Solution*, Vol. 3, K.L. Mittal and B. Lindman, Plenum, New York, 1984, p.1745

34. P.D.I. Fletcher and B.H. Robinson, *Ber. Bunsenges. Phys. Chem.*, **85**, 863 (1981)

35. H.F. Eicke and V. Arnold, *J. Colloid Interface Sci.*, **46**, 101 (1974)

Chapter 9

TERNARY INTERDIFFUSION IN WATER/2-PROPANOL/*n*-HEXANE MIXTURES – AN UNUSUAL MICROEMULSION SYSTEM

This chapter deals with ternary interdiffusion in an unusual surfactant-free microemulsion system: water/*2*-propanol/*n*-hexane. A chemical equilibrium model is proposed to describe the diffusion behaviour of this system.

9.1. Introduction

2-propanol, a common organic solvent, is not usually considered to be a surfactant. On the basis of centrifugation and conductivity data, however, Barden *et al.*[1] showed that microemulsions, stabilized by *2*-propanol, can be prepared without the addition of any other surfactants. A pseudo-phase diagram for the water/*2*-propanol/*n*-hexane is presented in Figure 9-1[1]. Region A contains unstable two-phase macroemulsions which are turbid and consist of immiscible water-rich and hexane-rich liquids. In region B, transparent and stable microemulsions are formed. Small aggregates of water and *2*-propanol form in region C. The mixtures in region D appear to behave as "normal" ternary solutions without aggregates and clusters. Region E includes compositions that give metastable microemulsions.

The work reported in this chapter focuses on ternary interdiffusion in microemulsion region B. Water/*2*-propanol/*n*-hexane microemulsions are more complicated than the water/AOT/*n*-heptane microemulsions treated in the previous chapter because *2*-propanol dissolves in the microemulsion droplets as well as in the hexane-continuous phase. Also, the water/*2*-propanol microdroplets are polydisperse.

9.2. Experimental Procedure

The microemulsions were prepared in calibrated volumetric flasks using distilled, deionized water, anhydrous *2*-propanol (BDH, < 0.05% water) and *n*-hexane (BDH, >99% purity). The densities of the mixtures were measured with 25-mL specific-gravity

Figure 9-1 Phase diagram for the *n*-hexane/water/2-propanol system at 25 °C reported by Barden *et al.*[1] The striped areas are unexplored due to practical limitations. The numerical values on the axes are mole fractions.
A: two-phase region; B: stable microemulsions; C: small aggregates of water and *2*-propanol; D: normal ternary solutions; E: metastable microemulsions.

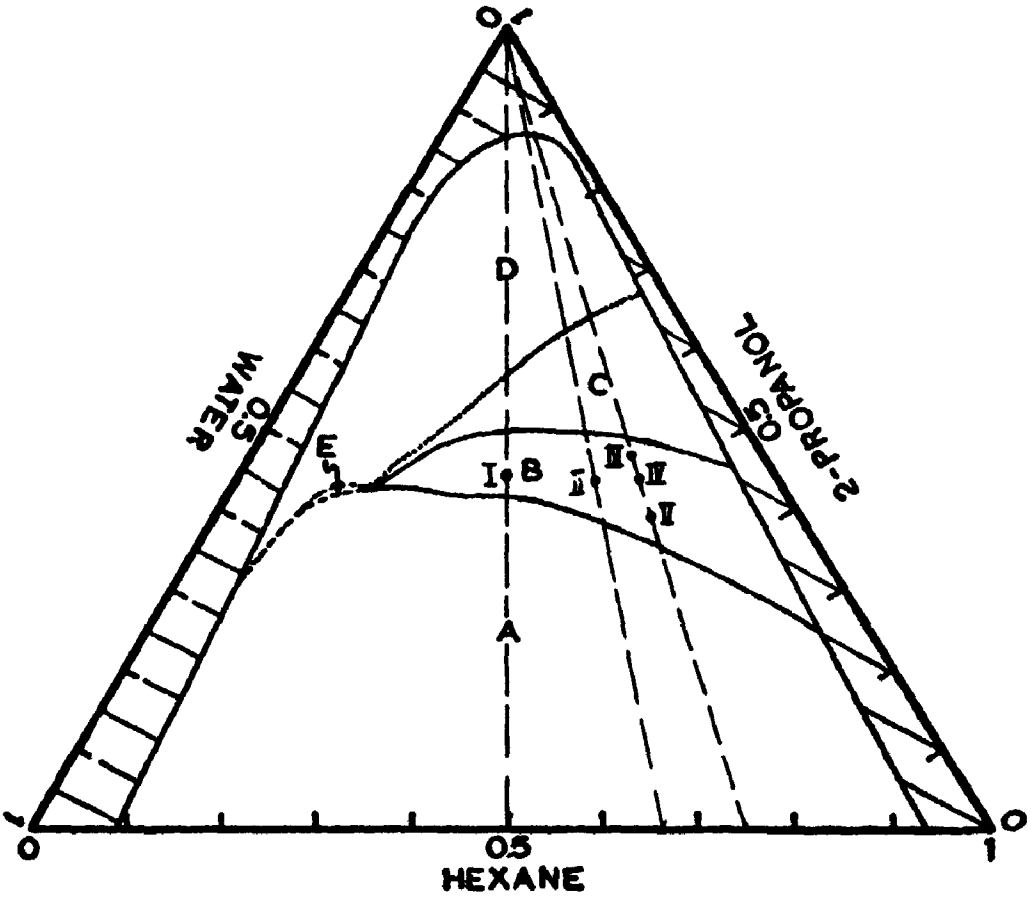
0
WATER
0.5
2-PROPANOL
0.5
0
0.5
1
HEXANE
D
C
A
B
E
I
II
III
IV
V

bottles in order to convert mole fractions given in the phase diagram to volumetric concentrations (mol L^{-1}). Viscosities were measured with a Cannon-Fenske viscometer.

Ternary interdiffusion coefficients of hexane(1)/water(2)/2-propanol microemulsions were measured by the Taylor dispersion technique. The dispersion tube used in this work was a Teflon capillary (length 3334 cm, inner radius 0.04738 cm). The tube was flushed overnight to achieve a stable baseline. A metering pump (Gilson Minipuls 2) maintained a steady flow of carrier solution. The retention times were about 8000 s. The sample solutions (20 μL) were injected through a low-pressure injection valve at the entrance to the dispersion tube. The diffusion coefficients were calculated by least-squares analysis of the refractive index profiles across the eluted samples. The coefficients were measured five or six times at each composition and then averaged.

9.3. Results

Figure 9-2 shows dispersion profiles obtained by injecting 0.40 mol L^{-1} excess hexane (peak 1) or 1.00 mol L^{-1} excess water (peak 2) into a microemulsion carrier stream containing 4.29 mol L^{-1} hexane and 1.43 mol L^{-1} water in 2-propanol.

Peak 2 shows that an initial concentration gradient in water(2) does not decay as a single Gaussian. Instead, it resembles a narrow Gaussian superimposed on a second broader Gaussian. This is an important result because it shows that a concentration gradient in water produces a coupled flow of hexane.

The compositions of the microemulsions that were studied are listed in Table 9-1 and indicated by points I-V in Figure 9-1. The D_{ik} values measured at each composition are summarized in Table 9-2. In addition to the diffusion coefficients, Table 9-2 includes ratios of the molar refractive index of hexane(1) and water(2). The R_2/R_1 values were calculated by measuring ratios of peak areas generated per mole of excess hexane or water in the injected samples. The ratio R_2/R_1 is quite small at each concentration. The relatively large values of R_1 allowed the dispersion of hexane to be followed more precisely than that of water. Consequently, diffusion coefficients D_{11} and D_{12} for hexane were determined more precisely than coefficients D_{21} and D_{22} for water.

Figure 9-2 Ternary dispersion profiles obtained by injecting 0.40 mol L^{-1} excess *n*-hexane (peak 1) or 1.00 mol L^{-1} excess water (peak 2) into a carrier stream containing 4.29 mol L^{-1} *n*-hexane and 1.43 mol L^{-1} water.

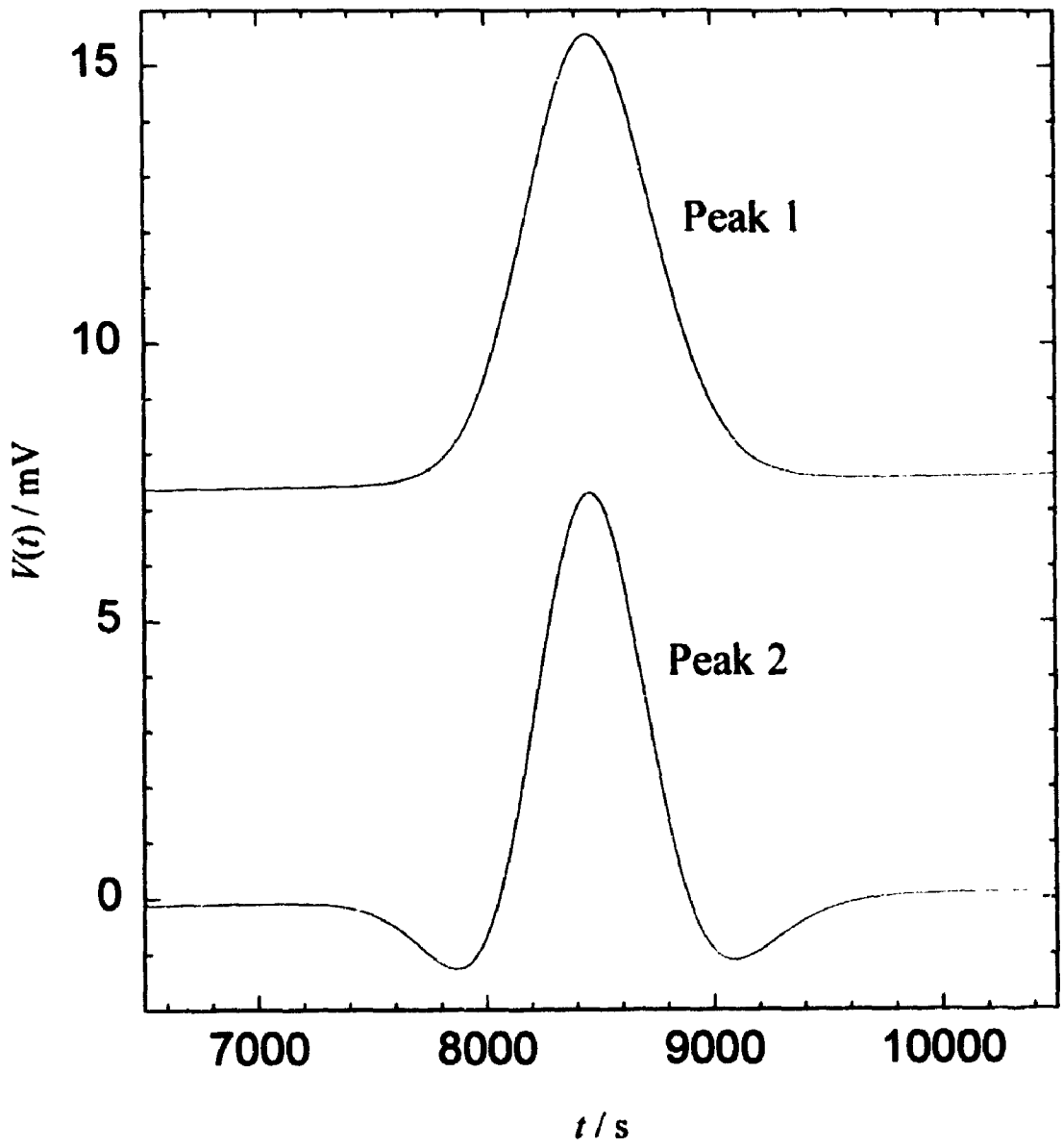
15
10
5
0
V(t) / mV
Peak 1
Peak 2
7000
8000
9000
10000
t / s

Table 9-1 Compositions of *n*-hexane(1)/water(2)/*2*-propanol(0) carrier solutions in region B used in the ternary interdiffusion measurements.

Point	C_0	X_0	C_1	X_1	C_2	X_2	$R = C_1/C_2$
I	5.94	0.450	3.61	0.275	3.61	0.275	1.00
II	5.22	0.450	4.25	0.367	2.13	0.183	2.00
III	5.28	0.480	4.29	0.390	1.43	0.130	3.00
IV	4.90	0.449	4.50	0.413	1.50	0.138	3.00
V	4.28	0.400	4.88	0.450	1.63	0.150	3.00

Units: C_i in mol L^{-1}.

Table 9-2 Ternary interdiffusion coefficients of *n*-hexane(1)/water(2)/*2*-propanol(0) in region B at 25 °C

Point	C_1	C_2	$D_{11}(\pm0.005)$	$D_{12}(\pm0.005)$	$D_{21}(\pm0.04)$	$D_{22}(\pm0.03)$	R_2/R_1
I	3.61	3.61	0.633	0.233	0.046	0.174	0.174
II	4.25	2.13	0.860	0.394	0.029	0.393	0.116
III	4.29	1.43	1.01	0.404	0.097	0.652	0.176
IV	4.50	1.50	0.974	0.478	0.090	0.586	0.094
V	4.88	3.00	1.63	[illegible]488	0.085	0.443	0.055

Units: C_i in mol L^{-1}; D_{ik} in 10^{-5} cm^2 s^{-1}.

It is interesting to note that one mole of diffusing water cotransports about one mole of hexane, whereas one mole of diffusing hexane cotransports only about 0.1 mol of water. The significant coupled flow of hexane caused by diffusing water indicates that there exists interaction between hexane and water. Since hexane and water are immiscible, the interaction between them may be attributable to the role of *2*-propanol which coats the water microdroplets and makes them soluble in the *2*-propanol/hexane continuous.

Since hexane is the major component in region B, this is a water-in-oil microemulsion system. For consistency with the treatment developed in Chapter 8, the D_{ik} coefficients measured for the *n*-hexane(1)/water(2)/*2*-propanol(0) system can be transformed to D_{ik}' coefficients for water(1')/*2*-propanol(2')/*n*-hexane(0') in which the oil (*n*-hexane) is chosen as a solvent. The transformation procedure is based on equations (2.45), (2.46) and (2.47):

$$D_{11}' = D_{22} - \frac{V_2}{V_1} D_{21} \tag{9.1}$$

$$D_{12}' = -\frac{V_{0m}}{V_{1m}} D_{21} \tag{9.2}$$

$$D_{21}' = \frac{V_2}{V_0} D_{11} - \frac{V_1}{V_0} D_{12} + \frac{V_2^2}{V_0 V_1} D_{21} - \frac{V_2}{V_0} D_{22} \tag{9.3}$$

$$D_{22}' = D_{11} + \frac{V_2}{V_1} D_{21} \tag{9.4}$$

where V_0, V_1 and V_2 are the partial molar volumes of *2*-propanol, *n*-hexane, and water, respectively. For our purposes, however, it is sufficiently accurate to use the molar volumes of the pure liquids: *2*-propanol, 7.62×10^{-2} L mol^{-1}; *n*-hexane, 1.30×10^{-1} L mol^{-1}; and water, 1.81×10^{-2} L mol^{-1}. The transformed diffusion coefficients are summarized in Table 9-3.

The molar volume and hence the effective molecular radius of *2*-propanol are much larger than the corresponding quantities for water. Thus water might be expected to diffuse more rapidly than *2*-propanol. In most cases, however, D_{22}' is 2 to 4 times larger than D_{11}'. This result suggests that water diffuses primarily in large, slowly moving

Table 9-3 Ternary interdiffusion coefficients for water(1′)/*2*-propanol(*2*′)/*n*-hexane(0′) at 25 °C

Point	C_1'	C_2'	D_{11}'	D_{12}'	D_{21}'	D_{22}'
I	3.61	5.94	0.17	-0.03	-0.29	0.64
II	2.13	5.22	0.39	-0.02	-0.56	0.86
III	1.43	5.28	0.64	-0.06	-0.66	1.02
IV	1.50	4.90	0.57	-0.05	-0.72	0.99
V	1.63	4.28	0.43	-0.05	-0.69	1.01

Units: C_i' in mol L^{-1}; D_{ik}' in 10^{-5} cm^2 s^{-1}.

Table 9-4 Average radius of water(1′)/*2*-propanol (2′) microemulsion droplets at 25 °C

Point	C_1'	C_2'	η	D_{11}'	r_m
III	1.43	5.28	5.65	0.64	0.60
IV	1.50	4.90	5.45	0.57	0.70
V	1.63	4.28	5.15	0.43	0.98
II	2.13	5.22	5.60	0.39	1.00
I	3.61	5.94	6.70	0.17	1.91

Units: C_i' in mol L^{-1}; η in 10^{-4} Pa s; D_{11}' in 10^{-5} cm^2 s^{-1}; r_m in nm.

microemulsion droplets. On the other hand, 2-propanol diffuses through the hexane solvent both in the droplets and as relatively mobile free 2-propanol molecules.

The values obtained for cross-coefficient D_{12}' for the water component are small and negative, whereas the values of D_{21}' for the 2-propanol component are large and negative. These results indicates that diffusing water produces a large countercurrent coupled flow of 2-propanol, but 2-propanol produces only a small counterflow of water.

9.4. Discussion

Size of the Microemulsion Droplets 2-propanol is completely miscible with both water and hexane. Therefore, 2-propanol is present both in the microemulsified water droplets and in the hexane solvent. On the other hand, nearly all of the water should reside in the microemulsion droplets because of the very low solubility of water in hexane. These considerations suggest that the diffusion coefficient of water (D_{11}') should be nearly equal to the diffusion coefficient of the microemulsion droplets. We can estimate the average droplet radius (r_m) by using the Stokes-Einstein equation (2.21)

$$r_m / \text{nm} = \frac{2.18 \times 10^{-9}}{(\eta / \text{Pa s})(D_{11}'/\text{cm}^2\text{s}^{-1})} \tag{9.5}$$

where η is the viscosity of binary solution consisting of 2-propanol and hexane at 25 °C. Table 9-4 gives the calculated radii of the microemulsion droplets. The results indicate that the average radius of the microemulsion droplets increases as the concentration of water (C_1') increases. The sizes of the water/2-propanol droplets are small relative to those of water/AOT droplets discussed in the previous chapter.

Composition of the Microemulsion Droplets Consider a microemulsion droplet containing m water molecules and n 2-propanol molecules. If we assume that the droplet is spherical, its volume V is given by

$$V = \frac{4}{3}\pi r_m^3 = mV_{1m} + nV_{2m} \tag{9.6}$$

where V_{1m} and V_{2m} are the molecular volumes of water and 2-propanol, respectively. Barden *et al.*[1] have reported that 2-propanol partitions nearly equally into water and hexane on a volumetric basis, and hence

Here η is the viscosity of the water-free binary solution consisting of *2*-propanol and hexane.

Table 9-5 Compositions of $(H_2O)_m$(*2*-propanol)$_n$ microemulsion droplets

Point	C_1'	C_2'	C_0'	β	*m/n*	*m*	*n*
III	1.43	5.28	4.29	0.0443	6.11	17.7	2.9
IV	1.50	4.90	4.50	0.0444	6.89	29.7	4.3
V	1.63	4.28	4.88	0.0444	8.58	88.4	10.3
II	2.13	5.22	4.25	0.0652	6.26	83.3	13.3
I	3.61	5.94	3.61	0.122	4.97	526	106

Unit: C_i' in mol L^{-1}.

Table 9-6 Comparison of predicted and measured D_{ik}' values for water(1')/*2*-propanol(2')/*n*-hexane(0') at 25 °C (measured values in parenthesis)

Point	C_1'	C_2'	D_{11}'	D_{12}'	D_{21}'	D_{22}'
I	3.61	5.94	0.60(0.17)	-0.04(-0.03)	-0.19(-0.29)	0.73(0.64)
II	2.13	5.22	0.59(0.39)	-0.02(-0.02)	-0.30(-0.56)	0.78(0.86)
III	1.43	5.28	0.59(0.64)	-0.02(-0.06)	-0.41(-0.60)	0.80(1.02)
IV	1.50	4.90	0.59(0.57)	-0.02(-0.05)	-0.39(-0.72)	0.81(0.99)
V	1.63	4.28	0.60(0.43)	-0.02(-0.05)	-0.34(-0.69)	0.83(1.01)

Units: C_i' in mol L^{-1}; D_{ik}' in 10^{-5} cm^2 s^{-1}.

$$\frac{C_2'(aq)}{C_1'(hex)} \approx 1 \tag{9.7}$$

where C_2' (aq) is the concentration of *2*-propanol in the aqueous phase (the droplets) and C_2' (hex) is the concentration of *2*-propanol in the hexane phase. If β denotes the fraction of *2*-propanol in the droplet and 1 - β is the fraction of *2*-propanol in the hexane phase, then

$$\frac{\beta C_2'/(C_1'V_{1m} + \beta C_2'V_{2m})}{(1-\beta)C_2'/[C_0'V_{0m} + (1-\beta)C_2'V_{2m}]} = 1 \tag{9.8}$$

and hence $\beta = C_1'V_{1m}/(1 - C_2'V_{2m})$. $C_1'V_{1m} + \beta C_2'V_{2m}$ is the volume fraction of the droplets and $C_0'V_{0m} + (1 - \beta)C_2'V_{2m}$ is the volume fraction of the hexane phase. The ratio of the concentration of water to the concentration of *2*-propanol in the microemulsion droplets is given by

$$\frac{C_1'}{\beta C_2'} = \frac{m}{n} \tag{9.9}$$

Equations (9.6) through (9.9) can be used to calculate *m* and *n*, and hence the average composition of the $(H_2O)_m$(*2*-propanol)$_n$ droplets. The results, which are summarized in Table 9-5, indicate that most of the *2*-propanol is in the hexane phase.

Interpretation of Diffusion Coefficients Assume that water and *2*-propanol form a series of molecular complexes $(H_2O)_m$(*2*-propanol)$_n$ which diffuse through *2*-propanol/ hexane-continuous solvent:

$$m\text{H}_2\text{O} + n\text{2-propanol} \rightleftharpoons (\text{H}_2\text{O})_m(\text{2-propanol})_n \tag{9.10}$$

The number of different solution species is potentially very large: H_2O and *2*-propanol monomers plus an infinite number of the molecular complexes, $(H_2O)_2$, $(H_2O)_1$(*2*-propanol)$_1$, (*2*-propanol)$_2$, $(H_2O)_3$, $(H_2O)_2$(*2*-propanol)$_1$, $(H_2O)_1$(*2*-propanol)$_2$, (*2*-propanol)$_3$, $(H_2O)_4$, $(H_2O)_3$(*2*-propanol)$_1$, ... Describing the diffusion of so many species is a daunting problem at first glance. Fortunately, however, the dissociation/association reactions are very rapid compared to diffusion. The concentration of each molecular complex is therefore constrained by the equilibrium relation:

$$K_{mn} = \frac{c_{(H_2O)_m(2\text{-propanol})_n}}{(c_{H_2O})^m (c_{2\text{-propanol}})^n} \tag{9.11}$$

at each point along the diffusion path. K_{mn} is the equilibrium constant for the formation of complex $(H_2O)_m(2\text{-propanol})_n$ from monomers, and c_i the concentration of species i.

Local chemical equilibrium has an important implication for diffusion: the formation of molecular complexes does not introduce additional independent fluxes (*i.e.* diffusional "degrees of freedom"). Consequently, the diffusion of total water and 2-propanol components can still be accurately described by the ternary Fick equations

$$J_1' = -D_{11}'\nabla C_1' - D_{12}'\nabla C_2' \tag{9.12}$$

$$J_2' = -D_{21}'\nabla C_1' - D_{22}'\nabla C_{22}' \tag{9.13}$$

despite the large number of solution species.

It is necessary to estimate the concentrations of the $(H_2O)_m(2\text{-propanol})_n$ species in order to use equation (8.9) through (8.12) to interpret the diffusion behaviour of the microemulsions. Consider the general case of two associating solutes A and B in an inert solvent. As a first step, we make the isodesmic approximation[121] for stepwise self-association of A and B. That is, the equilibrium constant for the formation of a dimer is identical to that for the successive association steps:

$$A_1 + A_{i-1} = A_i \qquad K_A = c_{A_i}/c_{A_1}c_{A_{i-1}} \tag{9.14}$$

$$B_1 + B_{i-1} = B_i \qquad K_B = c_{B_i}/c_{B_1}c_{B_{i-1}} \tag{9.15}$$

Accordingly, $c_{A_i} = K_A c_{A_1} c_{A_{i-1}} = K_A^{i-1} c_{A_1}'$ and $c_{B_i} = K_B c_{B_1} c_{B_{i-1}} = K_B^{i-1} c_{B_1}'$.

Similarly, we can estimate the concentration of the mixed A_1B_1 dimer by assuming that the equilibrium constant for the association of A_1 and B_1 monomers

$$A_1 + B_1 = A_1B_1 \qquad K_{A_1B_1} = (K_A^{1/2}K_B^{1/2}) = c_{A_1B_1}/c_{A_1}c_{B_1} \tag{9.16}$$

is the harmonic average of the equilibrium constants for the formation of A_2 and B_2.

$$c_{A_1B_1} = (K_A^{1/2}K_B^{1/2})c_{A_1}c_{B_1} \tag{9.17}$$

It is relatively complicated to estimate the concentrations of the higher-order mixed complexes owing to the formation of isomers. For example, the trimer represented by the overall formula A_2B_1 can exist as AAB or ABA isomers. We will assume that the

equilibrium constants for the formation of AAB and ABA from the monomers are simple mole-fraction w ighted averages of K_A and K_B:

$$A_1 + A_1B_1 = AAB \qquad K_{AAB} = (K_A^{2/3}K_B^{1/3})^2 = c_{AAB}/c_{A1}^2c_{B1} \tag{9.18}$$

$$A_1B_1 + A_1 = ABA \qquad K_{ABA} = (K_A^{2/3}K_B^{1/3})^2 = c_{ABA}/c_{A1}^2c_{B1} \tag{9.19}$$

and hence $c_{A2B1} = c_{AAB} + c_{ABA} = 2(K_A^{2/3}K_B^{1/3})^2\ c_{A1}^2c_{B1}$. The factor of two in this expression arises from the two isomeric forms of A_2B_1. Similar considerations lead to the expression for the concentration of the A_1B_2 complexes: $c_{A1B2} = 2(K_A^{1/3}K_B^{2/3})^2\ c_{A1}c_{B1}^2$.

If the above procedure is extended to the general case of species A_mB_n, the concentration of complex A_mB_n can be expressed as follows,

$$c_{AmBn} = N_{AmBn}\left(K_A^{\ m}K_B^{\ n}\right)^{\frac{+m-1}{n+m}} c_{A1}^{\ m}c_{B1}^{\ n} \qquad (m = 0, 1, 2,...;\ n = 0, 1, 2,...) \tag{9.20}$$

Here N_{AmBn} is the number of isomeric forms of complex A_mB_n (*e.g.*, 1 for A_1B_1; 2 for A_2B_1, A_1B_2; 3 for A_3B_1 and B_3A_1; 4 for A_2B_2; *etc.*).

In an interesting study, Longsworth[3] measured the diffusion coefficients of carboxylic acids and other hydrogen-bonded solutes in carbon tetrachloride, a nonpolar solvent. Plotting the limiting diffusion coefficients of these compounds against the logarithm of their molar volumes indicates that the diffusion coefficients are inversely proportional to the molar volume raised to the 2/3 power. Taking advantage of this result, we can estimate the diffusion coefficients of the various solution species as follows

$$D_{AmBn} = \left[\frac{v_B}{mv_A + nv_B}\right]^{2/3} D_{B1} \tag{9.21}$$

where D_{B1} is the diffusion coefficient of the B_1 monomer.

Given values for the association constants K_A(water), K_B(2-propanol), and the diffusion coefficient of 2-propanol monomer in the solution, the equations developed above can be used to calculate the D_{ik}' values of water(1′)/2-propanol(2′)/*n*-hexane water-in-oil microemulsions. Trial estimates of the monomer concentrations c_{A1} and c_{B1} were made at each composition. Newton's method was then used to solve the equilibrium equations for the concentrations of the various solution species. In most cases about 2500 different species were included in the model calculations.

The calculations were repeated with a number of different trial values for the association constants and the diffusion coefficient of B_1. The final value 1.0 was adopted for K_B, the effective equilibrium constant for self-association of *2*-propanol. This value is consistent with the association constants reported previously for alcohols in hydrocarbons, carbon tetrachloride, and other nonpolar solvents[3,4]. Values of association constant K_A for water have not been reported because water is almost insoluble in these solvents. We adopted the value $K_A = 1000$, which is much larger than the propanol association constant in order to reflect the higher polarity of water and its stronger tendency to associate. Using higher K_A values does not significantly improve the agreement between the measured and predicted D_{ik}' values. The diffusion coefficient of *2*-propanol in the propanol/hexane continuous phase must be smaller than the limiting diffusion coefficient of *2*-propanol in pure hexane, 4.2×10^{-5} cm^2 s^{-1}, because the viscosity of propanol/hexane mixtures increases with the concentration of propanol. The viscosity of a binary propanol/hexane mixture containing 0.4 mole fraction *2*-propanol is 5.0×10^{-4} Pa s, while the viscosity of pure hexane is 2.9×10^{-4} Pa s. Accordingly, the diffusion coefficient of *2*-propanol in the continuous phase of the microemulsions in region B, D_{B1}, is estimated to be 2.4×10^{-5} cm^2 s^{-1}.

The measured and predicted D_{ik}' coefficients for the water(1')/*2*-propanol(2')/*n*-hexane microemulsions are compared in Table 9-6. It is apparent that the fitted values are generally in good agreement with the measured diffusion coefficients, except for D_{11}'. It is encouraging that the predicted water diffusion coefficient L_{11}' is smaller than D_{22}' for *2*-propanol, even though water molecule is smaller than propanol molecule. The slower transport of water relative to propanol is caused by the stronger association of water molecules which leads to the formation of large slowly diffusing droplets.

A term-by-term study of the model equations suggested an explanation for the large, negative values of D_{21}'. When the concentration of water in the microemulsion is increased, the droplets grow in size and entrap more propanol molecules. Thus an increase in the concentration of water reduces the concentration of free propanol. The diffusion of relatively mobile free propanol "up" the water gradient to replace the propanol lost to the droplets appears as a coupled flow of propanol moving

countercurrent to the flow of water. The coupled flow of water produced by the propanol gradient is relatively small for two reasons. First, the tendency of propanol to associate is much weaker. Second, little free water is present.

Despite its qualitative success, the model for microemulsion diffusion developed here can be challenged on several points. For example, activity coefficients were set equal to unity even though the solutions are known to be nonideal. Also, the assumption of fixed equilibrium constants for the stepwise association reactions is a severe oversimplification because association often becomes stronger as the complexes grow in size[3,4]. For example, more stable cyclic complexes may form. This behaviour is not included in the model. These shortcomings are balanced by the fact that detailed predictions can be made based on very limited information: values for the effective association constants and the monomeric alcohol diffusion coefficient.

9.5. Conclusions

The results for water/*2*-propanol/*n*-hexane water-in-oil microemulsions indicate that water diffuses primarily in the form of large, slowly moving microemulsion droplets, whereas *2*-propanol diffuses both in the droplets and in the hexane solvent. The measured diffusion coefficients are used to estimate the average size and composition of the microemulsion droplets.

Coupled diffusion is important for this system. Diffusing water produces a large countercurrent coupled flow of *2*-propanol, but *2*-propanol produces only a small counterflow of water. This information provides a more complete picture of microemulsion diffusion than "pseudo-binary" treatments in which only a single "apparent" diffusion coefficient is determined.

A chemical equilibrium model is developed to describe interdiffusion in water/*2*-propanol/*n*-hexane. The calculated D_{ik}' values are in reasonably good agreement with the measured data. The model offers simple physical explanations for the system's interesting diffusion behaviour.

9.6. References

1 G D. Smith, C.E. Donelan and R.E. Barden, *J. Colloid Interface Sci.*, **60**, 488 (1976)

2. H. Høiland, A. Skauge and I. Stokkeland, *J. Phys. Chem.*, **88**, 6350 (1984).

3. L G. Longsworth, *J. Colloid Interface Sci.*, **22**, 3 (1966)

4. W C. Coburn and E.J. Grunwald, *J. Am. Chem. Soc.*, **80**, 1318 (1958).

Chapter 10

SUMMARY

Ternary interdiffusion in a number of micellar solutions and microemulsions was studied by using the Taylor dispersion technique. The results reported in this thesis provide new insights into the mass transport properties of these systems, especially the interactions between surfactants and solubilizates.

The diffusion coefficient of sodium dodecylsulfate (SDS) in aqueous NaCl solution determined by the dispersion method was smaller than the diffusion coefficient of the micelles suggested by quasi-elastic light scattering (QELS). This apparent disagreement arises from the neglect of cross-diffusion in the QELS measurements. In fact, QELS gives the lower eigenvalue of the interdiffusion coefficient matrix for SDS/NaCl solutions, not the micelle diffusion coefficient or the diffusion coefficient of the total SDS component.

The ternary diffusion measurements reported for aqueous SDS/*n*-hexanol and SDS/*n*-octanol solutions gave the diffusion coefficients of total SDS and total alcohol components as well as the cross-coefficients for the coupled flux of SDS caused by the concentration gradient in alcohol and *vice versa*. Coupled diffusion in these systems is particularly interesting. For example, virtually all of the octanol is solubilized and therefore diffuses through the solutions in SDS micelles, yet diffusing octanol produces large countercurrent coupled flows of SDS. To help understand the results, a model was developed for the interdiffusion of solubilizates and ionic micelles. The model takes into consideration changes in the extent of counterion binding caused by solubilization and coupled transport of solubilizate driven by the electric field which is generated by the diffusion of charged micelles and counterions. The ternary diffusion coefficients for aqueous sodium cholate (SC)/*n*-octanol and SC/*n*-decanol solutions predicted by using this model were in good agreement with the values measured by the Taylor dispersion technique. The results suggest that the model is applicable to a wide range of surfactant/solubilizate systems.

Ternary interdiffusion coefficients measured for water/AOT/*n*-heptane water-in-oil microemulsions showed that concentration gradients in AOT produced cocurrent coupled flows of water, but gradients in water produced counterflows of AOT. Moreover, the cross-coefficient for the coupled diffusion of water caused by the concentration gradient in AOT can even exceed the main diffusion coefficients. A size distribution model was developed to interpret these surprising results. The ternary diffusion coefficients predicted by this model were in good agreement with the measured values. This research provides an accurate picture of ternary interdiffusion in microemulsions because coupled diffusion is included.

Water/*2*-propanol/*n*-hexane water-in-oil microemulsions are unusual because this system is surfactant-free. *2*-propanol is completely soluble in both water and hexane. This consideration led to the development of a chemical equilibrium model for description of ternary interdiffusion in water/*2*-propanol/*n*-hexane water-in-oil microemulsions. Interdiffusion coefficients measured for water/*2*-propanol/*n*-hexane water-in-oil microemulsions were in reasonably good agreement with the values predicted by the chemical equilibrium model.

The research reported in this thesis explored the ternary diffusion behavior of surfactant/salt/water, surfactant/solubilizate/water and surfactant/oil/water systems. In many practical applications, however, surfactant solutions contain more than three components, such as surfactant/cosurfactant/oil/water or surfactant/salt/oil/water. In future studies, diffusion coefficients could be measured for four-component surfactant solutions. The diffusion properties of these systems, particularly coupled transport, promise to be very interesting.